Dynamics of Bodies Small Compared to the Mean Free Path in Gases

by

Karl Borg

May 2003
Technical Reports from
Royal Institute of Technology
Department of Mechanics
S-100 44 Stockholm, Sweden

Akademisk avhandling som med tillstånd av Kungliga Tekniska Högskolan i Stockholm framlägges till offentlig granskning för avläggande av teknologie doktorsexamen onsdagen den 11:e juni 2003 kl 10.15 i Kollegiesalen, Administrationsbyggnaden, Kungliga Tekniska Högskolan, Valhallavägen 79, Stockholm.

©Karl Borg 2003
Universitetsservice US AB, Stockholm, 2003

Dynamics of Bodies Small Compared to the Mean Free Path in Gases

Karl Borg, 2003

Department of Mechanics, Royal Institute of Technology SE-100 44 Stockholm, Sweden

Abstract

In the present thesis, aspects of the dynamics of bodies immersed in gases are investigated. The bodies under consideration are small compared to the mean free path in the gas. The study comprises both gases in equilibrium and gases subject to gradients in the temperature or the flow velocity. For the description of the inhomogeneous gas, the Chapman-Enskog distribution function is used.

In the case of an inhomogeneous gas, the dynamics of axially symmetric bodies is studied. The total force and torque exerted on the small body by the gas are calculated. The equations of motion are obtained, and the resulting transport, corresponding to stationary solutions, is investigated. For the case of a gas subject to a temperature gradient, the well-known thermophoresis phenomenon is recovered, where the bodies are transported towards the cooler parts of the gas. Previously known results for spherical bodies are generalised to axially symmetric bodies. For a gas subject to a velocity gradient, a new transport mechanism, Shearing Phoresis, is obtained, that transports the small bodies along the eigen directions of the shearing tensor.

In the case of a gas at equilibrium, the forces and torques acting on a spinning sphere are calculated. First, a sphere of finite thermal conductivity moving with a small speed is considered. A heat equation for the rotating sphere is solved, and the temperature field of the body surface is obtained. The total force acting on the spinning sphere is calculated, which is found to have three different components: a friction force, a force parallel to the angular velocity, and a transverse force of opposite direction compared to the corresponding force appearing in the continuum limit, the so-called Magnus force. Finally, the total force and torque acting on a spinning sphere of high thermal conductivity are obtained for arbitrary speeds. The result is applied to a spinning sphere in a Kepler orbit. In doing this, perturbation theory is employed. It is

shown that the force and torque, apart from slowly contracting the orbit radius, also slowly rotates the orbital plane.

Descriptors: rarefied gas, free molecular flow, distribution function, axially symmetric bodies, thermophoresis, transport phenomenon, Magnus effect, spinning sphere.

Preface

This thesis consists of one introduction to the subject and four papers.

Paper 1. Borg, K. I. & Söderholm, L. H. 2000 Thermophoresis of axially symmetric bodies. *Rarefied Gas Dynamics*, pp 867-874.

Paper 2. Söderholm, L. H. & Borg, K. I. 2001 Shearing Phoresis. *Phys. Rev. E.* Submitted.

Paper 3. Borg, K. I., Söderholm, L. H. & Essén, H. 2003 Force on a Spinning Sphere Moving in a Rarefied Gas. *Phys. Fluids*, pp 736-741.

Paper 4. Borg, K. I. & Söderholm, L. H. 2003 Effects of the reversed Magnus force on a Kepler orbit in a rarefied gas. Manuscript.

Division of work between authors

Paper 1: Karl Borg had the idea for paper 1. Karl Borg made all the calculations, theoretical and numerical, under Lars Söderholm's supervision.

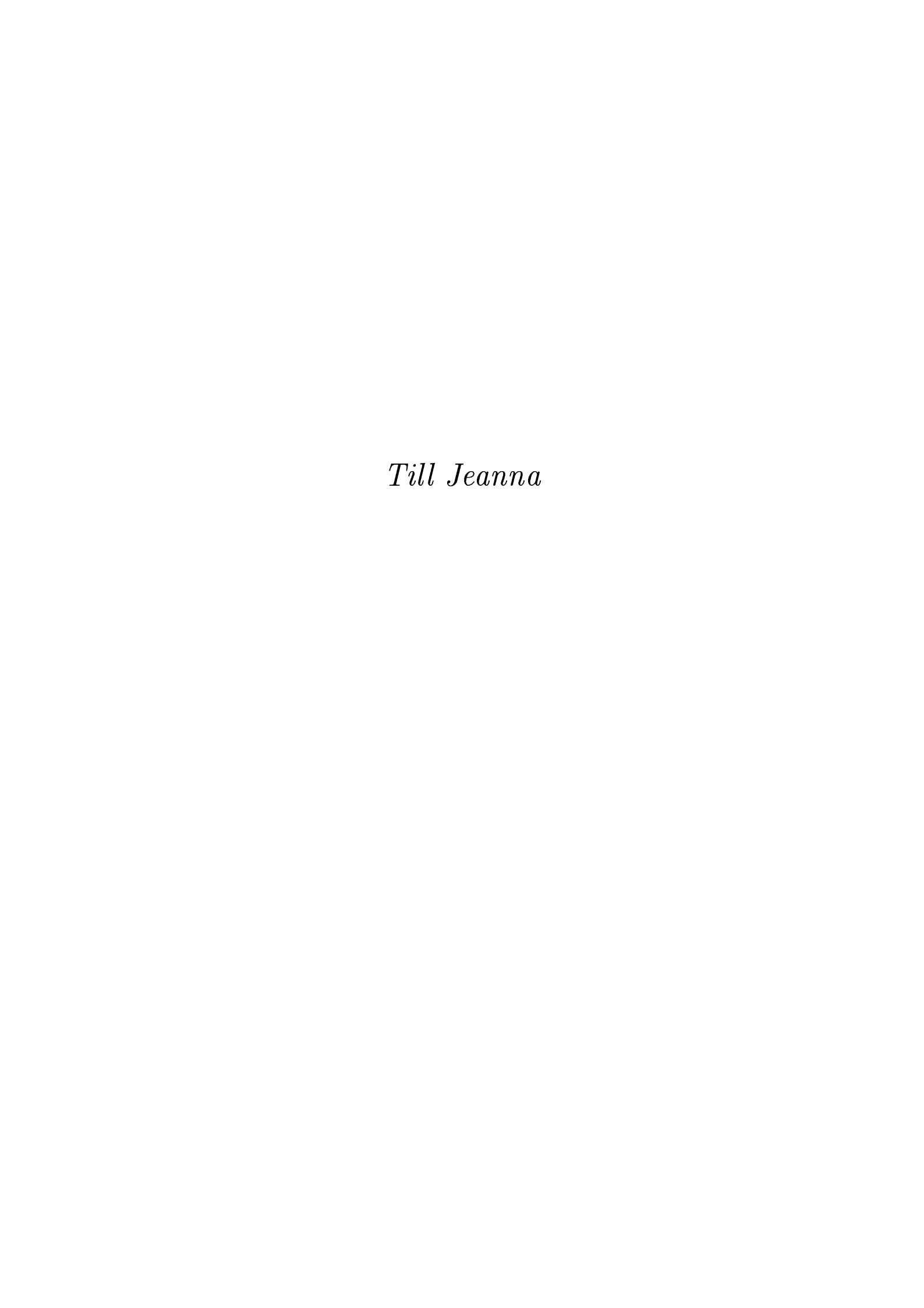
Paper 2: Lars Söderholm had the idea in paper 2 and made a preliminary calculation of the force and the torque. Karl Borg made the final calculation of force and the torque, calculated the asymptotics, and made the stability analysis, under Lars Söderholm's supervision. Karl Borg also made the numerical calculations.

Paper 3: Hanno Essén had the idea, and Karl Borg made the calculations under Lars Söderholm's supervision. Lars Söderholm also proposed the extension to finite heat conductivity of the body and conducted that investigation.

V

vi PREFACE

Paper 4: Lars Söderholm proposed the topic, and made a preliminary calculation of the effect. Karl Borg made all other calculations, under Lars Söderholm's supervision.



Contents

Prefac	e		v
Divi	sion of	work between authors	v
Chapt	er 1.	Thesis presentation	1
Chapt	er 2.	Introduction to kinetic theory	5
2.1.	The o	dilute gas	5
2.2.	Exan	aples of rarefied gas flows	8
Chapt	er 3.	The Boltzmann equation	9
3.1.	Boun	dary condition: The Maxwell model	11
3.2.	Cons	ervation properties	11
3.3.	Equil	librium distribution function (H-theorem)	13
Chapt	er 4.	Solutions of the Boltzmann equation	17
4.1.	The (Chapman-Enskog solution	17
4.2.	The l	Hilbert-Grad-Sone asymptotic method	18
4.3.	Free	Molecular Flow	19
4.4.	Solut	ions for length scales of the order of the mean free path	20
Chapt	er 5.	Spinning bodies and the Magnus effect	21
Chapt	er 6.	Introduction to the papers	23
6.1.	Axial	lly symmetric body	23
6.2.	Force	and torque on the body	24
6.3.	Asyn	aptotic solutions	24
6.4.	The l	Magnus effect	26
Chapt	er 7.	Papers Summary and Results	27

X	CONTENTS			
	7.1.	Paper (I)		

7.1.	Paper	(I)	27
7.2.	Paper	(II)	28
7.3.	Paper	(III)	29
7.4.	Paper	(IV)	31
Chap	ter 8.	"Beckham in for a surprise on Mars"	33
Chap	ter 9.	Future work	35
Ackno	owledge	ements	36
Refer Pape			37
Ther	nophor	esis of Axially Symmetric Bodies	41
1.	Introd	uction	41
2.	Local	momentum transfer to the body	42
3.	\mathbf{Body}	moving in a heat conducting gas	45
4.	Geom	etric integrals	47
5 .	Force	and torque on the body	48
6.	Equat	ions of motion	49
7.	Statio	nary solutions to the equations of motion	49
8.	\mathbf{Nume}	rical simulations	51
9.	Linear	stability analysis	52
10.	\mathbf{Body}	invariant under reflexion in a plane orthogonal	
	to th	e axis of symmetry	54
\mathbf{Ap}	pendix		57
Refer	ences		60
Shear	ing Ph	oresis	63
1.		uction	64
2 .	The d	istribution function of the shearing gas	65
3.	The fo	orce exerted by the gas on a body surface	66
4.		le and momentum fluxes	68
5.		and torque on the body	70
6.		ions of motion	72

	CONTENTS	xi
7.	Stationary solutions	73
8.	Numerical simulations	74
9.	Stability analysis	76
10	. Effects of inhomogeneities in the temperature field	
	of the body	79
11	. Conclusions	81
$\mathbf{A}_{\mathbf{I}}$	ppendix	82
A	cknowledgments	84
Refe	rences	85
Forc	e on a spinning sphere moving in a rarefied gas	89
1.	Introduction	90
2.	The distribution function	91
3.	The force exerted by the gas on a body surface	
	element	92
4.	Calculation of the force from a moving Maxwellian	94
5.	Effects of the nonuniform heating of the moving	
_	sphere	96
6.	Results for the force on the sphere	99
7.	Conclusions	101
Refe	rences	102
Effec	cts of the reversed Magnus force on a Kepler orbit in	
	a rarefied gas	105
1.	Introduction	105
2.	The distribution function	106
3.	The force on a body surface element	107
4.	Calculation of the force from a moving Maxwellian	109
5 .	Equilibrium temperature of a perfect conductor	112
6.	Perturbation of Kepler orbit	114
7.	Conclusion	120
A	cknowledgement	120
Refe	rences	121

Thesis presentation

There are several ways to read this thesis. One way is to start by chapter 8.

This thesis deals with the dynamics of small bodies immersed in gases. The bodies are small in the sense that their dimensions are much smaller than the mean free path of the gas.

Thermophoresis and Shearing Phoresis are the topics of papers (I) and (II). These belong to a class of interesting phenomena that appear in a gas with gradients in the temperature or the velocity in the limit where a continuum mechanical description breaks down.

If the gas is subject to a temperature gradient, we have the well-known phenomenon of thermophoresis: A small body suspended in the gas will be transported towards the cooler parts of the gas. Thermophoresis as a phenomenon has been known for a long time, and several authors have approached the problem. For example, Einstein calculated the final velocity of a spherical particle in a heat conducting gas using elementary kinetic theory. A recent review of the phenomenon is given in an article by Sone, [1].

Thermophoresis is used in some industrial processes, for instance, in manufacturing pure crystals. In that process, small particles in a gas are accumulated onto a solid boundary by applying a temperature gradient normal to the boundary. As a consequence, the small particles start to drift towards the cooler part of the gas, and finally wind up on the solid boundary. These applications are studied in [2] and in [3].

The first systematic attempt to describe the thermophoresis phenomenon using kinetic theory is found in an article by Waldmann from 1959, see [4]. That work was made under the assumption that the mean free path of the gas is much larger than the dimension of the body. Further results are found in a variety of articles, but these results mostly apply to bodies large compared to the mean free path. Some of these works deal with corrections to the Navier-Stokes equations. It should

2 1. THESIS PRESENTATION

be mentioned that in this region, negative thermophoresis may appear for bodies with very high thermal conductivity, cf [5].

The thermophoresis phenomenon if usually studied for spheres. In paper (I), thermophoresis is instead investigated for an axially symmetric body, in the limit where the typical length of the body is much smaller than the mean free path of the gas.

If the gas is subject to a gradient in the velocity, and if the suspended body is small compared to the mean free path in the gas, *Shearing Phoresis* occurs. This means that the small body will be transported along the eigendirections of the symmetric and traceless part of the velocity gradient.

Shearing phoresis is, to the best of our knowledge, a new phenomenon. Bell and Schaaf, [6], calculated the aerodynamic forces on a cylinder in shearing gas flow in 1953. Their result for the force from the shearing is valid for a finite Mach number. In paper (II) it is shown that the shearing will give rise to a force of first order in the Mach number. This force does not appear in the results in [6], because the cylinder is mirror symmetric. It is however apparent from their results that there exists a second-order force from the shearing acting on the cylinder.

Several authors, however, have studied the dynamics of larger bodies in a shearing gas, cf. [7],[8],[9]. These works deal with the problem in the continuum limit, and in particular corrections to the Navier-Stokes equations. A phenomenon of transverse diffusion of spherical particles in a shear layer is described in [10]. This phenomenon occurs in a dilute suspension of particles as a result of the collisions of the particles. Further results on this topic are found in [11] and [12]. The mechanism studied in paper (II) is however a different one, and does not require collisions between the particles.

Moreover, the force on a spinning sphere moving in a rarefied gas is the subject of interest in paper (III). The transverse force appearing in the continuum limit is a well-studied topic [13], not least in connection with sport balls. Here, the corresponding force is studied in the opposite limit. The calculations are made for a sphere with a moderate or higher thermal conductivity, moving with a speed much smaller than the thermal speed.

In paper (IV), the force and the torque acting on a spinning sphere of high thermal conductivity moving with arbitrary speed through a rarefied gas are calculated. The drag force was already calculated by Epstein for small speeds in [14]. So paper (IV) is an extension of his

work. These forces and torques are then applied to a spinning sphere in a Kepler orbit. It is found that these, apart from slowly contracting the orbit radius, also slowly turn the orbital plane.

Apart from the papers, the thesis also contains an introduction presenting some of the theory and nomenclature necessary to approach the papers. A summary of the papers is also included.

4 1. THESIS PRESENTATION

Introduction to kinetic theory

2.1. The dilute gas

The gas has in common with the liquid and the solid that it consists of a large collection of interacting molecules. If we however consider the relationship between the kinetic energy and the potential energy for these three different states, we find that in terms of this relationship, they differ very much among themselves.

In the solid, the molecules are closely bound to each other by intramolecular forces. The molecules perform thermal motion but remain in general rather fixed to an ordered lattice. For these molecules, the kinetic energy is not large enough to break the lattice ordering.

In the liquid, or in a dense gas, the kinetic energy of a particular molecule is large enough to destroy the ordered structure of the solid, but still small enough for the molecules to be in constant interaction with each other through the intermolecular forces.

In the dilute gas, the kinetic energy dominates over the potential energy in the sense that a gas molecule spends much of its time with only a negligible interaction with the other molecules in the gas. The interaction between the molecules can in the dilute gas be described as collisions, with a collision taking place during a time interval much shorter than the time spent by the molecules between collisions.

2.1.1. The molecular cross-section

For the dilute gas the interaction between the molecules can, as mentioned above, be reduced to collisions. The typical behaviour of the force between two molecules is a highly repulsive force for a small distance between the molecules (For larger distances the force falls of rapidly). There may also be a weak attractive part for large distances. The resulting collision is described by the cross-section. If the molecules are hard spheres with diameter d, the total cross section is then given by the area πd^2 .

The cross section is for realistic molecules energy dependent, and becomes smaller when the temperature is increased.

2.1.2. The dilute gas

Consider a simple gas (a gas that consists of one single chemical species) with density ρ . If we denote the mass of a molecule by m, we can compute the average number of molecules per unit volume, the *number density*, denoted by n, according to

$$n = \frac{\rho}{m}.$$

The value of the number density for air at standard temperature and pressure (293K and 101,3kPa), often abbreviated by STP, is $\sim 2.5 \cdot 10^{25}$ molecules per cubic meter. This, in turn, tells us that the average volume of gas per molecule is given by $1/n \sim 4 \cdot 10^{-26}$ cubic meters $= 4 \cdot 10^{-17}$ cubic millimetres. From the average volume per molecule, we can estimate the average spacing between the molecules, often denoted by δ , according to

$$\delta \sim \frac{1}{n^{1/3}}.$$

For air at STP, this estimate yields $\delta = 3.4 \cdot 10^{-9} \text{m}$. We are now in a position to define the *dilute gas* as a gas where the average spacing between the gas molecules is much larger than the diameter of the cross-section area, d. In a dilute gas, the time spent by the gas molecule travelling on the straight between two collisions is much larger than the time during which it interacts with another molecule in the gas. Air at STP has $\delta/d \sim 7$, and thus barely constitutes a dilute gas.

2.1.3. The mean free path

The mean free path of a gas is defined as the average distance a gas molecule travels between two successive collisions. It is possible to estimate the mean free path of a gas in the following way:

Consider a gas with number density n. We assume for simplicity that the gas is made up of spherical molecules with the radius r and diameter d=2r.

Let us start by placing an observer (A) on a particular molecule in the gas. Viewed from this observer, the molecules of the surrounding gas will perform some random motions with different velocities. Next, (A) calculates the average velocity of all the surrounding molecules. In order to proceed, we now perform the following artificial experiment: we replace all the different velocities of the different molecules by their mean velocity according to (A). We might say that all the surrounding molecules are replaced by a 'typical' molecule. When this is done, another observer (B) is placed on one of the surrounding molecules. From (B)'s point of view, we find that all the gas molecules are at rest except for our test molecule (A), which moves with the velocity of the same magnitude but opposite to the mean velocity calculated by (A). Moving along a straight line with this velocity, it will collide with the first molecule close enough to its trajectory. To be precise, it will hit another molecule if the distance between the centres of the molecules is less than 2r = d. Thus, any molecule with its centre within a cylinder, centred along the straight line-trajectory of our test molecule, with radius d, will be hit. If our test molecule travels in this way a distance l, the volume V of this cylinder is given by

$$V = \pi d^2 \cdot l$$
.

The mean free path λ is now defined as the distance this molecule travels before it collides with another molecule. This means that the volume of the cylinder by then is large enough to contain precisely one other molecule. Therefore this volume multiplied by the average number of molecules per unit volume equals one, or

$$V \cdot n = 1$$

or

$$\pi d^2 \cdot \lambda \cdot n = 1.$$

Solving this relation for the mean free path gives the estimate

$$\lambda = \frac{1}{\pi d^2 n}. (2.1)$$

2.1.4. The rarefied gas and the Knudsen number

If we now specify a particular problem for which the gas behaviour is sought for, there enter further length scales. These new length scales can be introduced by the boundary, i.e. the width of a channel through which the gas flows, or the length of an obstacle in a streaming gas. They may also enter through inhomogeneities in the gas properties, i.e. by the typical length over which the temperature varies in a non-uniformly heated gas.

In we denote this external length scale by L, we define the Knudsen number, Kn, as the quotient between the mean free path of the gas λ

and the external length L according to

$$Kn = \frac{\lambda}{L}$$
.

In a situation in which the external length scale L is much larger then the mean free path λ (thus for which $Kn \ll 1$), the gas may be regarded as a continuum. Usually one refers to a situation of this kind $(Kn \ll 1)$ as within the *continuum limit*, or sometimes the *fluid dynamic limit*. In this limit, the usual fluid dynamic equations can be used to calculate for instance the pressure and velocity fields of the gas. In this limit, the gas molecules perform a kind of random walk-like motion.

If, on the other hand, the length scale L approaches the mean free path λ in magnitude, the continuum description fail, and we enter the realm of Rarefied gases which is described by The Kinetic Theory of Gases. In this region, a number of striking non-continuum effects arise. For instance, a temperature gradient along a boundary may cause a gas flow along the boundary in the direction of the temperature gradient. This phenomenon is called the thermal creep flow, [15]. Another example is thermophoresis, which is a transport mechanism for small bodies causing them to move towards the cooler parts of a gas of non-uniform temperature.

2.2. Examples of rarefied gas flows

In the previous section it was claimed that for a dilute gas for which $Kn \geq 0.1$, ordinary fluid mechanics fails, and kinetic theory is required for the description of the gas flow. Of course, $Kn \geq 0.1$ can be achieved in two ways: either by making the external length L very small, or by making the mean free path λ very large. An example of the former case is the gas flow through the thin channels in a so-called micro electro mechanical system (MEMS), such as a micro nozzle. Further readings on gas flows in micro geometries is found in [16]. An example of the latter case is a satellite at the height of 140 km above the earth surface.

A further application of rarefied gas flows is the description of the thin layer (with the thickness of the order of a few mean free paths) of water vapour evaporating from the surface of the nucleus of a comet that surrounds the comet, and also the energy transport through channels and cracks in the comet's surface, [17].

The Boltzmann equation

In this section, we shall briefly review the so-called BBGKY-hierarchy [18, 19, 20, 21] derivation of the Boltzmann equation. Consider first an ensemble of N identical mono-atomic interacting molecules. This is the most simple case, poly-atomic gases posses further degrees of freedom: rotation and vibration. Further, both mono- and poly-atomic gases may undergo electronic transitions, but these require very much energy, that is, a high temperature. To describe the evolution of the entire system, we introduce the N-particle distribution function F_N , defined on the 6N-dimensional phase space spanned by the resp. positions and velocities of the N molecules. We call this space Γ -space. The 6-dimensional phase space of a single gas molecule we denote by γ -space. The interpretation of F_N is that $F_N d^3 x_1 d^3 c_1 d^3 x_2 d^3 c_2 ... d^3 x_N d^3 c_N$ is the probability that the position and velocity of molecule no 1 lie within $d^3x_1d^3c_1$; the position and velocity of molecule 2 lie within $d^3x_1d^3c_1$ etc. The interaction between the molecules is given by Newton's laws, and consequently the N-particle distribution function F_N satisfies the Liouville equation, which, in the absence of external forces is given by

$$\frac{\partial F_N}{\partial t} + \sum_{i=1}^{N} \mathbf{c}_i \cdot \frac{\partial F_N}{\partial \mathbf{x}_i} + \frac{1}{m} \sum_{i=1}^{N} \mathbf{X}_i \cdot \frac{\partial F_N}{\partial \mathbf{c}_i} = 0, \tag{3.2}$$

where X_i is the internal force acting on molecule *i*. The first assumption to be made is that the mono-atomic gas molecules interact via a spherically symmetric potential, that is, the potential satisfies

$$V(\mathbf{r}) = V(r).$$

We assume that the gas is dilute. This means that the typical diameter of the cross-section of the interaction between the molecules, d, is small compared to δ , the average distance between gas molecules. For air under standard conditions, $\frac{d}{\delta} \sim \frac{1}{7}$.

Since the gas molecules are identical, the state of the system is invariant under interchange of position of the molecules in γ -space. Therefore,

10

to an assembly of N molecules in γ -space, there corresponds N! points in Γ -space. We now introduce the function $f_N = f_N(t, \boldsymbol{x}_1, \boldsymbol{c}_1, ..., \boldsymbol{x}_N, \boldsymbol{c}_N)$ by writing the probability of finding the system at the points $(\boldsymbol{x}_i, \boldsymbol{c}_i)$ as

$$f_N(t, \boldsymbol{x}_1, \boldsymbol{c}_1, ..., \boldsymbol{x}_N, \boldsymbol{c}_N) d^3 x_1 d^3 c_1 \cdot ... \cdot d^3 x_N d^3 c_N;$$

Then we must have $f_N = N!F_N$.

The condition of molecular chaos is now imposed. This is a good approximation when the correlations can be neglected. This condition means that we can factorize the distribution function into a product of identical one-particle distribution functions, each describing a 'typical' gas molecule, that is,

$$f_N = f(\boldsymbol{x}_1, \boldsymbol{c}_1) \cdot f(\boldsymbol{x}_2, \boldsymbol{c}_2) \cdot \dots \cdot f(\boldsymbol{x}_N, \boldsymbol{c}_N). \tag{3.3}$$

Then the Liouville equation for a dilute gas is reduced to an integrodifferential equation for this one-particle distribution function: The Boltzmann equation. In the absence of external forces, if takes the form

$$\frac{\partial f}{\partial t} + \mathbf{c} \cdot \nabla f = \mathcal{J}(f, f), \tag{3.4}$$

where the *collision operator* $\mathcal{J}(f,f)$ is given by

$$\mathcal{J}(f,f) = \int \int \int \left(f'f_1' - ff_1 \right) gb db d\epsilon d^3 c_1, \tag{3.5}$$

The collision operator $\mathcal{J}(f,f)$ originates from the interaction term in the Liouville equation. In the expression for $\mathcal{J}(f,f)$, b is the impact parameter in the binary collision, ϵ is the angle of collision, $q = |c_1 - c|$ is the relative velocity of the colliding molecules, c is the velocity of the typical gas molecule, c_1 is the velocity of the molecule it collides with. c' and c'_1 are the corresponding velocities after the collision. Further, $f_1 = f(\mathbf{c}_1)$, $f' = f(\mathbf{c}')$ and $f'_1 = f(\mathbf{c}'_1)$. Note that the collision operator is bilinear in f. On the left-hand-side of the Boltzmann equation we have the material time derivative of the one-particle distribution function f. On the right-hand-side, the collision operator $\mathcal{J}(f,f)$ determines the rate of change in the one-particle distribution function due to collisions between the gas molecules. This equation is much simpler to handle than the Liouville equation. But the Boltzmann equation is still complicated enough as direct numerical solutions are possible only for simple geometries. The Bolzmann equation lacks the time-reversal symmetry satisfied by the Liouville equation. The essence of this derivation is thus that a coarse-graining is made in both time

and space. When this is done, the Boltzmann equation describes the probable evolution of the distribution f.

3.1. Boundary condition: The Maxwell model

The fate of a gas molecule that has collided with the body is not obvious. A rather well-established model that can be used is the Maxwell boundary condition. This model states that a fraction of the stream of molecules incident on the body surface is reflected specularly (or like a particle colliding with a solid wall). The remaining fraction of the incident stream of molecules reaches thermal equilibrium with the body (complete energy accommodation is assumed), and is reflected as a local Maxwellian. This fraction is said to be diffusely reflected. It is easy to see that the part specularly reflected on the surface element does not transfer any tangential momentum. Therefore, the fraction number is called, 'the accommodation coefficient of tangential momentum', and is usually denoted by α_{τ} . Put in mathematical terms, the reflected stream $f^{(r)}$ fulfils

$$f^{(r)}(\mathbf{c}) = (1 - \alpha_{\tau})f^{(i)}(\mathbf{c}') + \alpha_{\tau} \frac{n^{(r)}}{n} f^{(0)}(\mathbf{c}). \tag{3.6}$$

Here, $f^{(i)}$ is the distribution function describing the incident stream of molecules given by the first order Chapman-Enskog solution. Further, $c'_i = c_i - 2n_i n_j c_j$. $n^{(r)}$ is a number density that is determined by conservation of particles, and $f^{(0)}$ is a Maxwellian with the temperature of the body.

3.2. Conservation properties

The interpretation of the distribution function states that the average of a molecular quantity Q (such as the velocity or the kinetic energy), here denoted by $\langle Q \rangle$, is given by

$$\langle Q \rangle = \int Q f d^3c,$$
 (3.7)

where the integration is performed over all velocities. The averaged quantity $\langle Q \rangle$ corresponds to a macroscopic quantity (such as the flow velocity and the temperature). Here Q is a function of \boldsymbol{c} , the molecular velocity. The corresponding averaged quantity $\langle Q \rangle$, however, in general depends on time and position through the distribution function f. Since the Boltzmann equation (3.4) predicts the time evolution of the distribution function f, it is clear that also the time evolution of the averaged quantities $\langle Q \rangle$ are determined by the Boltzmann equation.

In an attempt to find the appropriate differential equation for < Q >, we multiply the Boltzmann equation by Q and integrate over velocity space. We then get

$$\int Q \frac{\partial f}{\partial t} d^3 c + \int Q \mathbf{c} \cdot \nabla f d^3 c = \int Q \mathcal{J}(f, f) d^3 c.$$

The molecular quantity Q is as mentioned above independent of position and time, and thus we may rewrite the terms of the left-hand side as

$$\int Q \frac{\partial f}{\partial t} d^3 c = \frac{\partial}{\partial t} \int Q f d^3 c = \frac{\partial \langle Q \rangle}{\partial t}.$$

and

$$\int Q \boldsymbol{c} \cdot \nabla f \, \mathrm{d}^3 c = \nabla \cdot \langle \boldsymbol{c} Q \rangle.$$

If we introduce the shorthand $\mathcal{I}[Q]$ for the rate of change of Q due to collisions, that is,

$$\mathcal{I}[Q] = \int Q \,\mathcal{J}(f, f) \,\mathrm{d}^3 c, \qquad (3.8)$$

we thus end up with a differential equation for $\langle Q \rangle$ given by

$$\frac{\partial \langle Q \rangle}{\partial t} + \nabla \cdot \langle cQ \rangle = \mathcal{I}[Q]. \tag{3.9}$$

This is the so-called transfer equation. It has the character of a transport equation with the source term $\mathcal{I}[Q]$. Using the symmetry properties of the collision operator $\mathcal{J}(f,f)$, $\mathcal{I}[Q]$ yields the following identity

$$egin{aligned} \mathcal{I}[Q] &= \int \int \int \int \ Q \ \left(f'f_1' - ff_1
ight) g b \mathrm{d}b \mathrm{d}\epsilon \mathrm{d}^3 c_1 \mathrm{d}^3 c \ &= rac{1}{2} \int \int \int \left(Q' + Q_1' - Q - Q_1
ight) f f_1 g b \mathrm{d}b \mathrm{d}\epsilon \mathrm{d}^3 c_1 \mathrm{d}^3 c. \end{aligned}$$

Written in this form, it is clear that if Q is either the mass, the momentum or the energy of a gas molecule, $Q' + Q'_1 = Q + Q_1$, as these are conserved during a collision, and consequently, $\mathcal{I}[Q] = 0$ for these quantities. It can be shown that these are the only quantities (or linear combinations of these) to be conserved during a collision.

Here it should be pointed out that when formulating the equation (3.9), the equation for $\langle Q \rangle$ depends on $\langle Q c \rangle$ through the second term of the transfer equation. Therefore, the equation for the mass will depend on the momentum, the equation for momentum on the energy etc. Thus, the transfer equations (3.9) will form a coupled, infinite system of equations.

3.3. Equilibrium distribution function (H-theorem)

In the six-dimensional γ -space, we denote the probability that there are N_1 molecules in the first cell of γ -space, N_2 molecules in the second cell, etc. by W, [18]. Using some algebra and Stirling's formula, it can be shown that W can be expressed in terms of the distribution function f according to

$$\ln W = -\int f \ln f \, \mathrm{d}^3 x \mathrm{d}^3 c. \tag{3.10}$$

The entropy σ is usually defined by $\sigma = (k_B/\rho) \ln W$, where k_B is the Boltzmann constant.

In this section, we shall study the so-called H-function for a region D of space defined by

$$H_D(t) = \int_D f \ln f \, d^3x d^3c.$$
 (3.11)

Here, f is a solution to the Boltzmann equation, and the functional $H_D(t)$ is thus related to the probability of this distribution via the entropy (3.10). We also define the corresponding H-function per unit volume, $H(t, \mathbf{x})$, by

$$H(t, \boldsymbol{x}) = \int f \ln f \, \mathrm{d}^3 c. \tag{3.12}$$

We shall now multiply the Boltzmann equation by $1+\ln f$, and integrate over velocity space. This cannot be done simply by putting $Q=1+\ln f$ and adopt the machinery of the previous section, since f depends on the time and space, and thus we proceed in a different way. First we observe that

$$(1 + \ln f)\frac{\partial f}{\partial t} = \frac{\partial}{\partial t}(f \ln f)$$

and

$$(1 + \ln f)\mathbf{c} \cdot \nabla f = \nabla \cdot (\mathbf{c} f \ln f).$$

Further, using the symmetry property employed in the preceding section, we obtain $\mathcal{I}[1 + \ln f]$:

$$\mathcal{I}[1+\ln f] = -\frac{1}{4} \int \int \int \int \ln \frac{f'f_1'}{ff_1} \left(f'f_1' - ff_1\right) gb \mathrm{d}b \mathrm{d}\epsilon \mathrm{d}^3 c_1 \mathrm{d}^3 c.$$

Now we define the function \boldsymbol{H} as

$$\boldsymbol{H} = \int \boldsymbol{c} f \ln f \, \mathrm{d}^3 c.$$

Accordingly, H is related to the entropy flux. The transfer equation for $1 + \ln f$ can thus be written

$$\frac{\partial H}{\partial t} + \nabla \cdot \boldsymbol{H} = \mathcal{I}[1 + \ln f]. \tag{3.13}$$

This equation should be interpreted as a transport equation for H with the source term $\mathcal{I}[1+\ln f]$, that corresponds to an entropy source. Now we integrate (3.13) over the region D. We then get, using Gauss' theorem on the second term of the left-hand side of (3.13)

$$\frac{\mathrm{d}H_D}{\mathrm{d}t} + \int_{\partial D} \boldsymbol{H} \cdot \boldsymbol{n} \, \mathrm{d}S = \int_D \mathcal{I}[1 + \ln f] \, \mathrm{d}^3 x,$$

where ∂D denotes the surface bounding the region D.

Inspecting the expression for $\mathcal{I}[1 + \ln f]$ shows the factors $f'f'_1 - ff_1$ and $\ln(f'f'_1/ff_1) = \ln(f'f'_1) - \ln(ff_1)$ always have the same sign, and thus make the integrand of $(3.3) \leq 0$. Therefore $\mathcal{I}[1 + \ln f] \leq 0$, that is,

$$\frac{\mathrm{d}H_D}{\mathrm{d}t} + \int_{\partial D} \boldsymbol{H} \cdot \boldsymbol{n} \, \mathrm{d}S \le 0. \tag{3.14}$$

This is the famous Bolzmann H-theorem [18].

Now we shall impose two defining conditions for the state of equilibrium: first we require that there is no net entropy flux through the volume D. Thus the surface integral vanishes in (3.14). Second, we require the equilibrium state to be stationary in the sense that the equality in (3.14) holds, which thus means that entropy is not produced within the region D. It is easy to see that the equality holds when $\ln(f'f'_1/ff_1) = 0$, or $\ln f' + \ln f'_1 = \ln f + \ln f_1$. This in turn implies that $\ln f$ is a linear combination of the mass, the momentum and the energy, according to

$$\ln f = Am + \mathbf{B} \cdot m\mathbf{c} + C,$$

where A, B and C are functions of time and space. These can be related to the number density n, the macroscopic flow velocity v and the temperature T by using their resp. definitions in terms of averages (integrals of f). When this is done, we finally obtain

$$f = f_0 = n \left(\frac{2\pi k_B T}{m}\right)^{-3/2} \exp\left[-\frac{m(\boldsymbol{c} - \boldsymbol{v})^2}{2k_B T}\right]$$
(3.15)

This distribution function is called the Maxwellian, or the equilibrium distribution function. It is the Normal distribution of the variable c,

3.3. EQUILIBRIUM DISTRIBUTION FUNCTION (H-THEOREM)

15

centred around the flow velocity $\boldsymbol{v},$ normalised according to

$$\int f \, \mathrm{d}^3 c = n,$$

with the standard deviation, or width of the distribution function, $\sigma^2 = k_B T/m$.

Solutions of the Boltzmann equation

In this chapter, we shall review approximate solutions to the Bolzmann equation.

If we denote the length scale of the problem for which we want to solve Boltzmann's equation by Λ , an order of magnitude estimate of the Boltzmann equation shows that the left-hand side is of the order of $\frac{\lambda}{\Lambda}$ times smaller than the collision term on the left hand side (we recall that λ denotes the mean free path of the gas. That is, in non-dimensional variables the Boltzmann equation looks like

$$\frac{\lambda}{\Lambda} \left(\frac{\partial f^*}{\partial t^*} + \mathbf{c}^* \cdot \nabla^* f^* \right) = \mathcal{J}^*(f^*, f^*). \tag{4.16}$$

(the *-superscript will be dropped in what follows.) For our purposes, there are two separate length scales for which we want to solve Boltzmann's equation: Firstly, we need a description of the gas subjected to the macroscopical gradients, that is, $\Lambda=L$. Secondly, we want to examine the situation for the small body, that is, $\Lambda=R$. Since by assumption $\frac{\lambda}{L}\ll 1$ and $\frac{\lambda}{R}\gg 1$, the corresponding investigations turns out to be quite different. For $\frac{\lambda}{L}\ll 1$ we use the so-called Chapman-Enskog solution, [22], to the Boltzmann equation. For $\frac{\lambda}{R}\gg 1$ we end up in the equations of Free Molecular Flow.

4.1. The Chapman-Enskog solution

In the limit where $\lambda \ll L$ the solution to the Boltzmann equation can be expanded in the small parameter $\frac{\lambda}{L} \equiv Kn$, where the *Knudsen number Kn* measures the rarefaction of the gas. To zeroth order in Kn, we obtain the solution for a gas in local equilibrium: the Maxwellian, $f^{(0)}$, given by

$$f^{(0)} = n \left(\frac{2\pi k_B T}{m}\right)^{-3/2} e^{-m(\mathbf{c} - \mathbf{v})^2/2k_B T}.$$
 (4.17)

In this expression, n is the number of molecules per unit area, k_B is Boltzmann's constant, T is the temperature, m is the mass of a gas

molecule, v is the flow velocity and c is the velocity of a gas molecules. Here n, v and T are functions of space and time. The Maxwellian is thus the solution of $\mathcal{J}(f,f)=0$. This solution describes a gas in local equilibrium, with no stresses and no heat currents.

To take into account the influence of the non-uniformity of the distribution function, we must include deviations from the Maxwellian in the distribution function. Therefore, we seek the solution to first order in Kn. This solution can be found through the Chapman-Enskog expansion. David Enskog (1884-1947) was Professor of Mechanics and Mathematics at KTH. Through his solution, the Navier-Stokes equations could for the first time be related to the Boltzmann equation [23]. In case of a gas subject to gradients in the temperature and the velocity v, a solution takes the form

$$f = f^{(0)} \left[1 - \frac{1}{nT} \sqrt{\frac{2k_B T}{m}} A(\mathcal{C}^2) \mathcal{C}_i T_{,i} - \frac{2}{n} B(\mathcal{C}^2) \mathcal{C}_{} v_{i,j} \right].$$
(4.18)

Here, $C_i \equiv \sqrt{m/2k_BT}c_i$ is a non-dimensional molecular velocity. The solutions A and B are related to the heat conductivity and the viscosity. A and B both depend on the intra-molecular potential and have the order of magnitude of Kn. Further, < ... > denotes the symmetric and traceless part.

This solution is well-established and gives correct values of the coefficients of heat conductivity and viscosity.

4.2. The Hilbert-Grad-Sone asymptotic method

An alternative approach to the Chapman-Enskog method that has come to be widely used was developed by Sone in the book [19] and by Sone, Aoki and others in a number of papers, c.f. [24, 25, 26, 27]. This method is a singular perturbation method, that resembles somewhat the boundary-layer methods of fluid dynamics. In this method, two expansions of a solution to the Boltzmann equation are made.

The first expansion is an exterior expansion made for small Kn. This corresponds to a slowly varying distribution function. This expansion yields the distribution function (or rather, the deviation of the distribution function from the Maxwellian) and equations for the hydrodynamic variables, valid away from the boundary.

The second expansion is an interior expansion made for the distribution function in the region close to the boundary, extending a distance of the order of the mean free path away from the boundary (the socalled Knudsen layer). Thus here a local Kn, based on the distance to the boundary, is no longer a small number. From this expansion, the boundary conditions for the hydrodynamic equations derived in the first expansion are derived.

4.3. Free Molecular Flow

We now consider a problem where the body has the length scale $R \ll \lambda$, and adopt for a moment its perspective of the gas. On the length scale of R the molecules of the surrounding gas do not collide with each other. As a consequence, the gas molecules move along straight lines. Still, they will of course collide with the small body. Accordingly, in the limit where $\frac{\lambda}{R} \gg 1$ the collision operator drops out of the Boltzmann equation, and we have

$$\frac{\partial f}{\partial t} + \boldsymbol{c} \cdot \nabla f = 0. \tag{4.19}$$

This is the Liouville equation for the one-particle distribution function f in the absence of forces. This means that f is constant along the trajectory of a molecule in γ -space.

Further, if the body is taken to be convex, a gas molecule will never undergo two consecutive collisions with the small body. In this limit, it is reasonable to assume that the body is small enough for the test-body approximation to be valid: the impact of the small body on the gas vanishes a distance $\sim \lambda$ away from the body, from where the gas molecules incident on the body surface originates. Thus, the distribution function describing the stream of molecules incident on the body surface can be approximated by the distribution function for the gas in the absence of the body, f. The particle flux incident on a surface element dS with unit normal n on the body, N is then expressed in terms of the distribution function f according to (here, f is the outward normal)

$$N = -\int_{\boldsymbol{n}\cdot\boldsymbol{c}<0} (\boldsymbol{n}\cdot\boldsymbol{c}) f \,\mathrm{d}^3 c, \qquad (4.20)$$

By the same argument, the momentum flux incident on the surface element is given by

$$P_i = -\int_{\boldsymbol{n}\cdot\boldsymbol{c}<0} (\boldsymbol{n}\cdot\boldsymbol{c}) m c_i f \,\mathrm{d}^3 c, \qquad (4.21)$$

and the energy flux is obtained from

$$E = -\int_{\boldsymbol{n} \cdot \boldsymbol{c} < 0} (\boldsymbol{n} \cdot \boldsymbol{c}) \frac{1}{2} m c^2 f \, d^3 c.$$
 (4.22)

4. SOLUTIONS OF THE BOLTZMANN EQUATION

With the Maxwell model we can also in a similar manner formulate the out-flux of mass and momentum by the stream of molecules that leave the surface. From demanding that the surface of the body is impermeable we can determine $n^{(r)}$. Then we are in a position to calculate the net momentum transferred from the gas to the surface element and thus arrive at an expression for the force and the torque exerted on the body surface element by the gas. The corresponding expressions can then be integrated over the total surface of the body to yield the total force and torque acting on the body.

4.4. Solutions for length scales of the order of the mean free path

In the region where the external length scale is of the order of the mean free path, that is, where $Kn \sim 1$, numerical methods are employed. One frequently used method is the DSMC (Direct-Simulation-Monte-Carlo) method. In this method, collisions between the molecules are modelled by random numbers, [28].

Direct numerical simulation of the Boltzmann equation is in general difficult, but has been carried out successfully for example for a shock wave, [29].

Further, a widely used method to approach problems numerically in this region is to use the BGK-equation. In this equation, the collision operator in the Boltzmann equation is replaced by a much simpler model, which is makes many problems much easier to handle numerically. The BGK-equation is employed also in other regions.

Spinning bodies and the Magnus effect

For those practising ball sports like table tennis and football, it is well known that the trajectory of the ball is curved if the ball is spinning. This effect has thus probably been known for as long as these ball sports have been practised.

Sir Isaac Newton (1642-1727) observed the effect and attributed it to a force, using his conclusions in *Philosophiae naturalis principia mathematica*.

In 1742, Benjamin Robins (1707-1751) published a book with the somewhat lengthy title: New principles of gunnery containing the determination of the force of gunpowder and investigation of the difference in the resting power of the air to swift and slow motions, containing a description of the Magnus effect (although he did not use the term 'Magnus Effect'). As the title suggests, the effect was here put in a ballistic context.

Ballistics was also the subject of interest of the German chemist Gustav Heinrich Magnus (1802-1870), after whom the Magnus effect is named. He described the effect on cannon projectiles in a work commissioned by the Preussian army.

In fact, there are quite a few names that could be associated with the influence of the spin on the trajectory: Euler, Maxwell, Magnus, Robins and Zhukovsky, [13].

The effect is usually explained in physical terms using Bernoulli's theorem [30] for irrotational flow:

$$p + \frac{1}{2}\rho u^2 = \text{constant} \tag{5.23}$$

This theorem states that the pressure is high where the velocity is low, and vice versa. To apply Bernoulli's theorem on the spinning ball, we proceed as follows:

Viewed from a rest frame of the centre of mass of the ball, at a certain point (A) the velocity of the surface of the sphere parallel to the

and Tiger Woods.

flow velocity is maximal. On the opposite side of the sphere, at the point (B), the situation is reversed: here the velocity of the sphere's surface opposite to the flow velocity assumes its maximum. By viscous action, the flow velocity is therefore increased at (A) and decreased at (B). This means, by Bernoulli's theorem, that the pressure is decreased at (A) and increased at (B). This pressure difference produces a force directed from (B) to (A), giving the ball a velocity in that direction. Thus, when a spinning ball is moving through the air, the spin of the ball will alter the trajectory, and the ball will be deflected. This is thus the origin of

To obtain a precise expression for the force, Rubinov and Keller [31] calculated the effect in the fluid dynamical limit using Navier-Stokes' equations, assuming small Reynolds number, Re, and found that the force acting on a sphere of radius R, velocity \boldsymbol{v} , and angular velocity $\boldsymbol{\omega}$, is given by

the effect so efficiently used by famous ball players like David Beckham

$$\mathbf{F} = [1 + \mathcal{O}(Re)]\pi R^3 \rho \,\mathbf{\omega} \times \mathbf{v},\tag{5.24}$$

where ρ is the density of the fluid. Experimental results show that the force (5.24) is adequate also for larger values of Re. A numerical calculation of the coefficient of the Magnus force for Reynolds numbers up to a few hundred is presented in [32].

Introduction to the papers

In the papers (I) and (II), it is shown that a body small compared to the mean free path in a nonuniform gas is set in a motion relative to the surrounding gas due to gradients in the temperature and the velocity. The typical length of the small body, R, is assumed to be much smaller than the mean free path of the gas. Further, the typical length over which the temperature and the velocity varies, L, is much larger than the mean free path of the gas. In the papers (III) and (IV), gas is in equilibrium. This can be regarded as $L \to \infty$. In all the papers, the surface of the body is convex, and the Free Molecular Flow approximation is used.

6.1. Axially symmetric body

The small bodies under consideration in the papers (I) and (II) are axially symmetric. This means that the body has no other geometrical direction than the axis of symmetry, N.

Axially symmetric bodies can posses an additional symmetry: If there exists a plane orthogonal to the axis of symmetry in which the body is mirror symmetric, the body is said to be equatorially symmetric, or mirror symmetric.

Further, geometric integrals over the total body surface of local geometrical quantities such as the unit normal n and the vector from the centre of mass of the body to a point on the body surface, x, must all be isotropic functions of the axis of symmetry N. That is, these geometric integrals are sums of products of N_i and the Kronecker delta δ_{ij} . An example of an integral of this type is given by $\int_S n_i n_j dS$, and due to isotropy it must fulfil

$$\int_{S} n_i n_j dS = S \left(c_1 \delta_{ij} + c_2 N_i N_j \right).$$

Here, S is the total body surface area. The non-dimensional scalar coefficients c_1 and c_2 can be found from successive contractions with products

of N_i and the Kronecker delta. When this is done, it is convenient to write the tensor as the sum of one isotropic part proportional to δ_{ij} and one symmetric traceless part proportional to $N_{< i}N_{j>} = N_iN_j - \frac{1}{3}\delta_{ij}$. These correspond to the l=0 and l=2 representation of the rotation group. The tensor integral then takes the form

$$\int_{S} n_i n_j dS = S\left(\frac{1}{3}\delta_{ij} + aN_{\langle i}N_{j\rangle}\right).$$

One finds that a measures symmetric deviations of the body shape from a sphere: For a coin shaped body, a = 1, and for a needle shaped body, $a = -\frac{1}{2}$. For a sphere, a = 0.

6.2. Force and torque on the body

The force, $d\mathbf{F}$, acting on a surface element of the body can now be obtained by calculating the net transfer of momentum to the surface element from the gas. This force will in general also produce a torque acting on the body surface element according to $d\mathbf{M} = \mathbf{x} \times d\mathbf{F}$, where \mathbf{x} is the vector from the centre of mass of the body to the surface element. As a consequence, the body will start to move and rotate, and a full rigid-body motion results. A body-fixed frame of reference is introduced, where one of the principal axes is chosen to be \mathbf{N} . The time evolution of this frame can then be related to the angular velocity by Euler's equations. The resulting motion of the body will generate additional forces and torques on the body.

Both the force and the torque acting on the surface element of the body will be tensor functions of the unit normal n and the vector x. To obtain the net force and torque acting on the body, we must integrate the force and the torque acting on a surface element of the body over the total body surface. This can be done using the method described above.

The total force will, to the present order of approximation, contain three different forces: one force arising from the non-uniformity of the gas, that is, from the heat currents or the stresses; one force depending on the velocity of the centre of mass of the body, and one force depending of the rotation of the body. The total torque on the body can be split up in a similar manner into three corresponding parts.

6.3. Asymptotic solutions

In paper (I) and (II), asymptotic solutions are studied. Given the force, the torque and Euler's equations, the equations of motion of the rigid

body can be formulated. This resulting system is a set of non-linear coupled ordinary differential equations, containing scalar coefficients that depend on the shape of the body.

With these at hand, asymptotic solutions with no rotation and a constant velocity can be found. These differ very much in character between thermophoresis and Shearing Phoresis. This is due to the difference in symmetry between the vectorial heat current and the tensorial stress tensor.

In order to investigate the stability of the resulting asymptotic states, the equations of motion of a test body are linearised close to these states. We choose as an example a 'double cone'. It consists of two cones, pointing in the opposite directions and glued together at their common base. The radius of the base is denoted by D, and the total length by R.

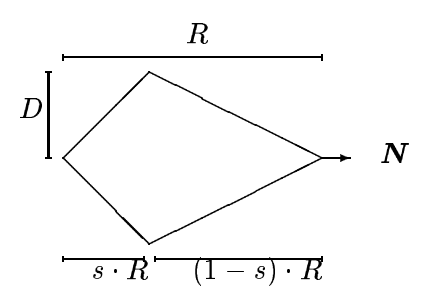


FIGURE 6.1. The 'double cone'

The base is situated a distance $s \cdot R$ from the left cusp, where the dimensionless parameter s obeys $0 \le s \le 1$. When s = 0 the double cone degenerates into a single cone with its cusp pointing in the direction of N. When s = 1 we recover another single cone, pointing in the direction of -N. This body is in general not equatorially symmetric, except when $s = \frac{1}{2}$.

In the case of Shearing Phoresis, the parameter s is restricted to vary in the interval $0 \le s \le \frac{1}{2}$; Thus, in this case, N always points in the same direction as the sharpest cusp of the double cone.

Given the linearised system, the eigenvalues of the infinitesimal motion of the double cone close to the asymptotic states can be calculated numerically. The stability character of these states can in this way be obtained for the double cone.

6.4. The Magnus effect

In papers (III) and (IV), the Magnus effect is studied. In case of phoresis, a linear approximation is adequate. But the Magnus force is quadratic (or bilinear). Here, a homogeneous spinning sphere is considered. In paper (III) the force is calculated to second order in the Mach number. A heat equation for the rotating sphere is solved. The boundary condition for this heat equation is obtained by calculating the net energy flux through the surface from the gas. In paper (IV), the calculations are made for arbitrary Mach numbers. Here the multiple-scale method is employed. In this method, two non-dimensional time scales are used: a 'fast' time t and a 'slow' time εt , where $\varepsilon \ll 1$, c.f. the weakly damped harmonic oscillator. Applying this method, a leading order solution is obtained in terms of the fast time, in which parameters depend on the slow time εt . These parameters are determined by a set of differential equations obtained from demanding that source terms producing resonance in the solution, and thus giving rise to irregular growth of the expansion, vanish.

CHAPTER 7

Papers Summary and Results

7.1. Paper (I)

In this paper, Thermophoresis of Axially Symmetric Bodies, the well-known thermophoresis phenomenon is studied. An axially symmetric test body is immersed in a heat conducting gas. The length scale of the temperature gradient (L) is much larger than the mean free path of the gas (λ) , and thus the Knudsen number Kn is much smaller than unity. Therefore the heat current can be described by the Chapman-Enskog distribution function.

The test body is assumed to be much smaller than the mean free path of the gas, and thus the method of free molecular flow is employed. Further, the body is assumed to have constant temperature: this corresponds to high thermal conductivity.

The Maxwell model is used for the boundary condition: a fraction $1-\alpha_{\tau}$ of the molecules incident on the body surface is reflected specularly, and the remaining fraction, α_{τ} , reaches thermal equilibrium with the body surface, and is reflected as a Maxwellian.

Assuming no net particle flux through the body surface, the net force and torque acting on the body are calculated to first order in Kn. The resulting speed is assumed to be small compared to the thermal speed $\sqrt{2k_BT/m}$: This assumption is shown to be consistent with our results.

In figure 7.1, the final thermophoretic speed of an axially symmetric body is plotted against the shape-dependent coefficient $c^{(2,0)}$, which measures the 'oblateness' of the body: for $c^{(2,0)} < 0$, the body is prolate, for $c^{(2,0)} = 0$, the body is a sphere, and for $c^{(2,0)} > 0$, the body is oblate.

Oblate bodies thus travel with a smaller speed than prolate bodies.

It is also shown, that for mirror-symmetric bodies, the rotational motion of the body decouples from the temperature gradient (an ellipsoid is mirror symmetric, but a half-sphere is not). This means that the axis of symmetry of the body does not align with the heat current,

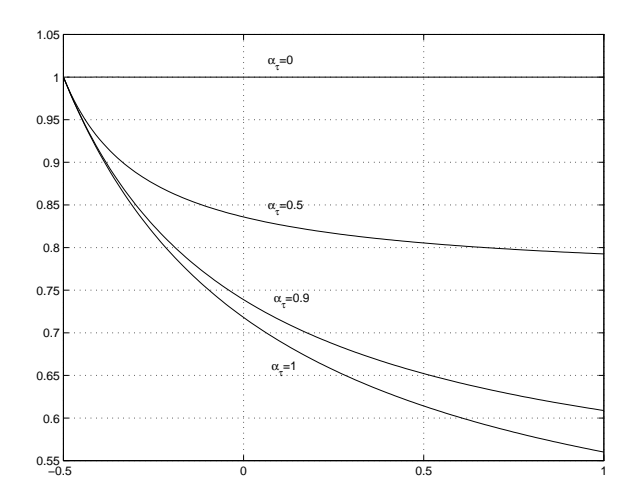


FIGURE 7.1. The non-dimensional final speed $|\mathcal{V}|/\frac{\gamma}{5p}|q|$ is plotted against the parameter $c^{(2,0)}$ for four different values of α_{τ} . On the horizontal axis, negative values corresponds to prolate bodies, whereas positive values corresponds to oblate bodies.

as is the case for bodies in general. As a consequence, the final thermophoretic velocity of such a body will in general have a component in the plane perpendicular to the heat current. In the figure 7.2, the orbit of a coin (mirror-symmetric) is compared to the orbit of a cone, for the same initial conditions. Thus, a body shaped as an ellipsoid or as a cylinder will with time travel without bound in a direction perpendicular to the heat current. It is likely, however, that higher-order terms in Kn will re-couple the angular momentum of mirror-symmetric bodies to the heat current. Since this coupling will be small, this effect will still prevail to a large extent for $Kn \ll 1$. This could be used to separate mirror symmetric bodies from general bodies in an assembly.

7.2. Paper (II)

In the paper *Shearing Phoresis*, a previously unknown mechanism of transport is obtained and studied. An axially symmetric body is immersed in a shearing gas. The body is small compared to the mean free path in the gas, and is assumed to have high thermal conductivity. The shearing gas is described by the Chapman-Enskog solution.

Calculating the linear and angular momentum transferred to the body by the gas, a force and a torque due to the shearing are obtained, together with a friction force and a friction torque. Stationary solutions

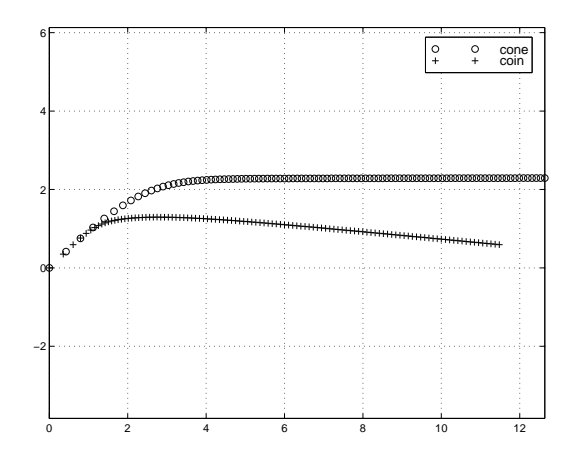


FIGURE 7.2. Orbit of one cone- and one coin-shaped body, with the heat current in the x-direction. Initially the axis of symmetry N of the two bodies makes the angle 45° with the heat current. The initial non-dimensional velocity of the two bodies is directed along N. Note that the cone assumes a final velocity parallel to the heat current, whereas the final velocity of the coin also has a component in the plane orthogonal to the heat current.

to these equations of motion are found, for which the velocity and the axis of symmetry of the body are parallel to an eigenvector of the shearing tensor. The speed of the body is constant and has the magnitude $\sim \lambda \, v_{x,y}$, where λ is the mean free path of the gas, and $v_{x,y}$ is the velocity gradient. This transport mechanism is not active if the body is mirror symmetric, which is the case in particular for spheres, ellipsoids, etc. In the figure 7.3, the orbits of blunt bodies (left figure) and slender bodies (right figure), subjected to a simple, one-component shearing $v_{x,y}$ are plotted.

Further, a linear stability analysis is made. It shows that the shape of the body determines along which eigen-vector of the shearing tensor the body will be transported.

7.3. Paper (III)

In the paper Force on a spinning sphere moving through a rarefied gas the force acting on the spinning sphere is calculated to second order in the non-dimensional speed (normalised for the thermal speed) for a sphere with moderately high thermal conductivity. A heat equation for the rotating body is solved, where the heat flux through the surface is

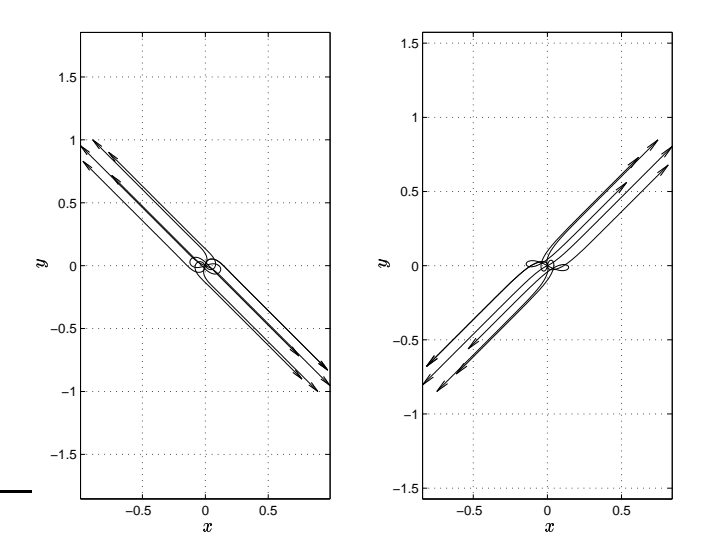


FIGURE 7.3. In each figure, 10 different orbits of bodies subject to a simple one-component shearing $v_{x,y}$ are represented for the case $\alpha_{\tau}=1/2$. They all start at t=0 in (x,y)=(0,0). In the left picture, the planar orbits of blunt bodies with R/L=2/5 end up parallel to the line x=-y. In the right picture, the orbits of more slender bodies, with R/L=1/4, finally end up along the line x=y. The initial angle between N and the x-axis is varied between 0 and 2π . The initial velocity is parallel to N, and the initial speed $|u_0|$ is set to approximately one tenth of the corresponding stationary velocity. The initial angular velocity is zero.

given by the energy conveyed to the body from the gas. The resulting temperature field of the surface of the sphere enters into the expression for the net momentum transferred to the body since the temperature determines the speed of recoil of the gas molecules that has reached thermal equilibrium with the sphere. It is shown that the resulting force has three components: One opposite to the velocity, one transverse force, and one proportional to the angular velocity of the sphere. The transverse force is found to have opposite sign compared to the corresponding transverse force appearing in the fluid dynamic limit. In the limit of infinitely high thermal conductivity, only the transverse component survives. Thus the trajectory of a spinning sphere is curved in the opposite direction compared to the corresponding well-known case of a spinning sphere in the continuum limit.

7.4. Paper (IV)

The sphere is assumed to be a perfect conductor. The total force and torque acting on a spinning sphere are calculated for arbitrary speed. It is shown that the transverse force coincides with the corresponding force in the small speed limit. The friction torque is found to have two components: one parallel to and one perpendicular to the velocity of the body. The coefficients of these torques are found to expose the same type of speed dependence as the friction force coefficient. They are constants for speeds small compared to the thermal speed. For speeds large compared to the thermal speed, they are proportional to the speed.

It is found that the force and the torque, when applied to a rotating body in a Kepler orbit, apart from slowly contracting the orbit radius also slowly rotates the orbital plane with an angular velocity proportional to the component of the initial angular velocity of the sphere parallel to the orbital plane. In the figure 7.4, the orbit of a rapidly rotating sphere in an initially circular Kepler orbit is shown.



FIGURE 7.4. The orbit in the figure above shows the evolution of an initially circular Kepler orbit of a sphere due to the damping and the action of the transverse force. The simulation exposes a slowly contracting orbit radius in a slowly rotating orbital plane. The angular velocity of the sphere has been exaggerated in order to produce a clearly visual effect on the orbit.

CHAPTER 8

"Beckham in for a surprise on Mars"

The 21:st February 2003, the journalist Philip Ball wrote an article in Nature with the title: "Beckham in for a surprise on Mars". In this article, he reviews paper (III) in this thesis and speculates on a possible application of the reversed Magnus force. Here follows two excerpt from his article:

"If a future interplanetary soccer competition is held on Mars, even David Beckham will struggle to bend the ball into the net, a new study suggests. Swedish physicists have found that a spinning ball would swerve in the opposite direction to the way it goes on Earth in the low-pressure atmosphere of the red planet."

He continues:

"Sports players understand the Magnus force intuitively. But in a gas much thinner than our atmosphere, their intuition would lead them astray. A ball swerves away from its spin in thin air, explain Karl Borg and colleagues at the Royal Institute of Technology in Stockholm. Footballers and baseball pitchers are used to balls that curve into their spin.

The problem is that, in a rarefied gas, the average distance that the molecules travel before colliding with one another is greater than the diameter of a ball. So more molecules hit the ball's forward-facing hemisphere than its rear hemisphere, the researchers calculate. These molecules bounce off in the direction of the ball's spin. Because of the conservation of momentum, this deflection of gas molecules pushes the ball itself in the opposite direction.

At intermediate gas pressure, the researchers point out, these two effects balance and a spinning ball won't swerve at all. "

But perhaps we cannot for sure promise the Earthly supporters of Beckham the spectacular experience of the ball swerving in the unexpected direction. It might take an atmosphere somewhat thinner than that on Mars. Alternatively, the game could be played with a smaller

34 8. "BECKHAM IN FOR A SURPRISE ON MARS"

football. But would really supporters then pay for the somewhat costly travel to the soccer game on Mars? On the other hand, with the whole solar system at our disposal we could of course choose another planet, with a thinner atmosphere than the one on Mars, for the interplanetary soccer competition. Beckham could then bring with him the football he is used to.

The article [33] (Ball, P., Beckham in for a surprise on Mars) can be found at: www.nature.com/nsu/030217/030217-11.html.

CHAPTER 9

Future work

The results of this thesis are obtained mainly by analytical methods in the free molecular flow limit. By means of Monte Carlo simulations, corresponding investigations for larger bodies (compared to the mean free path) would be of great interest. For instance, the critical density for which the transverse force (Magnus force) equals zero may be obtained by such a method.

For the Shearing phoresis phenomenon, there also remains to investigate if there exists a corresponding phenomenon in the continuum limit.

Further, it would be very interesting to extend the investigations made for the transverse force (Magnus force) in paper (IV) for a rotating body in a plasma. The outcome of such a study would probably have very interesting astrophysical applications.

Acknowledgements

First of all, I would like to thank my supervisor Dr. Lars Söderholm for his very competent and inspiring supervision, and for introducing me to the interesting field of the Kinetic Theory of Gases.

I would also like to thank Dr. Hanno Essén for rewarding and valuable discussions on various topics.

Further, Professor Anders Martin-Löf has been a great source of inspiration to me, and I would like to thank him for sharing some of his insights with me.

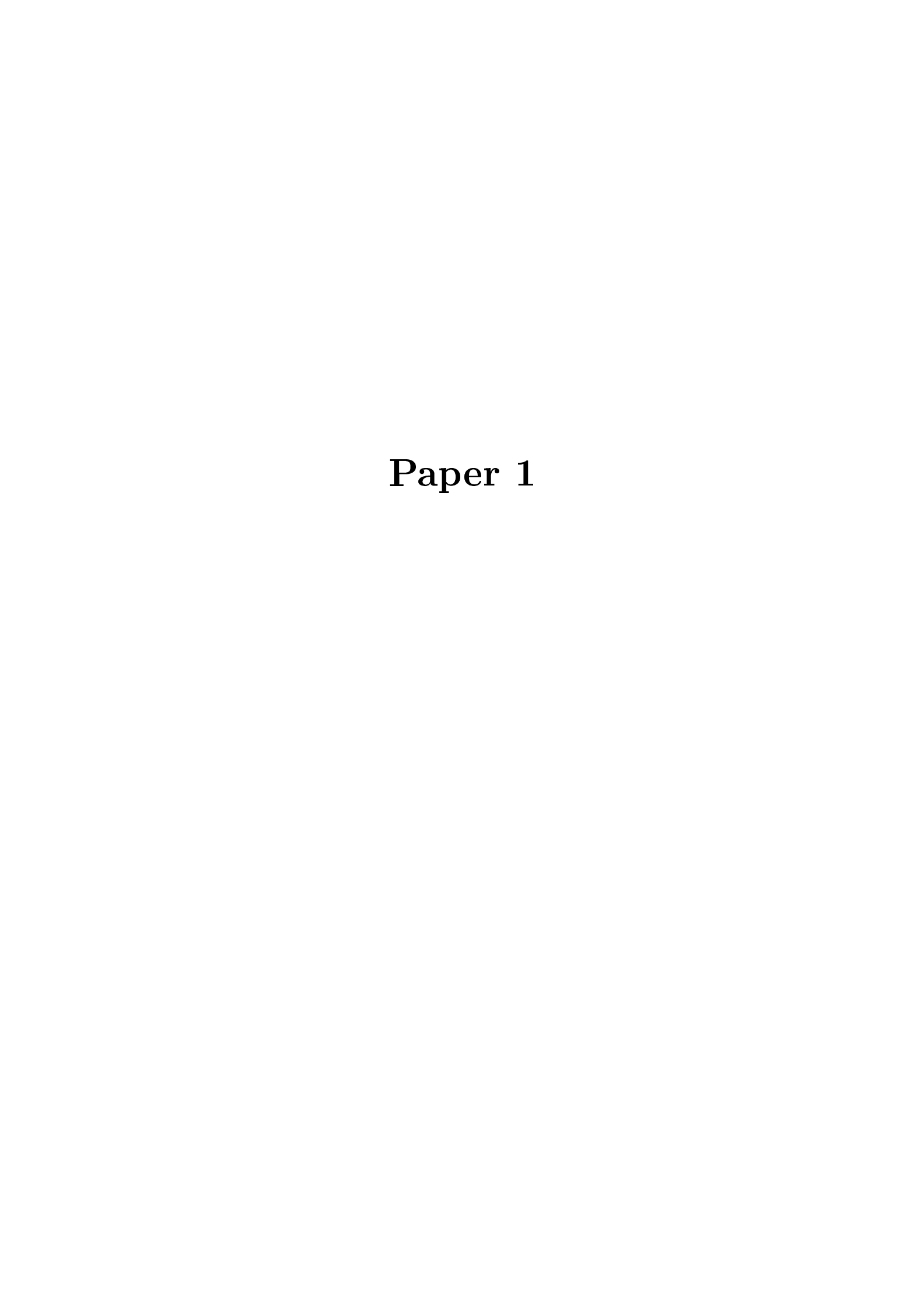
Moreover, my colleagues at the Department of Mechanics are gratefully acknowledged for providing a pleasant working atmosphere.

This work was partially supported by TFR.

References

- [1] Sone, Y. Flows induced by temperature fields in a rarefied gas and their ghost effect on the behaviour of a gas in the continuum limit. Ann. Rev. Fluid Mech., pp 779-811, 2000.
- [2] Guha, A., A unified Eulerian theory of turbulent deposition to smooth and rough surfaces. J. Aerosol Science, vol.28, no.8, pp. 1517-1537.
- [3] Opiolka, S., Schmidt, F., Fissan, H. Combined Effects of Electrophoresis and Thermophoresis on Particle Deposition onto Flat Surfaces J. Aerosol Sci., Vol. 25, No. 4, pp. 665-671, 1994
- [4] Waldmann, L. 1959 Über die Kraft eines inhomogenen Gases auf kleine suspendierte Kugeln. Z. Naturforsch. 14a: 589-99.
- [5] Ohwada, T., and Sone, Y. Analysis of thermal stress slip flow and negative termophoresis using the Boltzmann equation for hard-sphere molecules Eur. J. Mech., B/fluids 11, n:o 4, pp 389-414. (1992)
- [6] S. Bell and S. A. Schaaf, Aerodynamic Forces on a Cylinder for the free molecule flow of a Nonuniform gas, Journal of the American Rocket Society, vol 23, September-October 1953, pp. 314-317.
- [7] Cox, R. G. and Mason, S. G. Suspended particles in fluid flow through tubes. Ann. Rev. Fluid Mech. 3, p 291-316 (1971)
- [8] Goldsmith, H. L. and Mason, S. G. The flow of suspensions through tubes. 1: Single spheres, rods and discs. J. Colloid Sci. 17, pp 448-476 (1962)
- [9] Mortazavi, S. and Tryggvason, G. A numerical study of the motion of drops in Poiseuille flow. Part 1. Lateral migration of the drop. J. Fluid Mech. (2000), pp 325-350.
- [10] Wang, Y., Mauri, R. and Acrivos, A. The transverse shear-induced liquid and particle tracer diffusivities of a dilute suspension of spheres undergoing a simple shear flow. J. Fluid Mech. (1996), vol. 327, pp 255-272.
- [11] Leighton, D. and Acrivos, A. Measurement of shear-induced self-diffusion in concentrated suspensions. J. Fluid Mech. (1987a) vol. 177, p 109.
- [12] Leighton, D. and Acrivos, A. The shear-induced migration of particles in concentrated suspensions. J. Fluid Mech. (1987b) vol. 181, p 415.
- [13] Tokaty, G. A. A history and philosophy of fluid mechanics (Foulis, Henley on Thames, UK, 1971).
- [14] Epstein, P. S. On the resistance experienced by spheres in their motion through gases Phys. Rev. Series 2, 23, 710 (1924)
- [15] Sone, Y. (1966) Thermal creep in rarefied gas, J. Phys. Soc. Jpn 21, pp 1836-1837.

- [16] Karnadiakis, G. M. and Beskok, A. (2002) Micro Flows. Springer-Verlag New York.
- [17] Davidsson, B. J. R. (2003), Thermophysical Modelling and Mechanical Stability of Cometary Nuclei. Doctoral thesis.
- [18] Kogan, N. M. 1969 Rarefied Gas Dynamics New York: Plenum.
- [19] Sone, Y. (2002) Kinetic Theory and Fluid Dynamics. Birkhäuser, Boston.
- [20] Cercignani, C. (2000) Rarefied Gas Dynamics: From Basic Concepts to Actual Computations, Cambridge Texts in Applied Mathematics, Cambridge University Press.
- [21] Cercignani, C. (1988) The Boltzmann Equation and Its Applications, Springer-Verlag New York Inc.
- [22] S. Chapman and T. G. Cowling. The mathematical Theory of Nonuniform Gases, 3rd ed. (Cambridge U.P., Cambridge, England, 1958)
- [23] Enskog, D. (1917) Kinetische Theorie der Vorgange in massig verdünnten Gasen. Doctoral thesis.
- [24] Sone, Y. (1991) Asymptotic theory of a steady flow of a rarefied gas past bodies past bodies for small Knudsen numbers, in: Gatinol, R., and Soubbaramayer, Advances in Kinetic Theory and Continuum Mechanics, pp 19-31. Springer-Verlag, Berlin
- [25] Sone, Y. (1969) Asymptotic theory of flow of a rarefied gas over a smooth boundary I, in: Trilling, L. and Wachman, H. Y. eds., Rarefied Gas Dynamics, (Academic Press, New York) Vol. I, 243-253.
- [26] Sone, Y., and Aoki, K. (1987) Steady gas flows past bodies at small Knudsen numbers-Boltzmann and hydrodynamic systems, Transp. Theory and Stat. Phys. 16, pp 189-199.
- [27] Sone, Y., Aoki, K., Takata, S., Sugimoto, H., and Bobylev, A. V. (1996) Inappropriateness of the heat-conduction equation for description of a temperature field of a stationary gas in the continuum limit: Examination by asymptotic analysis and numerical computation of the Boltzmann equation, Phys. Fluids 8, pp 628-638; Erratum, Phys. Fluids 8, pp 841.
- [28] Bird, G. A. (1994) Molecular Gas Dynamics and the Direct Simulation of Gas Flows. Oxford University Press.
- [29] Ohwada, T. (1993) Structure of a shock wave, Phys. Fluids A, 5, pp 217-234.
- [30] Tritton, D. J. Physical Fluid Dynamics, 2nd ed, (Clarendon Press, Oxford, UK, 1988).
- [31] Rubinov, S. I. and Keller, J. B. (1961) The transverse force on a spinning sphere moving in a viscous fluid, J. Fluid Mech. 11, 447.
- [32] Bagshi, P. and Balachandar, S. (2002) Effect of free rotation on the motion of a solid sphere in linear shear flow at moderate Re. Phys. Fluids, 14, No. 8., pp 2719-2737.
- [33] Ball, P. (2003) Beckham in for a surprise on Mars. www.nature.com/nsu/030217/030217-11.html.



Thermophoresis of Axially Symmetric Bodies

By Karl I. Borg and Lars H. Söderholm

Department of Mechanics Royal Institute of Technology SE-100 44 Stockholm, Sweden

Published in Rarefied Gas Dynamics (2001), pp 867-874

Thermophoresis of axially symmetric bodies is investigated to first order in the Knudsen-number, Kn. The study is made in the limit where the typical length of the immersed body is small compared to the mean free path. It is shown that in this case, in contrast to what is the case for spherical bodies, the arising thermal force on the body is not in general anti-parallel to the temperature gradient. It is also shown that the gas exerts a torque on the body, which in magnitude and direction depends on the body geometry. Equations of motion describing the body movement are derived. Asymptotic solutions are studied.

1. Introduction

Thermophoresis as a phenomenon has been known for a long time, and several authors have approached the problem. For example, Einstein calculated the final velocity of a spherical particle in a heat conducting gas using elementary kinetic theory. A recent review of the phenomenon

is given in an article by Sone, see [1]. Another review is given by Talbot, see [2]. The first systematic attempt to describe the thermophoresis phenomenon using kinetic theory is found in an article by Waldmann from 1959, see [3]. That work was made under the assumption that the mean free path of the gas is much larger than the dimension of the body. Further results are found in a variety of articles, but these mostly apply to larger bodies, using asymptotic methods, and often to spheres. For example, Sone and Aoki analyzed negative thermophoresis in [4]. Further, in [5], thermophoresis of a moderately large and almost spherical particle is studied.

In this work, thermophoresis of axially symmetric bodies is considered. The typical macroscopical length L over which the temperature varies is assumed to be much larger than λ , the mean free path of the gas. Further, we define the Knudsen number according to $Kn = \lambda/L$. Thus $Kn \ll 1$, and we can use the first order Chapman-Enskog solution to the Boltzmann equation, see [6], to describe the heat conducting gas from the macroscopical viewpoint. The length R of the body is assumed to be much smaller than λ . R is also assumed to be much larger than d, the linear dimension of a gas molecule. In calculating the momentum transfer from the gas to the body we therefore use the equations of free molecular flow, [6]. We also assume that the speed of any point of the body is much smaller than the speed of sound. We define a Machnumber according to $M = v/c_s \ll 1$, where v is the speed of a body surface element and where c_s is the speed of sound.

2. Local momentum transfer to the body

If the one-particle distribution function $f = f(\boldsymbol{x}, \boldsymbol{c}, t)$ describing the gas is known and the proper gas-body surface boundary conditions are specified it is in principle possible to calculate the net transfer of momentum from the gas molecules to a body immersed in the gas. We shall now calculate the net force exerted by the surrounding gas on a surface element $d\boldsymbol{S} = \boldsymbol{n} dS$. Here \boldsymbol{n} is the outward unit normal of the surface element. It is convenient to perform the calculations in a frame of reference in which the unit surface element is momentarily at rest. This is possible since the force is a Galileian invariant (as the net mass flux through the surface element vanishes.) The force has two contributions: One from the stream of molecules incident on the surface element, and one from

the reflected stream, according to

$$dF_{i} = -\int_{c_{k}n_{k}<0} mc_{i}c_{j}n_{j}f^{(i)}(\boldsymbol{c})d^{3}cdS$$

$$-\left(\int_{c_{k}n_{k}>0} mc_{i}c_{j}n_{j}f^{(r)}(\boldsymbol{c})d^{3}cdS\right). \tag{1}$$

Here, m is the mass of a gas molecule, c_i is the molecular speed, $f^{(i)}$ and $f^{(r)}$ are the one-particle distribution functions describing the stream of molecules incident and reflected on the surface element. Since the body is small compared to the mean free path of the gas, and as the body is assumed to have a convex surface, the incident stream of molecules is approximated by f, the one-particle distribution function describing the gas in the absence of the body, that is, $f^{(i)}(\mathbf{c}) = f(\mathbf{c})$. The reflected stream of gas molecules is obtained from Maxwell's boundary condition. This means that the the reflected stream can be split in two separate parts: one part that is specularly reflected (that is, reflected as a particle hitting a solid wall), while the remaining part of the reflected stream has reached thermal equilibrium with the surface, and is reflected as an isotropic Maxwellian. We here assume complete energy accommodation [6], see below (25). Thus we write

$$f^{(r)}(\mathbf{c}) = (1 - \alpha_{\tau})f^{(i)}(\mathbf{c}') + \frac{n^{(r)}}{n}\alpha_{\tau}f^{(0)}(\mathbf{c}).$$
 (2)

Here, $c_i'=c_i-2n_in_jc_j$. The number α_{τ} is called the accommodation coefficient of tangential momentum, and measures the fraction of the reflected stream that is diffusely reflected. If $\alpha_{\tau}=0$, there is no transfer of tangential momentum between the gas molecules and the surface element. The unknown number density $n^{(r)}$ is to be determined from conservation of particles on the surface element. The Maxwellian is given by

$$f^{(0)}(\boldsymbol{c}) = n \left(\frac{2\pi k_B T}{m}\right)^{-3/2} \exp\left(-\frac{mc^2}{2k_B T}\right).$$

In this expression, the temperature of the reflected stream equals the temperature of the body.

We now demand that the net mass flux through the surface element vanishes. This means that

$$\int_{c_k n_k < 0} c_j n_j f^{(i)}(\mathbf{c}) d^3 c + \int_{c_k n_k > 0} c_j n_j f^{(r)}(\mathbf{c}) d^3 c = 0.$$
 (3)

This gives, [6],

$$\frac{n^{(r)}}{n} = -\frac{1}{n} \left(\frac{k_B T}{2\pi m}\right)^{-1/2} \int_{c_k n_k > 0} c_j n_j f(\mathbf{c}) d^3 c. \tag{4}$$

The force (1) becomes

$$dF_{i} = -\left[(1 - \alpha_{\tau}) \int_{c_{k}n_{k} < 0} m(c_{i} - c_{i}') c_{j} n_{j} f(\boldsymbol{c}) d^{3} c + \alpha_{\tau} \left(\int_{c_{k}n_{k} < 0} m c_{i} c_{j} n_{j} f(\boldsymbol{c}) d^{3} c + \frac{n^{(r)}}{n} \int_{c_{k}n_{k} > 0} m c_{i} c_{j} n_{j} f^{(0)}(\boldsymbol{c}) d^{3} c \right] dS.$$

$$(5)$$

We note that the last integral can be performed and equals $\frac{1}{2}pn_i$ where $p = nk_BT$. The velocity difference in the first integral can be written $c_i - c_i' = 2n_i n_j c_j$. Now we introduce a non-dimensional molecular velocity

$$C_i \equiv \sqrt{\frac{m}{2k_B T}} c_i, \tag{6}$$

a non-dimensional incident mass flux according to

$$\mathcal{M} \equiv -\frac{2\sqrt{\pi}}{n} \left(\frac{2k_B T}{m}\right)^{3/2} \int_{\mathcal{C}_k n_k < 0} \mathcal{C}_i n_i f^{(i)}(\mathcal{C}) d^3 \mathcal{C}, \tag{7}$$

and a non-dimensional incident momentum flux according to

$$\mathcal{M}_i \equiv \frac{4}{n} \left(\frac{2k_B T}{m} \right)^{3/2} \int_{\mathcal{C}_k n_k < 0} \mathcal{C}_i \mathcal{C}_j n_j f^{(i)}(\mathcal{C}) d^3 \mathcal{C}.$$
 (8)

These are normalized to give $\mathcal{M} = 1$ and $\mathcal{M}_i = n_i$ for the Maxwellian $f^{(0)}$. Now we write (4) as

$$\frac{n^{(r)}}{n} = \mathcal{M}. (9)$$

Then the force becomes

$$dF_i = -p \left[(1 - \alpha_\tau) n_i n_j \mathcal{M}_j + \frac{1}{2} \alpha_\tau \left(\mathcal{M}_i + \mathcal{M}_i n_i \right) \right] dS.$$
 (10)

3. Body moving in a heat conducting gas

In the present case, we shall consider a body which is small compared to the mean free path. This body will start to move under the influence of the force. Thus, in a frame of reference in which the body surface element is momentarily at rest the surface element will experience a homogeneous flow of the surrounding gas. This flow will exert an additional force on the surface element. It is convenient to perform the calculation of the force on the surface element (10) in this frame. Therefore, we consider a distribution function corresponding to a gas which is subject to a temperature gradient and a homogeneous flow. It is assumed that $Kn \equiv \lambda/L$, where λ is the mean free path and where L is the macroscopic length scale of the temperature gradient, is small. We also assume that the resulting motion of the surface element is small compared to the speed of sound. This is consistent with our result for the final velocity, see below.

For a gas subject to a non-uniform temperature distribution the distribution function takes, in the local rest frame of the gas, the form, [6],

$$f = f^{(0)} \left(1 + \phi_{\text{temp,grad.}} \right),$$
 (11)

where $\phi_{\text{temp.grad.}}$ can be found through the Chapman-Enskog expansion to first order in Kn. The result for pure heat conduction is

$$\phi_{\text{temp.grad.}} = -\frac{1}{nT} \sqrt{\frac{2k_B T}{m}} A(\mathcal{C}^2) \mathcal{C}_i T_{,i}. \tag{12}$$

The function A is usually expressed in Sonine polynomials according to

$$A(\mathcal{C}^2) = -\sum_{n=1}^{\infty} a_n S_{3/2}^{(n)}(\mathcal{C}^2), \text{ with } a_1 = -\frac{2m\kappa}{5k_B^2 T}.$$
 (13)

Here κ is the heat conductivity. If we introduce

$$\hat{A}(\mathcal{C}^2) \equiv A(\mathcal{C}^2)/a_1,$$

we may express $\phi_{\text{temp.grad.}}$ in terms of the heat current $q_i = -\kappa T_{,i}$ according to

$$\phi_{\text{temp.grad.}} = -\frac{4}{5p} \left(\frac{2k_B T}{m} \right)^{-1/2} \hat{A}(\mathcal{C}^2) \mathcal{C}_i q_i. \tag{14}$$

Now $\phi_{\text{temp.grad.}}$ is integrated to give the moments (7), (8) and one arrives at

$$\mathcal{M} = 1, \quad \mathcal{M}_i = n_i - \frac{2\gamma}{5p} \left(\frac{2\pi k_B T}{m} \right)^{-1/2} (\delta_{ij} + n_i n_j) q_j.$$
 (15)

The formulas (15) thus apply to a body surface element at rest. Here, the integral γ is given by

$$\gamma = \int_0^\infty \mathcal{C}^5 \hat{A}(\mathcal{C}^2) e^{-\mathcal{C}^2} d^3 \mathcal{C}. \tag{16}$$

If only the first term in the Sonine polynomial expansion of \hat{A} is retained, $\gamma = 1$. The corresponding integral in \mathcal{M} ,

$$\int_0^\infty \mathcal{C}^4 \hat{A}(\mathcal{C}^2) e^{-\mathcal{C}^2} d^3 \mathcal{C} = 0$$

as the gas is at rest.

The temperature gradient will give rise to a force on the immersed body and thus set the body in motion. This means that the motion of a particular point in the body will be given by $u = v + \omega \times x$, where v is the velocity of the body's center of mass, ω is the angular velocity of the body and x is the vector from the body's center of mass to the particular point we are considering. As the interaction between the gas and the body is mediated through the body surface, it is practical to take the motion of a body surface element into account by transforming the distribution function to a frame of reference where the surface element is momentarily at rest. Thus, for practical purposes, we consider a gas flowing with the velocity -u. The one-particle distribution function for the gas molecules can then be written

$$f = f^{(0)}(-\mathbf{u})(1 + \phi_{\text{temp.grad.}}),$$
 (17)

where $f^{(0)}(-\mathbf{u})$ is the Maxwellian with the flow $-\mathbf{u}$, and where $\phi_{\text{temp.grad.}}$ is the first-order Chapman-Enskog solution to Boltzmann's equation for a heat conducting gas. If the gas is moderately rarefied and if the velocity of the body is small compared to the speed of sound, $f^{(0)}(-\mathbf{u})$ can be linearized according to $f^{(0)}(-\mathbf{u}) \approx f^{(0)}(1 + \phi_{\text{flow}})$. $f^{(0)}$ is the Maxwellian describing the gas at rest. Under these circumstances we can also omit the cross-effect between the heat conduction and homogeneous flow. consequently, the moments \mathcal{M} and \mathcal{M}_i get additional

contributions of the order of M, and the result is

$$\mathcal{M} = 1 + \pi \left(\frac{2\pi k_B T}{m}\right)^{-1/2} n_i u_i, \tag{18}$$

47

$$\mathcal{M}_i = n_i - 2\left(\frac{2\pi k_B T}{m}\right)^{-1/2} \left(\delta_{ij} + n_i n_j\right) \left(\frac{\gamma}{5p} q_j - u_j\right). \tag{19}$$

The resulting force on a body surface element (10) becomes

$$dF_{i} = -pn_{i}dS + \left(\frac{2\pi k_{B}T}{m}\right)^{-1/2} \left\{\alpha_{\tau} \left(\frac{\gamma}{5}q_{i} - pu_{i}\right) + \left[\frac{\gamma}{5}(4 - 3\alpha_{\tau})q_{j} - p\left(4 - \left(3 - \frac{\pi}{2}\right)\alpha_{\tau}\right)u_{j}\right]n_{j}n_{i}\right\} dS$$
 (20)

This force will in general also produce a torque acting on the body through the surface element according to

$$dM_i = \epsilon_{ijk} x_i dF_k, \tag{21}$$

where \boldsymbol{x} is the vector from the center of mass of the body to the surface element.

4. Geometric integrals

In the expressions (20) and (21) there will appear tensor integrals all depending on the variables n and x. These have the general form

$$\int_{S} n_{i_1} n_{i_2} \dots n_{i_k} x_{j_1} x_{j_2} \dots x_{j_l} dS \equiv I_{i_1 i_2 \dots i_k | j_1 j_2 \dots j_l}^{(k,l)}.$$
 (22)

Here, the indices $i_n, j_n \in \{1, 2, 3\}$. In expression (20) for the force we have terms proportional to $I^{(0,0)} = S$. The integrals $I^{(k,l)}_{i_1 i_2 \dots i_k | j_1 j_2 \dots j_l}$ are tensors of rank k + l, and from symmetry, these integrals are all isotropic functions of N_i , where N_i is the body's axis of symmetry. This means that they are sums of products of N_i and δ_{ij} . It is convenient to use the symmetric and traceless part of the tensor $N_i N_j$, denoted by $N_{< i} N_{j>}$.

The scalar coefficients in these expansions will be contractions of the integrals. For example,

$$I_{i_1 i_2|}^{(2,0)} = S \left[\frac{1}{3} \delta_{i_1 i_2} + c^{(2,0)} N_{\langle i_1} N_{i_2 \rangle} \right]. \tag{23}$$

These coefficients will thus depend on the body geometry. In the expression (23) above,

$$c^{(2,0)} = \frac{3}{2S} \int_{S} \left[(\boldsymbol{N} \cdot \boldsymbol{n})^2 - \frac{1}{3} \right] dS.$$
 (24)

Here the coefficient $c^{(2,0)}$ is particularly important. It measures symmetric deviation of the body surface from spherical symmetry. For a needle-shaped body, its value is -1/2 and for a coin-shaped body it equals 1. For a sphere, it vanishes. A number of tensor integrals of this type appear. Along with the corresponding scalar coefficients, they are all calculated in the appendix. With these at hand we are in a position to write down the expressions for the force and the torque acting on the body.

5. Force and torque on the body

The force becomes

$$F_{i} = \left(\frac{2\pi k_{B}T}{m}\right)^{-1/2} \left\{ \frac{4\gamma S}{15} \left(\delta_{ij} + a_{1}N_{\langle i}N_{j\rangle}\right) q_{j} - pS \left(a_{2}\delta_{ij} + a_{3}N_{\langle i}N_{j\rangle}\right) v_{j} + 3pS^{3/2} a_{4}\epsilon_{ijk}N_{j}\omega_{k} \right\}.$$
(25)

The coefficients $a_1,...,a_4$ are calculated in the appendix. The first term on the right hand side of (25) is a thermal contribution to the force proportional to the heat current. The order of magnitude of this term is $\sim pSKn$. The second contribution to the total force is a friction force with geometrical features similar to the thermal force. The last term is a force acting on the body as a consequence of the body rotation. The two last terms both have the magnitude $\sim pSM$, where the M-number is based on \boldsymbol{v} in the first term and in the second term on $\boldsymbol{\omega}R$. We note that this expression is correct to first order in Kn and M. A corresponding calculation of the net energy transfer to the body will give the result 0+terms of higher order in Kn and M: Heating or cooling effects do not enter at this level of approximation. Thus it is consistent to assume that the temperature of the body is the same as the temperature of the gas.

The torque is given by

$$M_{i} = \left(\frac{2\pi k_{B}T}{m}\right)^{-1/2} \left\{ \frac{3\gamma S^{3/2}}{5} a_{5} \epsilon_{ijk} N_{j} q_{k} - 3p S^{3/2} a_{6} \epsilon_{ijk} N_{j} v_{k} - \frac{pS^{2}}{2} \left(a_{7} \delta_{ij} + a_{8} N_{\langle i} N_{j \rangle}\right) \omega_{j} \right\}.$$
(26)

The coefficients $a_1, ..., a_4$ are calculated in the appendix. In the expression for the torque, the first term is a thermal torque that acts to align the axis of symmetry parallel or anti-parallel to the heat current. This contribution is of the order of $\sim pS^{3/2}Kn$. The second term is active

whenever the axis of symmetry is not parallel or anti-parallel to the velocity. The third term is a friction torque. The two latter contributions are of the order of $\sim pS^{3/2}M$.

6. Equations of motion

In order to formulate the equations of motion for the body immersed in the heat conducting gas, we now introduce a body-fixed orthonormal frame of reference with the origin in the body's center of mass. The basis vectors are denoted by $e^{(\alpha)}$ where the index $\alpha = 1, 2, 3$ numbers the basis vectors. One of these basis vectors is naturally chosen to coincide with the axis of symmetry N. Newton's second law gives (m_B is the mass of the body)

$$m_B \frac{\mathrm{d}}{\mathrm{d}t} \boldsymbol{v} = \boldsymbol{F}.\tag{27}$$

The angular momentum equation becomes

$$\frac{\mathrm{d}}{\mathrm{d}t}\boldsymbol{L} = \boldsymbol{M},\tag{28}$$

where $L = I\omega$, and $\frac{d}{dt}L = L^{\circ} + \omega \times L$. Here L° denotes the rate of change of L with respect to the body-fixed frame. The basis vectors rotate with the angular velocity of the body, so

$$\frac{\mathrm{d}}{\mathrm{d}t}(\boldsymbol{e}^{(\alpha)}) = \boldsymbol{\omega} \times \boldsymbol{e}^{(\alpha)}.$$
 (29)

where I is the inertia tensor. This tensor has the form

$$I_{ij} = m_B S \left(B_1 \delta_{ij} + B_2 N_{\langle i} N_{i \rangle} \right). \tag{30}$$

For values of non-dimensional constants B_1, B_2 , see Appendix.

7. Stationary solutions to the equations of motion

In order to look for the asymptotic behavior of the bodies, we equate the force and the torque to zero. To do this we first make the ansatz $v = \mathcal{V}$ =constant and $\omega = 0$, and we get from the force equation (25)

$$\mathbf{0} = \frac{4\gamma S}{15} \mathbf{S}^{(q)} \mathbf{q} - pS \mathbf{S}^{(v)} \mathbf{V}, \tag{31}$$

and from the torque equation (26)

$$\mathbf{0} = \frac{3\gamma S^{3/2}}{5} a_5 \mathbf{N} \times \mathbf{q} - 3p S^{3/2} a_6 \mathbf{N} \times \mathbf{V}, \tag{32}$$

where the symmetrical tensors S are given by

$$\left(\mathbf{S}^{(q)}\right)_{ij} = \delta_{ij} + a_1 N_{< i} N_{j>}, \ \left(\mathbf{S}^{(v)}\right)_{ij} = a_2 \delta_{ij} + a_3 N_{< i} N_{j>}.$$

Note that these tensors are even functions of N. We obtain¹

$${f 0} = rac{\gamma}{5} \left(a_5 - rac{4}{9} a_6 rac{3 - a_1}{3a_2 - a_3}
ight) {m N} imes {m q}.$$

Two different types of solutions to this equation are possible:

- (I): $N \parallel \pm q$. From this condition we can compute the asymptotic velocity from the momentum equation.
- (II): $a_5 \frac{4}{9}a_6\frac{3-a_1}{3a_2-a_3} = 0$. This is the case when the body is mirror symmetric with respect to a plane orthogonal to the axis of symmetry. Here, any orientation of N relative to q is possible. Thus, the asymptotic velocity will in this case generally have a component perpendicular to q. This case will be studied in paragraph 10.

When $N \parallel \pm q$, we obtain from (31) is reduced to an expression for the asymptotic velocity \mathcal{V} :

$$\mathbf{\mathcal{V}} = \frac{4\gamma}{15p} \frac{3 + 2a_1}{3a_2 + 2a_3} \mathbf{q} = \frac{\gamma}{5p} \frac{1 + \frac{1}{2} (4 - 3\alpha_\tau) c^{(2,0)}}{1 + \frac{\pi}{8} \alpha_\tau + \frac{1}{4} [8 - (6 - \pi) \alpha_\tau] c^{(2,0)}} \mathbf{q}.$$
(33)

Here, γ is given by (16). It depends on the intramolecular forces of the gas molecules; $\gamma=1$ if only the first term of the Sonine polynomial expansion of the heat conducting part of the distribution function is retained. The new terms are those containing the parameter $c^{(2,0)}$, defined by

$$c^{(2,0)} = \frac{3}{2S} \int_{S} \left[(\boldsymbol{N} \cdot \boldsymbol{n})^2 - \frac{1}{3} \right] dS, \tag{34}$$

that depends on the body geometry. $c^{(2,0)}$ measures deformations of the body surface from a sphere: For a sphere, $c^{(2,0)} = 0$. In this case the asymptotic velocity (33) coincides with Waldmann's result, [3]. If the the body is extremely oblate, or shaped like a coin, $c^{(2,0)} = 1$. If the body is extremely prolate, or shaped like needle, $c^{(2,0)} = -\frac{1}{2}$. -The order of magnitude of this velocity is $Kn \cdot c_s$.

¹The equations (31) and (32) do not have solutions if the body is a coin or a needle and if $\alpha_{\tau} = 0$. This situation is unphysical and thus excluded in this context.

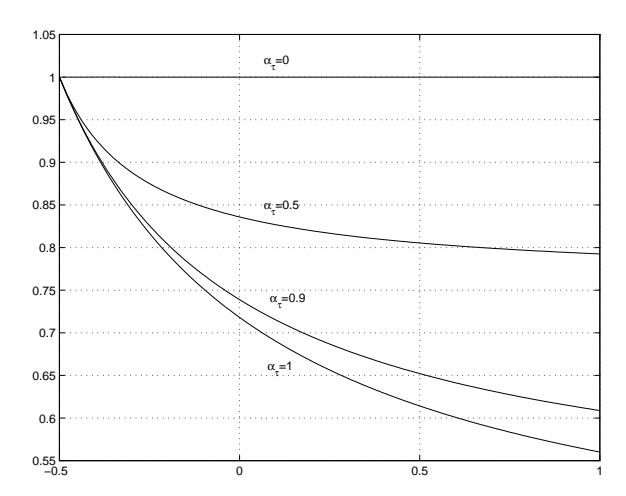


FIGURE 1. The non-dimensional final speed $|\mathcal{V}|/\frac{\gamma}{5p}|\mathbf{q}|$ is plotted against the parameter $c^{(2,0)}$ for four different values of α_{τ} .

8. Numerical simulations

Non-dimensional variables are now introduced according to $v_i = \frac{\gamma q}{5p} v_i^*$, $t = \frac{m_B}{pS} \left(\frac{2\pi k_B T}{m}\right)^{1/2} t^*$, and $\omega_i = \frac{pS}{m_B} \left(\frac{2\pi k_B T}{m}\right)^{-1/2} \omega_i^*$, where $q = |\boldsymbol{q}|$. The non-dimensional heat current is chosen to be $\hat{\boldsymbol{q}} = (1,0,0)$. Further, we introduce a non-dimensional tensor of inertia according to $\hat{I}_{ij} = I_{ij}/m_B S$. Then the system (27)-(28) becomes

$$\frac{dv_{i}^{*}}{dt^{*}} = \frac{4}{3} (a_{1}\delta_{ij} + a_{2}N_{\langle i}N_{j\rangle})\hat{q}_{j} - (a_{3}\delta_{ij} + a_{4}N_{\langle i}N_{j\rangle})v_{j}^{*}
-\mathcal{D}^{-1} \cdot 3a_{5}\epsilon_{ijk}N_{j}\omega_{k}^{*},$$

$$\frac{d}{dt^{*}} \left(\hat{I}_{ij}\omega_{j}^{*}\right) = \mathcal{D} \cdot 3a_{6}\epsilon_{ijk}N_{j}\hat{q}_{k} - \mathcal{D} \cdot 3a_{7}\epsilon_{ijk}N_{j}v_{k}^{*}
-\frac{1}{2} (a_{8}\delta_{ij} + a_{9}N_{\langle i}N_{j\rangle})\omega_{j}^{*}.$$
(35)

Here one non-dimensional parameter appears,

$$\mathcal{D} = \left(rac{2\pi k_B T}{m}
ight)^{1/2} rac{\gamma m_B q}{5p^2 S^{3/2}} \sim rac{\lambda}{d} \mathit{Kn} \, .$$

(The final order-of-magnitude estimate is made under the assumption that the density of the body equals the density of a gas molecule.) It is not obvious if this parameter is large or small. In the numerical calculations, we have set $\mathcal{D}=1$. The orbits of 10 identical double cones

with D/R = 2/5 and s = 1/4, but with different initial conditions, are shown in figure 2. In this figure, $\hat{q} = (1, 0, 0)$.

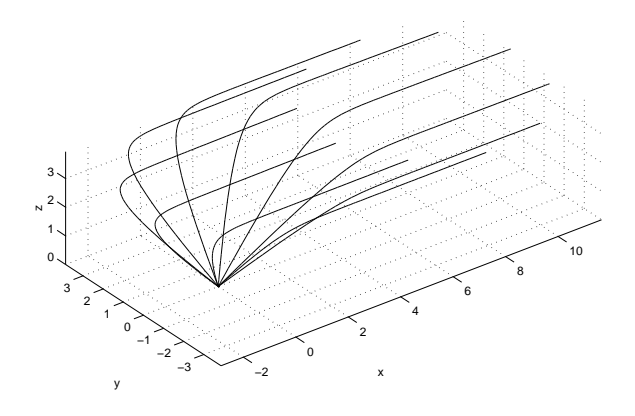


FIGURE 2. All the 10 orbits start at the origin. The all have the initial speed $v^*(0) = 10$, but with different directions of the axis of symmetry. N makes for all double cones the angle of 45^o with the z-axis. The angle the axes of symmetry make with the x-axis in the xy-plane is varied isotropically. The direction of the initial velocity coincides with that of the axes of symmetry. Despite the difference in initial condition, they all end up traveling along the heat current.

Simulations of the non-dimensional equations of motion of a cone-shaped body and a coin-shaped body are made, and the corresponding orbits are plotted in figure 3. Numerical simulations suggest that the bodies reach asymptotic states after a distance of the order of 1 in non-dimensional units, that is, $l = \left(\frac{2\pi k_B T}{m}\right)^{1/2} \frac{\gamma m_B q}{5p^2 S} \sim \frac{R}{d}\lambda \cdot Kn$ in dimensional units. Here, R is the dimension of the body, and d is the diameter of a gas molecule. This order-of-magnitude estimate is based on the assumption that the density of the body equals the density of a gas molecule. The difference in the final velocity is due to a symmetry in the coin-shaped body that is lacking in the body shape of the cone. This is investigated further later on.

9. Linear stability analysis

In order to investigate the stability of the two asymptotic states we linearize the equations of motion around the state where N is nearly

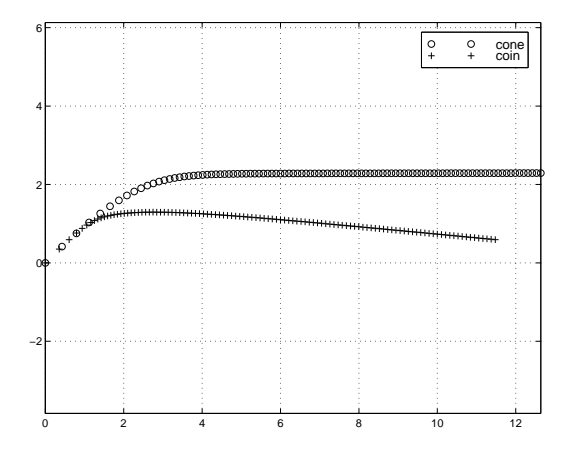


FIGURE 3. Orbit of one cone- and one coin-shaped body, with the heat current in the x-direction. Initially the axis of symmetry N of the two bodies makes the angle 45° with the heat current. The initial non-dimensional velocity of the two bodies is directed along N. Note that the cone assumes a final velocity parallel to the heat current, whereas the final velocity of the coin also has a component in the plane orthogonal to the heat current.

parallel to q. The eigenvalues of the resulting linear system are calculated for a special type of body, a 'double cone', shown in figure 4. This body consists of two cones with a common base. The radius of the base is denoted by D, and the total length by R. The base is situated a distance $s \cdot R$ from the left cusp, where the dimensionless parameter obeys $0 \le s \le 1$. When s = 0 the double cone degenerates to a single cone with its cusp pointing in the direction of N. When s = 1 we recover the same single cone, pointing in the opposite direction of N. A double cone with a given value of s = s' is identical to the double cone with s = 1 - s', but is pointing in the opposite direction.

The ansatz used for this linearization close to the asymptotic state $N\parallel q$ given by

$$\mathbf{N} = (1, \epsilon N_y, \epsilon N_z), \tag{37}$$

$$\boldsymbol{v}^* = \boldsymbol{\mathcal{V}}^* + (\epsilon v_x, \epsilon v_y, \epsilon v_z), \tag{38}$$

$$\boldsymbol{\omega}^* = (\epsilon \omega_x, \epsilon \omega_y, \epsilon \omega_z). \tag{39}$$

Note that since $N^2 = 1$, the correction to N_x is negligible. The non-dimensional asymptotic velocity $\mathbf{\mathcal{V}}^*$ is the non-dimensional final velocity.

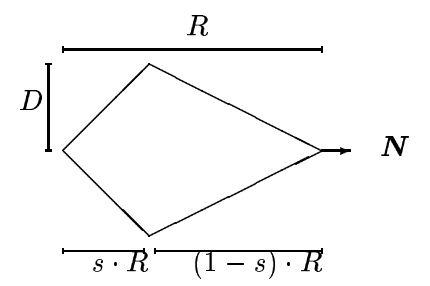


FIGURE 4. Test body: a 'double cone'

The ansatz is now substituted into the equations of motion, and a linear first-order system results. If we define the vector \boldsymbol{w} according to

$$\boldsymbol{w} = (N_y, N_z, v_x, v_y, v_z, \omega_x, \omega_y, \omega_z), \tag{40}$$

this linear system takes the form

$$\frac{d}{dt^*}\boldsymbol{w} = \mathcal{L}\boldsymbol{w},\tag{41}$$

where \mathcal{L} has been calculated with MAPLE, and is too large to give in explicit form here. The eigenvalues of the resulting linear systems are calculated for $\alpha_{\tau} = \frac{1}{2}$. The boundary between different stability areas is plotted in the plane spanned by s and D/R in the figure 5.

Plotting the real part of the eigenvalues against s yields a picture of the preferred orientation of the body. It turns out that stability is determined by two identical eigenvalues (the other eigenvalues are either negative or zero for all values of s). This eigenvalue is plotted against s in figure 5 for a somewhat prolate body (R/D=3) and for an oblate body (R/D=1/3).

It is apparent that the stable state for the prolate double cone occurs when the longer cone is pointing in the same direction as the heat current. For the oblate body the preferred orientation is in the opposite direction. For a symmetric body (s = 0.5) these eigenvalues vanish.

10. Body invariant under reflexion in a plane orthogonal to the axis of symmetry

Now we consider a body that is symmetric with respect to an equator plane, that is, a plane orthogonal to the axis of symmetry (ellipsoids, for example, possess this symmetry). Then the coefficients a_4, a_5 and a_6 vanish. It it easy to see that then the rotational motion decouples

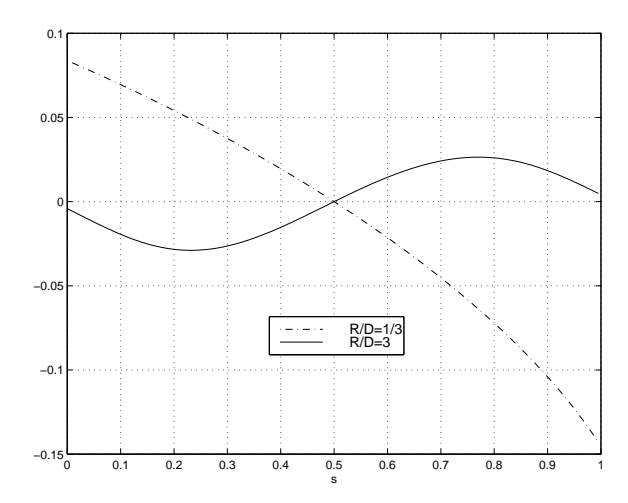


FIGURE 5. Critical eigenvalue plotted against s for two different double cones

from the translation and becomes independent of the heat current. The remaining part of the angular momentum equation states that as $t\to\infty$ all constant values of N are solutions. The asymptotic solution to the momentum equation in this case becomes

$$\tilde{V}_i = \left[\delta_{ij} + k \left(\delta_{ij} - N_i N_j\right)\right] V_j, \tag{42}$$

where V_j is the asymptotic velocity (33) found in the previous section. The tensor $\delta_{ij} - N_i N_j$ picks up the projection of \boldsymbol{q} that lies in the plane perpendicular to \boldsymbol{N} . The parameter k is introduced for simplicity and is given by (we recall that $c^{(2,0)}$ is a geometrical parameter encountered in (33))

$$k = 6\pi\alpha_{\tau}^{2}c^{(2,0)} \cdot \left\{ 2(8 + \pi\alpha_{\tau}) + [16 - (12 - 2\pi)\alpha_{\tau} - 3\pi\alpha_{\tau}^{2}]c^{(2,0)} - [32 - (48 - 4\pi)\alpha_{\tau} + (18 - 3\pi)\alpha_{\tau}^{2}] \left[c^{(2,0)}\right]^{2} \right\}^{-1}.$$
 (43)

In case of purely diffuse reflection, k takes the following values:

$$k=\frac{\pi}{4}=0.79~({\rm coin-shaped~body}),$$

$$k=-\frac{\pi}{6-\pi}=-0.34~({\rm needle-shaped~body}).$$

For a sphere, k=0. This means that a non-spherical body for general values of α_{τ} will acquire a velocity component in the plane perpendicular to the heat current. This effect is apparent in the final behavior exposed

by the body orbit of the coin in figure 3. If we let β denote the final angle between the N and q, it follows that the asymptotic speed of the body is now given by

$$|\tilde{\mathbf{\mathcal{V}}}| = |\mathbf{\mathcal{V}}|\sqrt{1 + (2k + k^2)\sin^2\beta},\tag{44}$$

and that the angle ψ that the velocity vector makes with the heat current obeys

$$\cos \psi = \frac{1 + k \sin^2 \beta}{\sqrt{1 + (2k + k^2)\sin^2 \beta}}.$$
 (45)

The maximum angle between the heat current and the body velocity, ψ_M , occurs in case of purely diffuse reflexion for an optimal value of the final orientation of the axis of symmetry relative to the heat current, and is given by

$$\psi_M = \arccos\left\{2\frac{\sqrt{1+k}}{2+k}\right\} = \begin{cases} 16.4^0 \text{ (coin - shaped body)} \\ 12.0^0 \text{ (needle - shaped body)} \end{cases}$$
(46)

These results thus predict that an initially localized assembly of equatorially symmetric bodies with different orientations relative to the heat current will, in the plane perpendicular to q, with time spread without bound. This is an interesting result, but perhaps not the whole story: Going to higher order contributions to the torque, a term of the order of Kn^2 ,

$$M_i \sim \epsilon_{ijk} N_j \tau_{kl}^{(B)} N_l \tag{47}$$

appears, where $\tau_{ij}^{(B)}$ is the stress tensor at the Burnett level in case of temperature gradients, given by

$$\tau_{ij}^{(B)} = \frac{\mu^2}{\rho T} \left(K_3 T_{,\langle ij \rangle} + K_5 \frac{1}{T} T_{\langle,i} T_{,j\rangle} \right). \tag{48}$$

Here μ is the viscosity and K_3 and K_5 are constants, cf [6]. This torque will re-couple the angular momentum of equatorially symmetric bodies to the temperature gradient. However, since in the present context $Kn \ll 1$, this coupling is clearly weak, and thus the typical time required for N to align with q is much larger for equatorially symmetric bodies.

Appendix

The geometric tensor integrals encountered when the expressions for the force and the torque are integrated over the body surface are listed below:

$$\begin{split} I_{i|}^{(1,0)} &= 0 \\ I_{|j}^{(0,1)} &= S^{3/2}c^{(0,1)}N_j \\ I_{i_1i_2|}^{(2,0)} &= S\left[\frac{1}{3}\delta_{i_1i_2} + c^{(2,0)}N_{< i_1}N_{i_2>}\right] \\ I_{i|j}^{(1,1)} &= S^{3/2}\left[c_1^{(1,1)}\delta_{ij} + c_2^{(1,1)}N_{< i}N_{j>}\right], \\ I_{|j_1j_2}^{(0,2)} &= S^2\left[c_1^{(0,2)}\delta_{j_1j_2} + c_2^{(0,2)}N_{< j_1}N_{j_2>}\right] \\ I_{i_1i_2|j}^{(2,1)} &= S^{3/2}\left[c_1^{(2,1)}\delta_{i_1i_2}N_j + c_2^{(2,1)}\left(\delta_{i_1j}N_{i_2} + \delta_{i_2j}N_{i_1}\right) + c_3^{(2,1)}N_{i_1}N_{i_2}N_j\right] \\ I_{i_1i_2|j_1j_2}^{(2,2)} &= S^2\left[c_1^{(2,2)}\delta_{i_1i_2}\delta_{j_1j_2} + c_2^{(2,2)}\left(\delta_{i_1j_1}\delta_{i_2j_2} + \delta_{i_1j_2}\delta_{i_2j_1}\right) + c_3^{(2,2)}\delta_{i_1i_2}N_{j_1}N_{j_2} + c_4^{(2,2)}\delta_{j_1j_2}N_{i_1}N_{i_2} \\ &+ \delta_{i_1j_2}N_{i_2}N_{j_1} + \delta_{i_2j_1}N_{i_1}N_{j_2} + \delta_{i_2j_2}N_{i_1}N_{j_1}\right] + c_6^{(2,2)}N_{i_1}N_{i_2}N_{j_1}N_{j_2} \end{split}$$

The coefficients $c_n^{(k,l)}$ in the expressions above are given by

$$c^{(0,1)} = \mathcal{J}_{2}$$

$$c^{(2,0)} = \frac{1}{2} (3\mathcal{J}_{1} - 1)$$

$$c^{(1,1)}_{1} = \frac{1}{3}\mathcal{J}_{2}$$

$$c^{(1,1)}_{2} = \frac{1}{2} (3\mathcal{J}_{3} - \mathcal{J}_{2})$$

$$c^{(0,2)}_{1} = \frac{1}{3}\mathcal{J}_{5}$$

$$c^{(0,2)}_{2} = \frac{1}{2} (3\mathcal{J}_{7} - \mathcal{J}_{5})$$

$$c^{(2,1)}_{1} = \frac{1}{2} (\mathcal{J}_{2} - \mathcal{J}_{4})$$

$$c^{(2,1)}_{2} = \frac{1}{2} (\mathcal{J}_{3} - \mathcal{J}_{4})$$

$$c^{(2,1)}_{3} = \frac{1}{2} (-2\mathcal{J}_{2} - 2\mathcal{J}_{3} + 5\mathcal{J}_{4})$$

$$c^{(2,1)}_{3} = \frac{1}{8} (-3\mathcal{J}_{4} + 17\mathcal{J}_{5} + 2\mathcal{J}_{6} - 8\mathcal{J}_{7} - 3\mathcal{J}_{8} + \mathcal{J}_{9})$$

$$c^{(2,2)}_{1} = \frac{1}{8} (2\mathcal{J}_{5} - 2\mathcal{J}_{6} - 3\mathcal{J}_{7} - 3\mathcal{J}_{8} + 4\mathcal{J}_{9} + \mathcal{J}_{10})$$

$$c^{(2,2)}_{2} = \frac{1}{8} (-\mathcal{J}_{5} + 2\mathcal{J}_{6} + \mathcal{J}_{7} + \mathcal{J}_{8} - 4\mathcal{J}_{9} + \mathcal{J}_{10})$$

$$c^{(2,2)}_{3} = \frac{1}{8} (-3\mathcal{J}_{5} + 2\mathcal{J}_{6} + 7\mathcal{J}_{7} + 3\mathcal{J}_{8} - 4\mathcal{J}_{9} - 5\mathcal{J}_{10})$$

$$c^{(2,2)}_{4} = \frac{1}{8} (-3\mathcal{J}_{5} + 2\mathcal{J}_{6} + 3\mathcal{J}_{7} + 7\mathcal{J}_{8} - 4\mathcal{J}_{9} - 5\mathcal{J}_{10})$$

$$c^{(2,2)}_{5} = \frac{1}{8} (-\mathcal{J}_{5} - 2\mathcal{J}_{6} - \mathcal{J}_{7} - \mathcal{J}_{8} - 8\mathcal{J}_{9} - 5\mathcal{J}_{10})$$

$$c^{(2,2)}_{6} = \frac{1}{8} (\mathcal{J}_{5} + 2\mathcal{J}_{6} - 5\mathcal{J}_{7} - 5\mathcal{J}_{8} - 5\mathcal{J}_{9} + 35\mathcal{J}_{10})$$

In these coefficients the integrals $\mathcal{J}_1 - \mathcal{J}_{10}$ are given by

Integrals

Integrals
$$\mathcal{J}_{1} = S^{-1} \int_{S} (\boldsymbol{N} \cdot \boldsymbol{n})^{2} dS$$

$$\mathcal{J}_{2} = S^{-3/2} \int_{S} \boldsymbol{x} \cdot \boldsymbol{N} dS$$

$$\mathcal{J}_{3} = S^{-3/2} \int_{S} (\boldsymbol{x} \cdot \boldsymbol{n}) (\boldsymbol{n} \cdot \boldsymbol{N}) dS$$

$$\mathcal{J}_{4} = S^{-3/2} \int_{S} (\boldsymbol{x} \cdot \boldsymbol{N}) (\boldsymbol{n} \cdot \boldsymbol{N})^{2} dS$$

$$\mathcal{J}_{5} = S^{-2} \int_{S} \boldsymbol{x}^{2} dS$$

$$\mathcal{J}_{6} = S^{-2} \int_{S} (\boldsymbol{x} \cdot \boldsymbol{n})^{2} dS$$

$$\mathcal{J}_{7} = S^{-2} \int_{S} (\boldsymbol{x} \cdot \boldsymbol{N})^{2} dS$$

$$\mathcal{J}_{8} = S^{-2} \int_{S} \boldsymbol{x}^{2} (\boldsymbol{n} \cdot \boldsymbol{N})^{2} dS$$

$$\mathcal{J}_{9} = S^{-2} \int_{S} (\boldsymbol{x} \cdot \boldsymbol{n}) (\boldsymbol{x} \cdot \boldsymbol{N}) (\boldsymbol{n} \cdot \boldsymbol{N}) dS$$

$$\mathcal{J}_{10} = S^{-2} \int_{S} (\boldsymbol{x} \cdot \boldsymbol{N})^{2} (\boldsymbol{n} \cdot \boldsymbol{N})^{2} dS$$

In the following table, the values of the coefficients $a_1..a_8$ and there resp. equatorial symmetry (E.S.) are listed:

Coefficient	Value	$\mathbf{E.S.}$
a_1	$\frac{1}{6} \left(4 - 3\alpha_{\tau}\right) \left(3\mathcal{J}_{1} - 1\right)$	+
a_2	$\frac{1}{6}\left(8+\pi\alpha_{ au} ight)$	+
a_3	$\frac{1}{4} \left[8 - (6 - \pi) \alpha_{\tau} \right] (3\mathcal{J}_1 - 1)$	+
a_4	$\frac{1}{12} \left\{ \left[8 + (\pi - 2) \alpha_{\tau} \right] \mathcal{J}_2 - \left[8 - (6 - \pi) \alpha_{\tau} \right] \mathcal{J}_3 \right\}$	_
a_5	$\frac{1}{6}[(4-lpha_{ au})\mathcal{J}_2-(4-3lpha_{ au})\mathcal{J}_3]$	_
a_6	$\frac{1}{12} \left\{ \left[8 + (\pi - 2) \alpha_{\tau} \right] \mathcal{J}_2 - \left[8 - (6 - \pi) \alpha_{\tau} \right] \mathcal{J}_3 \right\}$	_
a_7	$\frac{1}{12} \left\{ \left[8 + (\pi - 2) \alpha_{\tau} \right] \mathcal{J}_5 - \left[8 - (6 - \pi) \alpha_{\tau} \right] \mathcal{J}_6 \right\}$	+
a_8	$\frac{1}{8} \{ [16 - (10 - 2\pi) \alpha_{\tau}] \mathcal{J}_5 - [16 - (12 - 2\pi) \alpha_{\tau}] \mathcal{J}_6 \}$	
	$-[24-(12-3\pi)\alpha_{\tau}]\mathcal{J}_{7}-[24-(18-3\pi)\alpha_{\tau}]\mathcal{J}_{8}$	
	$+ [48 - (36 - 6\pi) \alpha_{\tau}] \mathcal{J}_9 $	+

The tensor of inertia, I_{ij} , is conveniently expressed according to (30) with the choice

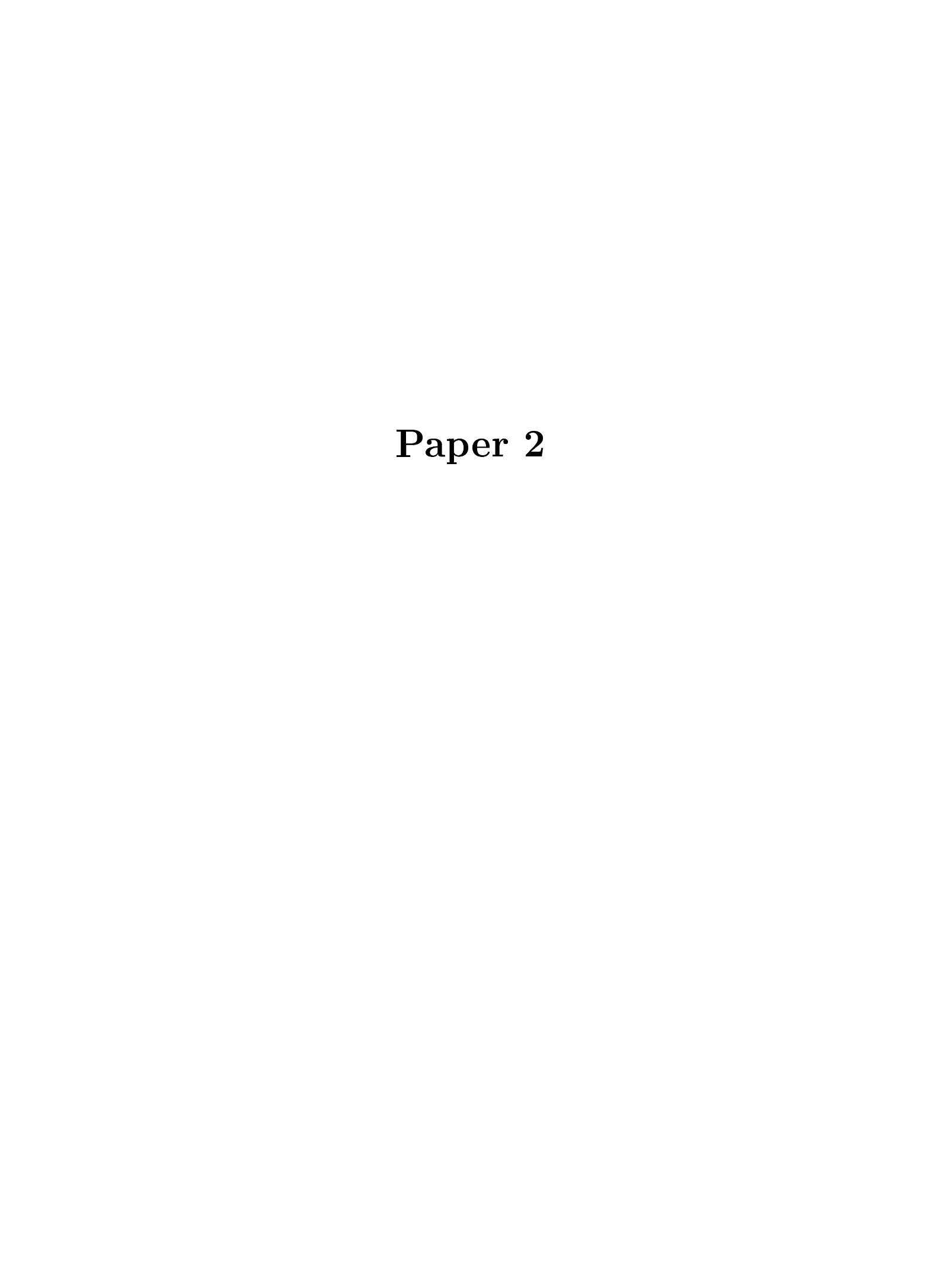
$$I_0 \equiv m_B S$$
,

and the coefficients \mathcal{B}_1 and \mathcal{B}_2 become

$$B_1 = rac{2}{3m_B S} \int_V
ho(m{x}) m{x}^2 \mathrm{d}^3 x, \ B_2 = rac{1}{2m_B S} \int_V
ho(m{x}) \left[m{x}^2 - 3(m{N}\cdotm{x})^2
ight] \mathrm{d}^3 x.$$

References

- [1] Sone, Y., Flows induced by temperature fields and their ghost effect on the behavior of a gas in the continuum limit. Ann. Rev. Fluid Mech., pp 779-811, 2000.
- [2] Talbot, L., Rarefied Gas Dynamics, ed. SS Fisher, Part I, pp 467-88. New York: AIAA, 1981.
- [3] Waldmann, L., Z. Naturforsch. 14a, 589. (1959).
- [4] Sone, Y. and Aoki, K., (1981) $Rarefied\ Gas\ Dynamics\ ed.$ SS Fisher, Part I, pp 489-503.
- [5] Yalamov, Yu. I., Chermoshentsev, A. V., and Chermoshentseva O. F., Thermophoresis of a Moderately Large Aerosol Particle Having a Slightly Deformed Spherical Shape. High Temperature, Vol. 35, No. 3, pp 425-431 (1997).
- [6] Kogan, N. M., Rarefied Gas Dynamics, New York: Plenum Press (1969).



Shearing Phoresis

By Lars H. Söderholm and Karl I. Borg

Department of Mechanics Royal Institute of Technology 100 44 Stockholm, Sweden

An axially symmetric body small compared with the mean free path is free to move in a shearing gas. The body is treated as a test particle. The force and torque acting on the body are calculated. The body will be set in motion, which asymptotically will take place in one of the eigendirections of the rate of deformation tensor. The axis of the body then points in the same direction. For a velocity field $v_x(y)$ the final motion is parallel to one of the lines x = y and x = -y, and the speed of the motion relative to the gas is given by

$$V = \frac{9\beta_N}{8} \sqrt{\frac{2\pi k_B T}{m}} \frac{\alpha_\tau b_1}{4 + \frac{1}{2}\pi \alpha_\tau + [8 - (6 - \pi \alpha_\tau)]b_3} \frac{\mu v_{x,y}}{p}.$$

Here μ is the viscosity of the gas, p is the pressure, β_N is a number close to unity, T is the temperature, m is the mass of a gas molecule, and α_{τ} is the accommodation coefficient of tangential momentum. The non-dimensional numbers b_1 and b_3 depend on the shape of the body. This speed is of the order of the mean free path of the gas multiplied by the shearing. -This means that there is a phenomenon of phoresis in a shearing gas, which is analogous to thermophoresis in a gas with a temperature gradient.

1. Introduction

Thermophoresis is a widely studied phenomenon. There are three length scales: that of the body, that of the mean free path and that of the temperature field of the gas. The assumption is made that the mean free path of the gas is much smaller than the length scale of the temperature field. So this phenomenon is characterised by two small parameters.

For small Knudsen numbers, however, there are two basic deformations of the local Maxwellian. One from a temperature gradient and one from shearing. In an earlier paper of one of the authors, [1], the influence of shearing on the heat transfer to a body was studied. It was found there, that due to the tensorial nature of the shearing, shearing did not influence the heat transfer to a spherical body, so bodies of arbitrary symmetry were considered. It was found that the equilibrium temperature of an axially symmetric small body was influenced by the shearing and thus was different from that of the surrounding gas.

In an other work by the present authors, [2], thermophoresis was studied for axially symmetric bodies and also their full rigid body motion.

In the present work, focus is again on the influence of shearing on axially symmetric bodies. But now force and torque on the body exerted by the surrounding gas are calculated. It is found that there is a motion, a phoresis, in a shearing gas, which is analogous to that of thermophoresis. It vanishes for bodies, which are mirror symmetric with respect to a plane perpendicular to the axis of symmetry of the body, in particular for spheres. We name this motion shearing phoresis. It is found that there will be a resulting slow transport of the particles relative to the gas. It takes place in the direction of one of the eigenvectors of the traceless rate of deformation tensor. The axis of symmetry of the body lines up with the direction of the velocity of the body. In the case of a simple shearing, where $v_x(y)$ is the only non-vanishing component of the velocity field of the surrounding gas, the resulting motion is either parallel to the line x = y, or parallel to the line x = -y, depending on the shape of the body.

A phenomenon of transverse diffusion of spherical particles in a shear layer is described in [3]. This phenomenon occurs in a dilute suspension of particles only if the particles are interacting. The mechanism described in the present work is an entirely different one.

In this work the problem will be approached in the way outlined by Waldmann in [4]. Thus the method of free molecular flow is applied, which means that the body is small enough for the molecules incident on the body surface to be unaffected by the presence of the body. Thus one can express the total momentum conveyed to the body from the distribution function for the incoming molecules only.

2. The distribution function of the shearing gas

We consider a convex high conductivity body, small compared to the mean free path of the gas. The gas is subjected to a velocity gradient. As a consequence the small body will start to move. This means that the velocity of a point in the body will be given by $u' = u + \omega \times x$, where u is the velocity of the body's center of mass, ω is the angular velocity of the body and x is the vector from the body's center of mass to the point under consideration. As the interaction between the gas and the body is mediated through the body surface, it is convenient to take the motion of a body surface element into account by transforming the distribution function to a frame of reference where the surface element is momentarily at rest. In this frame, the gas is flowing with the velocity -u'. In the absence of the shearing, to zeroth order in the mean free path, the distribution function is thus given by the Maxwellian

$$f_0(-\boldsymbol{u'}) = n \left(rac{2\pi k_B T}{m}
ight)^{-3/2} e^{-m(\boldsymbol{c} + \boldsymbol{u'})^2/2k_B T}.$$

Here n is the number density of the gas, k_B is Boltzmann's constant, T is the gas temperature, m is the mass of a gas molecule, and c is the velocity of a gas molecule. Now the assumption that the speed |u'| is much smaller than the speed of sound is made (this assumption will be consistent with our results for the final speed of the body), and thus the distribution function can be approximated by

$$f_0(-\boldsymbol{u}') \approx f_0(\boldsymbol{0}) \left[1 + \phi_{(\text{flow})} \right],$$

where

$$\phi_{ ext{(flow)}} = -rac{m}{k_B T} m{c} \cdot m{u'}$$

has been introduced for convenience. In what follows $f_0(\mathbf{0})$, the Maxwellian at rest, will be denoted by f_0 .

To first order in the mean free path, the distribution function for the gas molecules can then be written [5]

$$f = f_0(-\mathbf{u'})[1 + \phi_{(\text{shear})}],$$

where $\phi_{(\text{shear})}$ is given by the first-order Chapman-Enskog solution to Boltzmann's equation for a shearing gas. $\phi_{(\text{shear})}$ has the explicit form [5]

$$\phi_{\text{(shear)}} = -\frac{2\mu}{p} \hat{B}(\mathcal{C}^2) \mathcal{C}_{\langle i} \mathcal{C}_{j\rangle} v_{\langle i,j\rangle},\tag{1}$$

where the nondimensional molecular velocity $C_i \equiv \sqrt{m/2k_BT}c_i$ has been introduced. Under these circumstances one can also omit the cross-effect between the shearing and the homogeneous flow, and thus

$$f = f_0 \left[1 + \phi_{\text{(shear)}} + \phi_{\text{(flow)}} \right]. \tag{2}$$

In this expression, < ... > denotes the symmetric and traceless part. The scalar function $\hat{B}(\mathcal{C}^2)$ is usually expanded in Sonine polynomials. It is normalised so that $\hat{B}=1$ if only the first term in the Sonine expansion is retained.

3. The force exerted by the gas on a body surface element

We shall now calculate a general expression for the net force exerted by the surrounding gas on a resting surface element $dS_i = n_i dS$. Here n_i is the unit outward normal of the surface element. This force is given by the difference of the momentum brought to the surface element by the incident stream of gas molecules and the momentum carried out by the reflected stream, and can be written

$$dF_k = \left[P_k^{(i)} - P_k^{(r)} \right] dS, \tag{3}$$

where the momentum flux incident on the surface element $P_k^{(i)}$ is given by

$$P_k^{(i)} = -\int_{c_j n_j < 0} m c_k c_j n_j f^{(i)} d^3 c.$$
 (4)

If the surrounding gas is described by a resting Maxwellian distribution, $P_k^{(i)}$ takes the value $-P_M n_i$, where

$$P_M = \frac{1}{2}nk_BT. (5)$$

The momentum flux carried out by reflected molecules $P_k^{(r)}$ is given by

$$P_k^{(\mathbf{r})} = \int_{c_j n_j > 0} m c_k c_j n_j f^{(\mathbf{r})} d^3 c.$$
 (6)

Here, $f^{(i)}$ and $f^{(r)}$ are the distribution functions of the stream of molecules incident and reflected on the surface element. Since the body is small compared to the mean free path of the gas, and as the body is convex, the incident stream of molecules can be approximated by the distribution function describing the gas in the absence of the body, that is, $f^{(i)} = f$. The reflected stream of gas molecules is given by Maxwell's boundary condition, cf Kogan [6]. One part is specularly reflected (that is, reflected like a particle hitting elastically a solid wall). The remaining part has reached thermal equilibrium with the surface, and is reflected as a Maxwellian. Thus we have

$$f^{(r)}(\boldsymbol{c}) = (1 - \alpha_{\tau}) f^{(i)}(\boldsymbol{c} - 2(\boldsymbol{c} \cdot \boldsymbol{n}) \boldsymbol{n})$$
$$+ \alpha_{\tau} n^{(w)} \left(\frac{2\pi k_B T^{(w)}}{m} \right)^{-3/2} \exp\left(-\frac{mc^2}{2k_B T^{(w)}} \right). \tag{7}$$

The number α_{τ} is called the accommodation coefficient of tangential momentum, and measures the fraction of the reflected stream that is diffusely reflected. If $\alpha_{\tau}=0$, there is no transfer of tangential momentum between the gas molecules and the surface element. $T^{(\mathrm{w})}$ is the temperature of the surface of the body. The unknown number density $n^{(\mathrm{w})}$ can be determined from the condition that the net particle flux through the surface vanishes, that is, $0=N^{(\mathrm{i})}-N^{(\mathrm{r})}$, where the incident particle flux $N^{(\mathrm{i})}$ is given by

$$N^{(i)} = -\int_{c_j n_j < 0} c_j n_j f^{(i)} d^3 c.$$
 (8)

For a Maxwellian distribution at rest $N^{(i)}$ takes the value

$$N_M = n\sqrt{\frac{k_B T}{2\pi m}}. (9)$$

The reflected particle flux $N^{(r)}$ is found from (7) to be

$$N^{(r)} = (1 - \alpha_{\tau}) N^{(i)} + \alpha_{\tau} N_M^{(w)}, \tag{10}$$

where $N_M^{(w)}$ is given by (9) but with wall-values of T and n. Therefore, due to conservation of gas molecules at the surface, $n^{(w)}$ fulfils

$$N^{(i)} = n^{(w)} \sqrt{\frac{k_B T^{(w)}}{2\pi m}}.$$
 (11)

We are now in a position to calculate the net momentum flux transferred to the surface element according to (3). In the case of pure specular reflection, it is given by $2n_k n_j P_j^{(i)}$. In case of purely diffuse reflection, the corresponding momentum can be written $P_M^{(w)} n_i$, where $P_M^{(w)}$ is (5) with wall-values of T and n. $P_M^{(w)}$ can be expressed according to

$$P_M^{(\mathrm{w})} = \sqrt{rac{T^{(\mathrm{w})}}{T}} rac{N^{(\mathrm{i})}}{N_M} P_M.$$

Here, (11) has been used. The force on the surface element (3) can thus be written

$$dF_k = \left[(1 - \alpha_\tau) 2n_k n_j P_j^{(i)} + \alpha_\tau \left(P_k^{(i)} - \sqrt{\frac{T^{(w)}}{T}} \frac{N^{(i)}}{N_M} P_M n_k \right) \right] dS.$$
(12)

The first term is the momentum transferred to the body from the specularly reflected stream. The second term, $\alpha_{\tau}P_k^{(i)}$, is the part of the incident momentum to be reflected diffusely. The last term is the momentum carried out from the surface by the diffusely reflected stream. Note that N_M and P_M depend on the gas parameters only. The influence of the wall is collected in $T^{(w)}$. In what follows the approximation $T^{(w)} \approx T$ will be used. This will be justified in Section 11.

4. Particle and momentum fluxes

Now the splitting of the distribution function (2) is used and the particle and momentum fluxes incident on a body surface element with unit outward normal n given by (8) and (4) are calculated. The contributions to these from the resting Maxwellian have already been calculated and are given by (9) and (5)

Now the contribution to the particle flux incident on a body surface element from the shearing is calculated:

$$\begin{split} N_{(\mathrm{shear})}^{(\mathrm{i})} &= \frac{4\mu}{\pi p} \int_{\mathcal{C}_{i} n_{i} < 0} \mathcal{C}_{k} n_{k} \hat{B}(\mathcal{C}^{2}) e^{-\mathcal{C}^{2}} \mathcal{C}_{< i} \mathcal{C}_{j>} \mathrm{d}^{3} \mathcal{C} v_{< i, j>} \\ &\equiv \frac{4\mu}{\pi p} I_{< ij>} v_{< i, j>}. \end{split}$$

From symmetry,

$$I_{\langle ij \rangle} = I_1 n_{\langle i} n_{j \rangle},$$

where I_1 is a scalar integral. Using spherical coordinates, one finds

$$I_1 = \int_{\mathcal{C}_i n_i < 0} \mathcal{C}_k n_k \hat{B}(\mathcal{C}^2) e^{-\mathcal{C}^2} \mathcal{C}_{< i} \mathcal{C}_{j>} n_{< i} n_{j>} \mathrm{d}^3 \mathcal{C} = -\frac{\pi}{6} \beta_N.$$

Here

$$\beta_N \equiv \int_0^\infty \mathcal{C}^5 \hat{B}(\mathcal{C}^2) e^{-\mathcal{C}^2} d\mathcal{C} = \frac{1}{2} \int_0^\infty x^2 \hat{B}(x) e^{-x} dx. \tag{13}$$

If $\hat{B}(x)$ is expanded in Sonine polynomials and only the first term is retained, $\beta_N = 1$. Thus the shearing contribution to (8) takes the form

$$N_{\text{(shear)}}^{(i)} = -\beta_N \frac{\mu}{\sqrt{2\pi m k_B T}} n_{< i} n_{j>} v_{< i, j>}.$$
 (14)

When calculating the momentum flux one finds that the shearing contribution to the influx of momentum (4) is proportional to

$$\int_{\mathcal{C}_j n_j < 0} \mathcal{C}^4 \hat{B}(\mathcal{C}^2) e^{-\mathcal{C}^2} d^3 \mathcal{C}. \tag{15}$$

Due to the definition of temperature, which is given by the total kinetic energy of the gas molecules, the Chapman-Enskog solution [5] fulfils

$$0 = \int rac{1}{2} m \mathcal{C}^2 f_0 \phi_{
m (shear)} {
m d}^3 \mathcal{C},$$

which means that the integral (15) vanishes. Thus the shearing does not contribute to the momentum flux (to this order).

4.2. Fluxes from the homogeneous flow

For the homogeneous flow the incident particle flux (8) becomes

$$N_{(\text{flow})}^{(i)} = \frac{n}{2} n_i u_i' \tag{16}$$

Similarly, the incident momentum flux (4) is given by

$$P_{(\text{flow})k}^{(i)} = -p\sqrt{\frac{m}{2\pi k_B T}} \left(\delta_{kj} + n_k n_j\right) u_j'. \tag{17}$$

Having obtained the fluxes, the total force on a surface element according to (12) can be calculated.

5. Force and torque on the body

The fluxes (14), (16) and (17) are now substituted into (12), and one gets three different contributions to the force on the surface element of the body:

$$dF_i = -pn_i dS + \frac{1}{2} \mu \alpha_\tau \beta_N n_i n_{\langle j} n_{k \rangle} v_{\langle j,k \rangle} dS$$
(18)

$$-\sqrt{\frac{m}{2\pi k_B T}} p \left\{ \alpha_{\tau} u_i' + \left[4 - \left(3 - \frac{\pi}{2} \right) \alpha_{\tau} \right] u_j' n_j n_i \right\} dS$$

The first force stems from the resting Maxwellian, the second from the shearing and the third from the homogeneous flow.

The object of this section is to integrate the force over the surface of an axially symmetric body, for which we denote the axis of symmetry N. In addition, the gas will in general also produce a torque acting on the body. For this purpose, we introduce a frame of reference with the origin at the center of mass of the body. The torque then becomes (here ϵ_{ijk} is the totally antisymmetric permutation pseudotensor, with $\epsilon_{123} = 1$)

$$dM_i = \epsilon_{ijk} x_j dF_k. \tag{19}$$

Here, \boldsymbol{x} is the position vector of the surface element with the normal \boldsymbol{n} in this frame. Integrated over the surface of the body it gives the total torque.

To calculate the force and torque, several purely geometrical tensor integrals of the type

$$\int_{S} n_{i_1} n_{i_2} ... n_{i_k} x_{j_1} x_{j_2} ... x_{j_l} dS \equiv I_{i_1 i_2 ... i_k | j_1 j_2 ... j_l}^{(k,l)}$$

have to be performed. Their tensorial features can be found from symmetry and isotropy, and the scalar coefficients are found by successively forming contractions with δ_{ij} or N_i . They are listed in the appendix.

It is well known that a gas at equilibrium will not exert forces or torques on a resting body. This is easy to show: The Maxwellian contribution, $-pn_i\mathrm{d}S$, is proportional to n. Since the surface of the body, S, is closed, the force vanishes when it is integrated over the surface of the body. The corresponding torque acting on the surface element is proportional to $x \times n$. By virtue of Gauss' theorem, the integrated torque also vanishes. Thus the resting Maxwellian does not exert forces or torques on the body. We will now proceed to calculate the forces from the shearing and from the homogeneous flow.

5.1. Force and torque from the shearing

The force due to the shearing becomes

$$F_{\text{(shear)}i} = \frac{1}{2}\mu\alpha_{\tau}\beta_{N} \int_{S} n_{i}n_{} dSv_{}$$

$$\equiv \frac{1}{2}\mu\alpha_{\tau}\beta_{N}J_{ijk}v_{}, \tag{20}$$

where the tensor integral J_{ijk} is given by

$$J_{ijk} = \int_{S} n_i n_j n_k \mathrm{d}S$$

and must therefore be proportional to the body surface area. From isotropy, and since all traces vanish, one can write

$$J_{ijk} = -rac{1}{2}Sb_1\left(\delta_{ij}N_k + \delta_{ik}N_j + \delta_{jk}N_i - 5N_iN_jN_k
ight),$$

where S is the body's surface area. The factor -1/2 is chosen for convenience. Contracting with $N_i N_j N_k$ one finds

$$b_1 = \frac{1}{S} \int_S (\boldsymbol{n} \cdot \boldsymbol{N})^3 \, \mathrm{d}S.$$

Note that $b_1 = 0$ if there exists a plane orthogonal to the axis N in which the body is mirror symmetric. The force (20) becomes, since $v_{\langle j,k\rangle}$ is symmetric and traceless,

$$F_{(\text{shear})}$$

$$= -\frac{1}{12} \mu \alpha_{\tau} \beta_{N} S b_{1} \left(\delta_{ij} - 15 N_{\langle i} N_{j \rangle} \right) v_{\langle j,k \rangle} N_{k}. \tag{21}$$

Using the previously obtained expression for the force from the shearing (18) the corresponding torque (19) is integrated and the total torque due to the shearing acting on the body becomes

$$M_{(\text{shear})i} = \frac{1}{2} \mu \alpha_{\tau} \beta_N S^{3/2} b_2 \epsilon_{ijk} N_j v_{\langle k,l \rangle} N_l.$$
 (22)

The coefficient b_2 is a scalar integral given in appendix. Note that b_2 , in contrast to b_1 , does not in general vanish if the surface is mirror symmetric in a plane orthogonal to the axis of symmetry.

5.2. Force and torque from the homogeneous flow

Again, integration over the surface is performed in the way described above. Now the transformation to the frame where the gas is at rest is made, in which the body is in motion. The force and the torque are invariants under this transformation. In terms of the velocity of the body's center of mass u and the angular velocity of the body, ω , one gets the force and the torque due to the motion of the body (c.f. [2])

$$F_{\text{(flow)} i} = \sqrt{\frac{m}{2\pi k_B T}} \left[-pS \left(a_1 \delta_{ij} + a_2 N_{< i} N_{j>} \right) u_j + 3pS^{3/2} a_3 \epsilon_{ijk} N_j \omega_k \right],$$

$$M_{\text{(flow)} i} = \sqrt{\frac{m}{2\pi k_B T}} \left[-3pS^{3/2} a_3 \epsilon_{ijk} N_j v_k - \frac{pS^2}{2} \left(a_4 \delta_{ij} + a_5 N_{< i} N_{j>} \right) \omega_j \right].$$
(23)

The coefficients $a_1..a_5$ are listed in the appendix.

6. Equations of motion

To formulate the equations of motion of the system, the body mass m_B and the tensor of inertia I_{ij} are introduced. The latter is written

$$I_{ij} = m_B S \left(I_1 \delta_{ij} + I_2 N_{< i} N_{j>} \right).$$

Here the coefficients I_1 , I_2 are dimensionless moments of inertia. They are given in Appendix. Further, we introduce a body-fixed orthonormal frame of reference with the origin in the body's center of mass. The basis vectors are denoted by $e^{(\alpha)}$ where the index $\alpha = 1, 2, 3$ numbers the basis vectors. One of these basis vectors is naturally chosen to coincide with the axis of symmetry N. The basis vectors of the body fixed frame move according to Euler's kinematic equations

$$\frac{\mathrm{d}\boldsymbol{e}^{(\alpha)}}{\mathrm{d}t} = \boldsymbol{\omega} \times \boldsymbol{e}^{(\alpha)}$$

Further, Newton's second law now gives (c.f. Goldstein [7]), with the forces calculated in the previous section,

$$m_B \frac{\mathrm{d}u_i}{\mathrm{d}t} = -\frac{1}{12} \mu \alpha_\tau \beta_N Sb_1 \left(\delta_{ij} - 15N_{< i} N_{j>} \right) v_{< j,k>} N_k$$

$$+\sqrt{\frac{m}{2\pi k_B T}} \left[-pS \left(a_1 \delta_{ij} + a_2 N_{< i} N_{j>} \right) u_j + 3pS^{3/2} a_3 \epsilon_{ijk} N_j \omega_k \right]. \tag{25}$$

73

The other equation needed, giving the time derivative as the angular momentum as the torque, is Euler's equation (see Goldstein [7])

$$I_{ij} \frac{\mathrm{d}\omega_{j}}{\mathrm{d}t} + \epsilon_{ijk}\omega_{j}I_{kl}\omega_{l} = \frac{1}{2}\mu\alpha_{\tau}\beta_{N}S^{3/2}b_{2}\epsilon_{ijk}N_{j}u_{\langle k,l\rangle}N_{l} + \sqrt{\frac{m}{2\pi k_{B}T}} \left[-3pS^{3/2}a_{3}\epsilon_{ijk}N_{j}u_{k} - \frac{pS^{2}}{2} \left(a_{4}\delta_{ij} + a_{5}N_{\langle i}N_{j\rangle} \right) \omega_{j} \right\}.$$

$$(26)$$

7. Stationary solutions

A first attempt to understand the equations of motion is provided by seeking a stationary solution. For this solution, the assumptions $\omega = \mathbf{0}$ and a constant velocity \mathcal{U} are made. From the equations (25), (26) one then gets the system

$$\begin{cases} 0 = -\frac{1}{12}\mu\alpha_{\tau}\beta_{N}b_{1}\left(\delta_{ij} - 15N_{< i}N_{j>}\right)v_{< j,k>}N_{k} \\ -\sqrt{\frac{m}{2\pi k_{B}T}}p\left(a_{1}\delta_{ij} + a_{2}N_{< i}N_{j>}\right)U_{j} \\ 0 = \epsilon_{ijk}N_{j}\left[\frac{1}{2}\mu\alpha_{\tau}\beta_{N}b_{2}v_{< k,l>}N_{l} - 3\sqrt{\frac{m}{2\pi k_{B}T}}pa_{3}U_{k}\right] \end{cases}$$

From the second of these equations, one can see that the sum within the square brackets must be parallel to N_k . Hence the vector $v_{\langle i,j\rangle}N_j$ must be a linear combination of N_i and U_i . This result is substituted into the first equation, and one finds that \mathcal{U} is parallel with N. Using again the second equation, it is apparent the vectors $v_{\langle i,j\rangle}N_j$ and N_i are parallel, that is, N is an eigenvector of $v_{\langle i,j\rangle}$. We conclude that

$$U_{i} = \frac{9\mu\beta_{N}}{4p}\sqrt{\frac{2\pi k_{B}T}{m}}\frac{\alpha_{\tau}b_{1}}{4 + \frac{1}{2}\pi\alpha_{\tau} + [8 - (6 - \pi\alpha_{\tau})]b_{3}}lN_{i}.$$
(27)

Here, the the values of a_1 and a_2 from appendix have been inserted. In this expression, N coincides with an eigenvector of the traceless rate of deformation tensor $v_{\langle i,j\rangle}$, and l is the corresponding eigenvalue. For a velocity field with only one non-vanishing component, $v_x(y)$, there are two eigenvectors with non-vanishing eigenvalues of the corresponding traceless rate-of-deformation tensor. The eigenvectors are $(\pm \boldsymbol{e}_x + \boldsymbol{e}_y)/\sqrt{2}$, and the corresponding eigenvalues $l = \pm v_{x,y}/2$, respectively.

In the expression for the stationary velocity (27), the purely geometrical parameter b_3 , given by, see appendix,

$$b_3 \equiv \frac{3}{2S} \int_S \left[(\boldsymbol{n} \cdot \boldsymbol{N})^2 - \frac{1}{3} \right] dS, \tag{28}$$

depends on the shape of the body: For a coin shaped body, or an extremely oblate body, $b_3 = 1$. For needle shape, or an extremely prolate body, $b_3 = -1/2$. For a sphere, $b_3 = 0$.

As mentioned earlier, b_1 is given by

$$b_1 = rac{1}{S} \int_S \left(m{n} \cdot m{N}
ight)^3 \mathrm{d}S.$$

We recall that $b_1 = 0$ if the body is mirror symmetric in a plane orthogonal to the axis of symmetry. If the velocity field of the gas is $v_x(y)$, a simple order of magnitude estimate of this velocity is given by, if λ denotes the mean free path of the gas,

$$|\mathcal{U}| \sim \lambda v_{x,y}$$

8. Numerical simulations

8.1. Scaling and nondimensional variables

To obtain numerical solutions to the equations of motion, a time-scale τ is introduced according to

$$\tau = \frac{m_B}{pS} \sqrt{\frac{2\pi k_B T}{m}}. (29)$$

This time scale is obtained from the force proportional to \boldsymbol{u} in (25). For the flow field of the surrounding gas a simple velocity field $v_x(y)$ is considered. For the traceless rate of deformation tensor \mathbf{D} the only non-vanishing components then become

$$v_{\langle x,y\rangle} = v_{\langle y,x\rangle} = \frac{1}{2}v_{x,y}. (30)$$

The corresponding eigendirections are the lines $x = \pm y$ with the corresponding eigenvalues $l = \pm v_{x,y}/2$.

To form a non-dimensional shearing tensor, we write

$$D_{ij}^* = 2v_{\langle i,j \rangle}/|v_{x,y}|.$$

The eigenvalues of this non-dimensional shearing are given by $l_{\pm}^* = \pm 1$. Further, a non-dimensional tensor of inertia is introduced according to $I_{ij}^* = I_{ij}(m_B S)^{-1}$.

It is convenient to chose the velocity scale V from the stationary speed, as

$$V = \frac{9\beta_N}{8} \sqrt{\frac{2\pi k_B T}{m}} \frac{\mu v_{x,y}}{p}.$$

The dimensionless variables $t^*, v_i^*, x_i^*, \omega_i^*$ are now defined by

$$t = \tau t^*, \ u_i = V u_i^*, \ x_i = V \tau x_i^* \ \omega_i = \tau^{-1} \omega_i^*.$$

In what follows, the *-superscript will be skipped. With this choice, the dimensionless equations of motion take the form

$$\begin{split} \frac{\mathrm{d}u_{i}}{\mathrm{d}t} &= -\frac{1}{27}\alpha_{\tau}b_{1}\left(\delta_{ij} - 15N_{< i}N_{j>}\right)D_{jk}N_{k} \\ &- \left(a_{1}\delta_{ij} + a_{2}N_{< i}N_{j>}\right)u_{j} + \mathcal{D}a_{3}\epsilon_{ijk}N_{j}\omega_{k}, \end{split}$$

and

$$I_{ij} \frac{\mathrm{d}\omega_j}{\mathrm{d}t} + \epsilon_{ijk}\omega_j \hat{I}_{kl}\omega_l = \mathcal{D}^{-1} \frac{2}{3}\alpha_\tau b_2 \epsilon_{ijk} N_j D_{kl} N_l$$
$$-\mathcal{D}^{-1} 9 a_3 \epsilon_{ijk} N_j u_k - \frac{1}{2} \left(a_4 \delta_{ij} + a_5 N_{< i} N_{j>} \right) \omega_j.$$

Here the dimensionless number \mathcal{D} is given by

$$\mathcal{D} = rac{8}{3} \left(rac{2\pi k_B T}{m}
ight)^{-1} rac{p^2 S^{3/2}}{m_B eta_N \mu v_{x,y}} \sim rac{p}{\mu v_{x,y}} rac{nm}{
ho}.$$

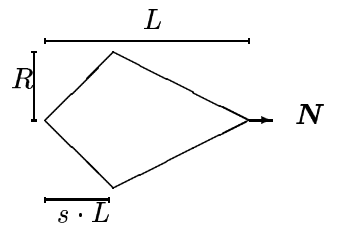
(In this expression, dimensional units are used.) Here n is the number density of the gas, m is the mass of a gas molecule, and ρ is the density of the body. This number is not definitely large or small. In the numerical calculations and in the stability analysis we have unless otherwise indicated, for simplicity chosen $\mathcal{D}=1$. The non-dimensional version of the asymptotic velocity (27) becomes, with the present scaling

$$U_i = \frac{\alpha_\tau b_1}{4 + \frac{1}{2}\pi\alpha_\tau + [8 - (6 - \pi\alpha_\tau)]b_3} lN_i.$$
 (31)

8.2. Orbits of a double cone.

To be specific, we now introduce a geometrically simple body for which the coefficients that depend on the shape can be calculated easily. This body, a 'double cone', is shown in the figure below.

This body is axially symmetric. It is mirror symmetric (with respect to a plane orthogonal to the axis of symmetry) precisely when s = 1/2. This body is homogeneous and consists of two cones with a common base. The radius of the base is denoted by R, and the total length by L. The base is situated a distance sL from the left cusp, where the dimensionless parameter obeys $0 \le s \le 1/2$. N points in the direction of the sharpest cusp of the double cone. When s = 0 the double cone degenerates to a single cone. It should also be pointed out that $b_1 < 0$ when $s \in [0, 1/2]$.



The equations of motion are now solved numerically for the double cone. The figures 1 show the resulting orbits of two different double cones, both with s=1/4, in a gas subject to the simple shearing given by (30). It is obvious from these figures that the asymptotic transport of the blunt double cones takes place parallel the line x=-y, and for the more slender bodies parallel to x=y. It is found that in the final orientation of the blunt double cones, the sharpest cusp is directed parallel to the final velocity, whereas for the slender double cones, the sharpest cusp is directed in the direction opposite to the final velocity. This is in agreement with the expression for the final velocity (27), when $s \in [0,1/2]$. It should also be pointed out that the bodies in the left figure travel in both directions along the line x=y in the right figure. This symmetry stems from the tensor character of the shearing: It is invariant under rotation by an angle of π .

9. Stability analysis

The numerical simulations of the orbits in figure (1) in the previous section suggest that the stability of the double cone depends on the ratio

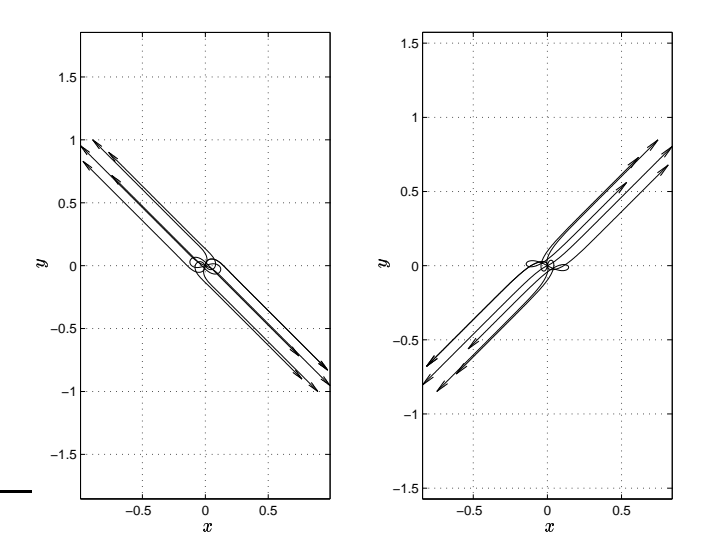


FIGURE 1. In each figure, 10 different orbits of bodies subject to the simple shearing given by (30) are represented for the case $\alpha_{\tau}=1/2$. They all start at t=0 in (x,y)=(0,0). In the left picture, the planar orbits of blunt bodies with R/L=2/5 end up parallel to the line x=-y. In the right picture, the orbits of more slender bodies, with R/L=1/4, finally end up along the line x=y. The initial angle between N and the x-axis is varied between 0 and 2π . The initial velocity is parallel to N, and the initial speed $|u_0|$ is set to approximately one tenth of the corresponding stationary velocity. The initial angular velocity is zero.

R/L. In order to investigate the stability of the orbits close to the lines x=y and x=-y the equations of motion are linearised for the double cone close to these final states. For simplicity, a new coordinate frame $\{x',y',z'\}$ is introduced in which the shearing tensor (30) is diagonal. In this frame, the basis vectors are rotated by an angle $\pi/4$ about the z-axis. In the frame $\{x',y',z'\}$, the x'-axis corresponds to the positive eigenvalue, and the line y'-axis corresponds to the negative eigenvalue.

The Ansatz used for this linearisation close to the asymptotic state along the y'-axis is given by

$$\mathbf{N} = (\epsilon N_{x'}, 1, \epsilon N_{z'}),$$

$$\boldsymbol{u} = \boldsymbol{\mathcal{U}} + (\epsilon v_{x'}, \epsilon v_{y'}, \epsilon v_{z'}),$$

$$\boldsymbol{\omega} = (\epsilon \omega_{x'}, \epsilon \omega_{y'}, \epsilon \omega_{z'}).$$

As $N^2 = 1$, the correction to $N_{y'}$ is of second order. The non-dimensional stationary velocity \mathcal{U} is given by (31). The linearisation close to the x'-axis is made in a similar manner.

The ansatz is now substituted into the equations of motion, and a linear first-order system results for each eigendirection. If one defines the vector \mathbf{w} according to

$$\mathbf{w} = (N_{x'}, N_{z'}, v_{x'}, v_{y'}, v_{z'}, \omega_{x'}, \omega_{y'}, \omega_{z'}),$$

this linear system takes the form

$$\frac{\mathrm{d}\mathbf{w}}{\mathrm{d}t} = \mathbf{L}\mathbf{w},$$

where **L** has been calculated with MAPLE, and is too large to give in explicit form here. **L** is different for the two different asymptotic states, that is, x=y and x=-y. The eigenvalues of the resulting linear systems are calculated for $\alpha_{\tau}=1/2$. The eigenvalues of a slender double cone with R/L=1/4 (cf FIG. 1, right figure) are plotted in figure 2. It is clearly seen that the stability of the body depends on its shape.

The boundary between different stability areas is plotted in the plane spanned by s and R/L in the figure 3.

There exist however cases where none of these states is stable. For small values of \mathcal{D} (heavy body or very rarefied gas), limit cycles appear in the body orbits, see figure 4. Here $s=0.1,\,R/L=0.25,\,\alpha_{\tau}=0.9$ and $\mathcal{D}=10^{-2}$. For these cases, no macroscopic transport will occur due to the shearing. In general, for the cases with linear instability, effects of the heating may be large and produce additional forces and torques on the body. For the orbit in figure 4, however, the timescales are large enough for these effects to be small. This is discussed in the next section.

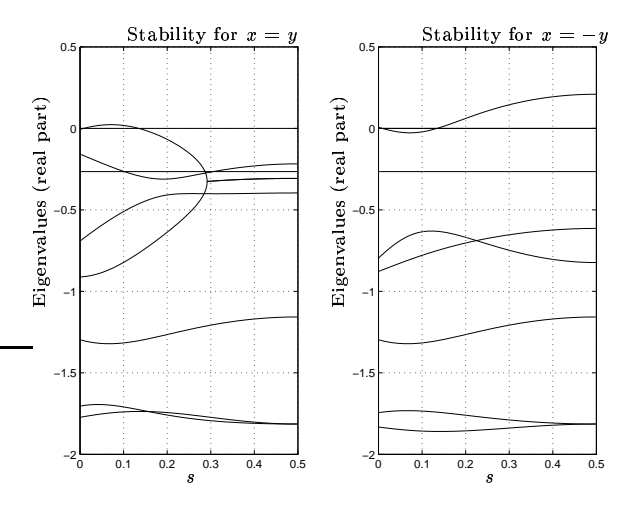


FIGURE 2. In the left figure the real part of the eigenvalues of the linearised equations of motion close to the line x=y are plotted, and in the right figure, the corresponding eigenvalues for x=-y are shown. The scale of eigenvalues on the vertical axes is τ^{-1} . On the horizontal axis, s is varied. It is apparent that the shape of the cone determines the stability. In particular, one critical eigenvalue changes sign as s is varied: For small values of s the line s=-y is the stable one, whereas for larger values of s, the line s=-y is the stable one.

10. Effects of inhomogeneities in the temperature field of the body

(In what follows, dimensional variables are used.) For a body with typical length R and with the heat conductivity κ , the time scale of the heat conduction in the body is given by $c_p\rho R^2/\kappa$, where c_p and ρ are the heat capacity and density of the body. In this case, except for bodies with poor heat conductivity, the heat conduction is much faster than the rate of change in the dynamics close to the stable states. This follows from the magnitude of the eigenvalues close to the stationary states in the previous section together with the assumption of free molecular flow. Thus the stationary heat equation can be used here. This also holds for the limit cycle orbit exposed in figure 4, since the time elapsed during one period is of the order of τ .

Energy is transferred to the body both by the shearing and by the homogeneous flow of the surrounding gas [1]. For example, from the

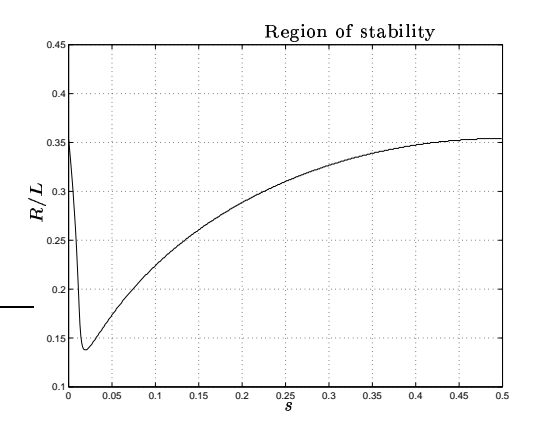


FIGURE 3. On the vertical axis, R/L-values are represented. On the horizontal axis, s is varied. Double cones with values of s and R/L below the boundary curve are stable on the line x=y, whereas bodies with values above the curve are stable along the line x=-y. Here, $\alpha_{\tau}=1/2$.

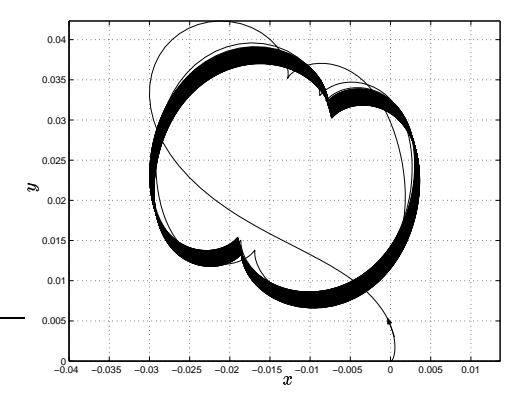


FIGURE 4. A body orbit forms a limit cycle. For the case above, $s=0.1,\ R/L=0.25,\ \alpha_{\tau}=0.9$ and $\mathcal{D}=10^{-2}.$

shearing the influx of energy gets the contribution

$$\frac{3}{2}\mu\beta_E\frac{v_{< ij>}}{p}n_{< i}n_{j>}E_M,$$

where β_E is a number close to unity, and where $E_M = 2k_BTN^{(i)}$. The stationary heat equation for the body is solved with the net influx of

energy through the surface as a boundary condition. The resulting temperature field will get an inhomogeneous contribution proportional to

$$\chi = lpha_{ au} rac{nk_B R}{\kappa} \sqrt{rac{k_B T}{2\pi m}} \sim rac{ au_q}{ au},$$

where $\tau_q = R^2 \rho c_p/\kappa$ (in which ρ and c_p are the density and the heat capacity of the body), and where τ is the typical damping time given by (29). Except for bodies of poor heat conductivity, one finds from explicite calculation that $\chi \ll 1$ in the free molecular flow region, and consequently, the force dF_k on the a surface element with unit normal n_k that stems from the temperature field (12) at the body surface will thus be a factor χ times smaller than the other forces calculated here. Thus, it is legitimate to neglect these forces.

11. Conclusions

It has been shown that a body small compared to the mean free path in a shearing gas is subject to a, to the best of the knowledge of the authors, previously unknown transport mechanism we call the *Shearing Phoresis*. This transport takes place along the directions of the eigenvectors of the traceless part of the rate of deformation tensor. The final velocity of a transported body depends on the body shape, and is given by

$$U_{i} = \frac{9\mu\beta_{N}}{4p} \sqrt{\frac{2\pi k_{B}T}{m}} \frac{\alpha_{\tau}b_{1}}{4 + \frac{1}{2}\pi\alpha_{\tau} + [8 - (6 - \pi\alpha_{\tau})]b_{3}} lN_{i}.$$

Here, N is one of the eigenvectors of the symmetrical and traceless part of the velocity gradient $(v_{\langle i,j\rangle})$, and l is the corresponding eigenvalue. For the simple type of shearing discussed above, we have the eigenvectors $(\pm \boldsymbol{e}_x + \boldsymbol{e}_y)/\sqrt{2}$ with the corresponding eigenvalues $l = \pm v_{x,y}/2$.

For bodies mirror symmetric in a plane orthogonal to the axis of symmetry, such as spheres, ellipses and right circular cylinders, this velocity vanishes.

Numerical simulations of the equations of motion for a double cone have been made for the case with a one-component shearing, $v_{x,y}$. A linearised version of the equations of motion has been obtained to investigate the stability close to the asymptotic states of a double cone.

Appendix

The geometric tensor integrals encountered when the expressions for the force and the torque are integrated over the body surface are listed below:

$$\begin{split} I_{i|}^{(1,0)} &= 0 \\ I_{|j}^{(0,1)} &= S^{3/2}c^{(0,1)}N_{j} \\ I_{i_{1}i_{2}|}^{(2,0)} &= S\left[\frac{1}{3}\delta_{i_{1}i_{2}} + c^{(2,0)}N_{< i_{1}}N_{i_{2}>}\right] \\ I_{i|j}^{(1,1)} &= S^{3/2}\left[c_{1}^{(1,1)}\delta_{ij} + c_{2}^{(1,1)}N_{< i}N_{j>}\right], \\ I_{|j_{1}j_{2}}^{(0,2)} &= S^{2}\left[c_{1}^{(0,2)}\delta_{j_{1}j_{2}} + c_{2}^{(0,2)}N_{< j_{1}}N_{j_{2}>}\right] \\ I_{i_{1}i_{2}|j}^{(2,1)} &= S^{3/2}\left[c_{1}^{(2,1)}\delta_{i_{1}i_{2}}N_{j} + c_{2}^{(2,1)}\left(\delta_{i_{1}j}N_{i_{2}} + \delta_{i_{2}j}N_{i_{1}}\right) + c_{3}^{(2,1)}N_{i_{1}}N_{i_{2}}N_{j}\right] \\ I_{i_{1}i_{2}|j_{1}j_{2}}^{(2,2)} &= S^{2}\left[c_{1}^{(2,2)}\delta_{i_{1}i_{2}}\delta_{j_{1}j_{2}} + c_{2}^{(2,2)}\left(\delta_{i_{1}j_{1}}\delta_{i_{2}j_{2}} + \delta_{i_{1}j_{2}}\delta_{i_{2}j_{1}}\right) + c_{3}^{(2,2)}\delta_{i_{1}i_{2}}N_{j_{1}}N_{j_{2}} + c_{4}^{(2,2)}\delta_{j_{1}j_{2}}N_{i_{1}}N_{i_{2}} + \delta_{i_{2}j_{1}}N_{i_{1}}N_{j_{2}} + c_{5}^{(2,2)}\left(\delta_{i_{1}j_{1}}N_{i_{2}}N_{j_{2}} + \delta_{i_{1}j_{2}}N_{i_{2}}N_{j_{1}} + \delta_{i_{2}j_{1}}N_{i_{1}}N_{j_{2}} + \delta_{i_{2}j_{2}}N_{i_{1}}N_{j_{1}}\right) + c_{6}^{(2,2)}N_{i_{1}}N_{i_{2}}N_{j_{1}}N_{j_{2}} \end{bmatrix} \end{split}$$

The coefficients $c_n^{(k,l)}$ in the expressions above are given by

$$c^{(0,1)} = \mathcal{J}_{2}$$

$$c^{(2,0)} = \frac{1}{2} (3\mathcal{J}_{1} - 1)$$

$$c^{(1,1)}_{1} = \frac{1}{3}\mathcal{J}_{2}$$

$$c^{(1,1)}_{2} = \frac{1}{2} (3\mathcal{J}_{3} - \mathcal{J}_{2})$$

$$c^{(0,2)}_{1} = \frac{1}{3}\mathcal{J}_{5}$$

$$c^{(0,2)}_{2} = \frac{1}{2} (3\mathcal{J}_{7} - \mathcal{J}_{5})$$

$$c^{(2,1)}_{1} = \frac{1}{2} (\mathcal{J}_{2} - \mathcal{J}_{4})$$

$$c^{(2,1)}_{2} = \frac{1}{2} (\mathcal{J}_{3} - \mathcal{J}_{4})$$

$$c^{(2,1)}_{3} = \frac{1}{2} (-2\mathcal{J}_{2} - 2\mathcal{J}_{3} + 5\mathcal{J}_{4})$$

$$c^{(2,2)}_{1} = \frac{1}{8} (-3\mathcal{J}_{4} + 17\mathcal{J}_{5} + 2\mathcal{J}_{6} - 8\mathcal{J}_{7} - 3\mathcal{J}_{8} + \mathcal{J}_{9})$$

$$c^{(2,2)}_{1} = \frac{1}{8} (2\mathcal{J}_{5} - 2\mathcal{J}_{6} - 3\mathcal{J}_{7} - 3\mathcal{J}_{8} + 4\mathcal{J}_{9} + \mathcal{J}_{10})$$

$$c^{(2,2)}_{2} = \frac{1}{8} (-\mathcal{J}_{5} + 2\mathcal{J}_{6} + \mathcal{J}_{7} + \mathcal{J}_{8} - 4\mathcal{J}_{9} + \mathcal{J}_{10})$$

$$c^{(2,2)}_{3} = \frac{1}{8} (-3\mathcal{J}_{5} + 2\mathcal{J}_{6} + 7\mathcal{J}_{7} + 3\mathcal{J}_{8} - 4\mathcal{J}_{9} - 5\mathcal{J}_{10})$$

$$c^{(2,2)}_{4} = \frac{1}{8} (-3\mathcal{J}_{5} + 2\mathcal{J}_{6} + 3\mathcal{J}_{7} + 7\mathcal{J}_{8} - 4\mathcal{J}_{9} - 5\mathcal{J}_{10})$$

$$c^{(2,2)}_{5} = \frac{1}{8} (-\mathcal{J}_{5} - 2\mathcal{J}_{6} - \mathcal{J}_{7} - \mathcal{J}_{8} - 8\mathcal{J}_{9} - 5\mathcal{J}_{10})$$

$$c^{(2,2)}_{6} = \frac{1}{8} (\mathcal{J}_{5} + 2\mathcal{J}_{6} - 5\mathcal{J}_{7} - 5\mathcal{J}_{8} - 5\mathcal{J}_{9} + 35\mathcal{J}_{10})$$

In these coefficients the integrals $\mathcal{J}_1 - \mathcal{J}_{11}$ are given by

Integrals

Integrals
$$\mathcal{J}_{1} = S^{-1} \int_{S} (\boldsymbol{N} \cdot \boldsymbol{n})^{2} dS$$

$$\mathcal{J}_{2} = S^{-3/2} \int_{S} \boldsymbol{x} \cdot \boldsymbol{N} dS$$

$$\mathcal{J}_{3} = S^{-3/2} \int_{S} (\boldsymbol{x} \cdot \boldsymbol{n}) (\boldsymbol{n} \cdot \boldsymbol{N}) dS$$

$$\mathcal{J}_{4} = S^{-3/2} \int_{S} (\boldsymbol{x} \cdot \boldsymbol{n}) (\boldsymbol{n} \cdot \boldsymbol{N}) dS$$

$$\mathcal{J}_{5} = S^{-2} \int_{S} \boldsymbol{x}^{2} dS$$

$$\mathcal{J}_{6} = S^{-2} \int_{S} (\boldsymbol{x} \cdot \boldsymbol{n})^{2} dS$$

$$\mathcal{J}_{7} = S^{-2} \int_{S} (\boldsymbol{x} \cdot \boldsymbol{N})^{2} dS$$

$$\mathcal{J}_{8} = S^{-2} \int_{S} \boldsymbol{x}^{2} (\boldsymbol{n} \cdot \boldsymbol{N})^{2} dS$$

$$\mathcal{J}_{9} = S^{-2} \int_{S} (\boldsymbol{x} \cdot \boldsymbol{n}) (\boldsymbol{x} \cdot \boldsymbol{N}) (\boldsymbol{n} \cdot \boldsymbol{N}) dS$$

$$\mathcal{J}_{10} = S^{-3/2} \int_{S} (\boldsymbol{x} \cdot \boldsymbol{n}) (\boldsymbol{n} \cdot \boldsymbol{N}) dS$$

$$\mathcal{J}_{11} = S^{-3/2} \int_{S} (\boldsymbol{x} \cdot \boldsymbol{n}) (\boldsymbol{n} \cdot \boldsymbol{N})^{2} dS$$

In the following table, the values of the coefficients $a_1..a_5$ and b_2, b_3 are listed:

Coefficients

Coefficients
$$a_{1} = \frac{1}{6} (8 + \pi \alpha_{\tau})$$

$$a_{2} = \frac{1}{4} [8 - (6 - \pi) \alpha_{\tau}] (3\mathcal{J}_{1} - 1)$$

$$a_{3} = \frac{1}{12} \{ [8 + (\pi - 2) \alpha_{\tau}] \mathcal{J}_{2} - [8 - (6 - \pi) \alpha_{\tau}] \mathcal{J}_{3} \}$$

$$a_{4} = \frac{1}{12} \{ [8 + (\pi - 2) \alpha_{\tau}] \mathcal{J}_{5} - [8 - (6 - \pi) \alpha_{\tau}] \mathcal{J}_{6} \}$$

$$a_{5} = \frac{1}{8} \{ [16 - (10 - 2\pi) \alpha_{\tau}] \mathcal{J}_{5} - [16 - (12 - 2\pi) \alpha_{\tau}] \mathcal{J}_{6} \}$$

$$- [24 - (12 - 3\pi) \alpha_{\tau}] \mathcal{J}_{7} - [24 - (18 - 3\pi) \alpha_{\tau}] \mathcal{J}_{8}$$

$$+ [48 - (36 - 6\pi) \alpha_{\tau}] \mathcal{J}_{9} \}$$

$$b_{2} = \mathcal{J}_{10} - \mathcal{J}_{11}$$

$$b_{3} = \frac{1}{2} (3\mathcal{J}_{1} - 1) (= c^{(2,0)})$$

The tensor of inertia, I_{ij} , contains two non-dimensional moments of inertia I_1 and I_2 become

$$I_1 = \frac{2}{3m_B S} \int_V \rho(\boldsymbol{x}) \boldsymbol{x}^2 d^3 x$$

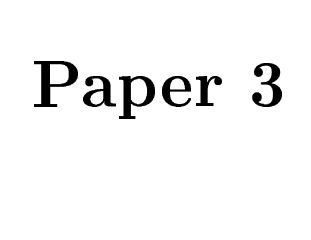
$$I_2 = \frac{1}{2m_B S} \int_V \rho(\boldsymbol{x}) \left[\boldsymbol{x}^2 - 3(\boldsymbol{N} \cdot \boldsymbol{x})^2 \right] d^3 x$$

Acknowledgments

L. Söderholm wishes to acknowledge a valuable discussion with Prof. I. Goldhirsch. -This work has been supported by the Swedish Research Council for Engineering Sciences.

References

- [1] Söderholm, L. H. 2002 Equilibrium Temperature of a Convex Body in Free Molecular Shearing Flow, Phys. Rev. E, **66**: 031204.
- [2] Borg, K. I., and Söderholm, L. H., *Thermophoresis of Axially Symmetric Bodies*. Submitted to Rarefied Gas Dynamics.
- [3] Wang, Y., Mauri, R. and Acrivos, A. The transverse shear-induced liquid and particle tracer diffusivities of a dilute suspension of spheres undergoing a simple shear flow. J. Fluid Mech. (1996), vol. 327, pp 255-272.
- [4] Waldmann, L. 1959 Über die Kraft eines inhomogenen Gases auf kleine suspendierte Kugeln. Z. Naturforsch. 14a: 589-99.
- [5] S. Chapman and T. G. Cowling. The mathematical Theory of Nonuniform Gases, 3rd ed. (Cambridge U.P., Cambridge, England, 1958)
- [6] Kogan, N. M. 1969 Rarefied Gas Dynamics New York: Plenum.
- [7] Goldstein, H. (1981) Classical Mechanics Addison-Wesley publishing company



Force on a spinning sphere moving in a rarefied gas

By Karl I. Borg, Lars H. Söderholm and Hanno Essén

Department of Mechanics Royal Institute of Technology SE-100 44 Stockholm, Sweden

Published in *Physics of Fluids* (2003), **3**, n:o 8, pp 736-741.

The force acting on a spinning sphere moving in a rarefied gas is calculated. It is found to have three contributions with different directions. The transversal contribution is of opposite direction compared to the so-called Magnus force normally exerted on a sphere by a dense gas. It is given by

$$m{F} = -lpha_{ au} \xi rac{2}{3} \pi R^3 mn \, m{\omega} imes m{v},$$

where α_{τ} is the accommodation coefficient of tangential momentum, R is the radius of the sphere, m is the mass of a gas molecule, n is the number density of the surrounding gas, ω is the angular velocity and v is the velocity of the center of the sphere relative to the gas. The dimensionless factor ξ is close to unity, but depends on ω and κ , the heat conductivity of the body.

1. Introduction

The force acting on a sphere moving in a fluid has been a subject of great interest in the history of fluid physics. This is also true for spinning spheres. Newton observed that a transverse force acts on spinning sphere moving through a fluid. In 1742 Robins described the effect in connection with the trajectory of cannon balls. The early history of the subject is described in Tokaty [1]. Nowadays the effect is usually called the Magnus effect. Rubinov and Keller [2] calculated the effect in the fluid dynamical limit using the Navier-Stokes equations, assuming small Reynolds number, Re, and found that the force acting on a sphere of radius R, velocity v, and angular velocity ω , is given by

$$\mathbf{F} = [1 + \mathcal{O}(Re)]\pi R^3 mn \,\boldsymbol{\omega} \times \boldsymbol{v},\tag{1}$$

where m is the mass of a gas molecule and n the number density of the fluid. This force has attracted much interest in connection with sports balls [3, 4]. Experimental studies, on the whole, confirm formula (1) [4, 5, 6] and indicate that, in fact, it is quite reasonable also for high Reynolds numbers. For large Reynolds numbers but small $\omega R/v$, however, the force sometimes changes sign [6, 7]. This is called the inverse Magnus effect. Here it is shown that if the sphere moves through a rarefied gas the force also will have the opposite sign.

There are a few studies in the literature on other forces acting on rotating objects in rarefied gases. One of some relevance is Bowyer [8], who studied the drag on a rotating cylinder in a rarefied gas.

Consider a homogeneous sphere with radius R and heat conductivity κ immersed in a gas with number density n. The mass of a gas molecule is denoted by m. The gas is assumed to be rarefied enough for the mean free path of the gas (the average distance a gas molecule travels between collisions) to be large compared to R. Therefore we may employ the method of free molecular flow [9]. The distribution function describing the gas that surrounds the sphere can then be approximated with the distribution function for the gas in the absence of the sphere. For further results of this method, see Schaaf [10].

The sphere is set into motion relative to the gas in equilibrium. The velocity of the center of mass of the sphere is denoted by \boldsymbol{v} and the angular velocity by $\boldsymbol{\omega}$. We further assume that the heat conduction of the sphere is much faster than the damping of \boldsymbol{v} and $\boldsymbol{\omega}$. One can show that this applies when $(c_s R/k) \cdot (mn/\rho) \ll 1$. Here c_s is the speed of sound, $k = \kappa/\rho c_p$, where κ is the heat conductivity and c_p is the heat

capacity of the body, and where ρ is the density of the body. The surface of the body interacts with the gas according to Maxwell's boundary condition: a fraction $1 - \alpha_{\tau}$ of the stream of molecules incident on the surface is reflected as a light beam hitting a mirror, and a fraction α_{τ} of the incident stream reaches thermal equilibrium with the body surface, and is reflected as a Maxwellian.

The object here is to, under these circumstances, calculate the force acting on the rotating sphere. This is done by calculating an expression for the force acting on a surface element of the body and then by integrating this expression over the surface of the sphere. The calculations will be made to second order in $\omega R/c_s$ and v/c_s , and to arbitrary $\omega R^2/k$.

2. The distribution function

If we introduce a frame of reference with origin at the center of the sphere, the velocity of a point x_i on the surface of the sphere is given by $v_i + \epsilon_{ijk}\omega_j x_k$. For a sphere, a point on the surface can be written as $x_i = Rn_i$, where n is the unit normal in the point, and where n is the radius. It is convenient to make the calculations in a frame of reference in which the surface element is momentarily at rest. In this frame, the surrounding gas has the velocity $u_i = -(v_i + R\epsilon_{ijk}\omega_j n_k)$. Consequently, the surrounding gas is described by the distribution function

$$f(\mathbf{c}) = n \left(\frac{2\pi k_B T}{m}\right)^{-3/2} \exp\left[-\frac{m(c_i - u_i)^2}{2k_B T}\right]. \tag{2}$$

Here, n is the number density of the gas, k_B is Boltzmann's constant, T is the temperature, m is the mass of a gas molecule and c_i is a component of the velocity of a gas molecule. This is the Maxwell distribution function describing a gas in equilibrium subjected to the homogeneous flow u_i . It is normalized according to

$$n = \int f(\boldsymbol{c}) \mathrm{d}^3 c,$$

where d^3c is a unit volume in velocity space. To this end, we introduce the non-dimensional velocities $\mathcal{C}_i \equiv c_i \sqrt{m/2k_BT}$ and $\mathcal{U}_i \equiv u_i \sqrt{m/2k_BT}$. For a monoatomic gas, $\mathcal{U} = \sqrt{6/5}M$, the Mach-number, here based upon the translation of the body. The corresponding dimensionless number, based on the rotation, $\omega R \sqrt{m/2k_BT}$, is assumed to be of the same order of magnitude as \mathcal{U} .

3. The force exerted by the gas on a body surface element

We shall now calculate a general expression for the net force exerted by the surrounding gas described by f, the distribution function of the gas in the absence of the body, on a resting surface element $dS_i = n_i dS$. Here n_i is the unit normal of the surface element. The object of this section is to express this force completely in terms of f. In doing this, the procedure outlined by Waldmann [11] is employed.

The net force exerted on the surface element is the difference of the momentum carried in to the surface element by the incident stream of gas molecules and the momentum carried out by the reflected stream, and can be written

$$dF_k = \left[P_k^{(i)} - P_k^{(r)}\right] dS, \tag{3}$$

where the momentum flux incident on the surface element $P_k^{(\mathrm{i})}$ is given by

$$P_k^{(i)} = -\int_{c_j n_j < 0} m c_k c_j n_j f^{(i)} d^3 c.$$
 (4)

If the surrounding gas is described by a resting Maxwellian distribution, (4) takes the value $-P_M n_i$, where

$$P_M = \frac{1}{2}nk_BT. (5)$$

The momentum flux carried out by reflected molecules $P^{(r)}$ is given by

$$P_k^{(r)} = \int_{c_j n_j > 0} m c_k c_j n_j f^{(r)} d^3 c.$$
 (6)

Here, $f^{(i)}$ and $f^{(r)}$ are the distribution functions describing the stream of molecules incident and reflected on the surface element. Since the body is small compared to the mean free path of the gas, and as the body is convex, the incident stream of molecules can be described by the distribution function of the gas in the absence of the body, that is, $f^{(i)} = f$. The reflected stream of gas molecules is given by Maxwell's boundary condition, cf Kogan [9]. This means that the the reflected stream has two separate parts: one part is specularly reflected (that is, reflected as a particle hitting elastically a solid wall). The other part of the reflected stream has reached thermal equilibrium with the surface and is reflected as Maxwellian.

Thus we have

$$f^{(r)} = (1 - \alpha_{\tau}) f^{(i)} (\boldsymbol{c} - 2(\boldsymbol{c} \cdot \boldsymbol{n}) \boldsymbol{n})$$

$$+\alpha_{\tau} n^{(\mathbf{w})} \left(\frac{2\pi k_B T^{(\mathbf{w})}}{m} \right)^{-3/2} \exp\left(-\frac{mc^2}{2k_B T^{(\mathbf{w})}} \right). \tag{7}$$

The number α_{τ} is called the accommodation coefficient of tangential momentum and measures the fraction of the reflected stream that is diffusely reflected. If $\alpha_{\tau}=0$, there is no transfer of tangential momentum between the gas molecules and the surface element. $T^{(\mathrm{w})}$ is the temperature of the surface of the body. The unknown number density $n^{(\mathrm{w})}$ can be determined from the condition that the net particle flux through the surface vanishes, that is, $0=N^{(\mathrm{i})}-N^{(\mathrm{r})}$, where the incident particle flux $N^{(\mathrm{i})}$ is given by

$$N^{(i)} = -\int_{c_j n_j < 0} c_j n_j f^{(i)} d^3 c.$$
 (8)

For a Maxwellian distribution at rest $f^{(i)} = f^{(0)}$, (8) takes the value

$$N_M = n\sqrt{\frac{k_B T}{2\pi m}}. (9)$$

The reflected particle flux $N^{(r)}$ obeys (7):

$$N^{(r)} = (1 - \alpha_{\tau}) N^{(i)} + \alpha_{\tau} N_M^{(w)}, \tag{10}$$

where $N_M^{(\mathrm{w})}$ is given by (9) but with wall values of T and n. Therefore, due to conservation of gas molecules on the surface, $n^{(\mathrm{w})}$ fulfils

$$N^{(i)} = n^{(w)} \sqrt{\frac{k_B T^{(w)}}{2\pi m}}.$$
 (11)

We are now in a position to calculate the net momentum flux transferred to the surface element according to (3). It is easy to see that in case of pure specular reflection, the momentum transferred to the surface element is given by $2n_k n_j P_j^{(i)}$. The diffusely reflected momentum can be written $P_M^{(w)} n_i$, where $P_M^{(w)}$ is (5) with wallvalues of T and n. Here $P_M^{(w)}$ is given by

$$P_M^{(\mathrm{w})} = \sqrt{rac{T^{(\mathrm{w})}}{T}} rac{N^{(\mathrm{i})}}{N_M} P_M.$$

Here we have used (11). The force on the surface element (3) can thus be written

$$dF_{k} = \left[2(1 - \alpha_{\tau}) n_{k} n_{j} P_{j}^{(i)} + \alpha_{\tau} \left(P_{k}^{(i)} - \sqrt{\frac{T^{(w)}}{T}} \frac{N^{(i)}}{N_{M}} P_{M} n_{k} \right) \right] dS.$$
 (12)

The first term is the momentum transferred to the body from the specularly reflected stream. The second term, $\alpha_{\tau}P_k^{(\mathrm{i})}$, is the part of the incident momentum to be reflected diffusely. The last term is the momentum carried out from the surface by the diffusely reflected stream. Note that N_M and P_M only depends on the gas parameters. The influence of the wall is contained in $T^{(\mathrm{w})}$. The only real complication of this problem is finding $\sqrt{T^{(\mathrm{w})}/T}$, which requires the heat conduction equation to be solved for the rotating sphere.

4. Calculation of the force from a moving Maxwellian

The situation investigated here is the case where $v \ll c_s$ and $\omega R \ll c_s$. Hence the forces (12) are expanded in \mathcal{U} . We recall here that for a monoatomic gas, $\mathcal{U} = \sqrt{6/5}M$, the Mach-number.

To zeroth-order in \mathcal{U} , $f = f^{(0)}$, a Maxwellian at rest and the force (12) simply takes the form $dF_i = -pn_i dS$, where $p = nk_BT$, which vanishes when integrated over the body surface.

To obtain the forces that depend on the rotation, we shall calculate the force (12) to order of \mathcal{U}^2 . The force is split into two separate parts: one part that depends on the inhomogeneous temperature field on the body surface, and one part that does not. To that end the relative temperature deviation is introduced according to $\tau \equiv T^{(\mathrm{w})}/T - 1$. $N^{(\mathrm{i})}$, $P_j^{(\mathrm{i})}$ and τ are then Taylor expanded to second order in \mathcal{U} . The resulting τ -independent part will be treated below. The τ -dependent part of the force (12) becomes

$$-\alpha_{\tau}\sqrt{1+\tau}\frac{N^{(i)}}{N_{M}}P_{M}n_{k}dS$$

$$=-\alpha_{\tau}\frac{1}{2}\tau_{[1]}P_{M}n_{k}dS - \alpha_{\tau}\left[\frac{1}{2}\tau_{[1]}\frac{N^{(i)}_{[1]}}{N_{M}} + \left(\frac{1}{2}\tau_{[2]} - \frac{1}{8}\tau^{2}_{[1]}\right)\right]P_{M}n_{k}dS. (13)$$

Here, the subscript [n] in $\tau_{[n]}$ denotes the contribution of order \mathcal{U}^n to τ (and similarly for $N^{(i)}$). We shall postpone the treatment of (13) to Section 5, where the heat conduction equation for the sphere is solved.

To calculate the incident particle and momentum flux from the moving Maxwellian $N^{(i)}$ and $P_j^{(i)}$, the distribution function is expanded (here $\mathcal{U} = -\sqrt{m/2k_BT}\left(\boldsymbol{v} + R\boldsymbol{\omega} \times \boldsymbol{n}\right)$)

$$f(\mathcal{C}) = n \left(\frac{2\pi k_B T}{m} \right)^{-3/2} \exp \left[- \left(\mathcal{C}_i - \mathcal{U}_i \right)^2 \right]$$

to second order in \mathcal{U} , and get

$$f = f^{(0)} \left[1 - 2C_i \mathcal{U}_i - \mathcal{U}^2 + 2 \left(C_i \mathcal{U}_i \right)^2 \right].$$

Using this expansion, we get $N^{(i)}$ and $P_j^{(i)}$ according to

$$N^{(i)} = N_M \left[1 - \sqrt{\pi \mathcal{U}_k n_k} + (\mathcal{U}_k n_k)^2 \right]$$
 (14)

$$P_j^{(i)} = P_M[-n_j + \frac{2}{\sqrt{\pi}}(\mathcal{U}_j + n_k \mathcal{U}_k n_j) - 2n_k \mathcal{U}_k \mathcal{U}_j]. \tag{15}$$

These expressions are then substituted into formula (12). The first order in \mathcal{U} the well-known linear damping force derived by Epstein [12] is obtained

$$-\frac{8R^2}{3}n\sqrt{2\pi mk_BT}(1+\frac{\pi}{8}\alpha_{\tau})v_i.$$
 (16)

The second order contribution becomes

$$\frac{1}{2} \left[-\left(2 - \frac{3}{2}\alpha_{\tau}\right) n_{i} n_{j} n_{k} - \frac{1}{2}\alpha_{\tau} \left(\delta_{jk} n_{i} + \delta_{ik} n_{j}\right) \right] \mathcal{U}_{i} \mathcal{U}_{j} P_{M} dS.$$

Now we use

$$U_iU_j =$$

$$\frac{m}{2k_BT}\left(v_iv_j+R^2\epsilon_{ikl}\omega_kn_l\epsilon_{jmn}\omega_mn_n+Rv_i\epsilon_{jkl}\omega_kn_l+Rv_j\epsilon_{ikl}\omega_kn_l\right).$$

From symmetry follows that the first two terms within the bracket will not contribute to the force. It is impossible to construct a force to second order that does not mix ω and v. Using $P_M = nk_BT/2$, the remaining contributions are written

$$-\frac{1}{2}Rmn\left[\left(2-\frac{3}{2}\alpha_{\tau}\right)n_{i}n_{j}n_{k}+\frac{1}{2}\alpha_{\tau}\left(\delta_{jk}n_{i}+\delta_{ik}n_{j}\right)\right]\left(v_{i}\epsilon_{jlm}\omega_{l}n_{m}+v_{j}\epsilon_{ilm}\omega_{l}n_{m}\right)dS.$$

$$(17)$$

In expression (17), the first term within the bracket will give rise to terms proportional to $\epsilon_{ijk} \int_S n_j n_k n_l n_m dS$, which vanish since the tensor

 $\int_{S} n_{i} n_{j} n_{k} n_{l} dS$ is totally symmetric. The second term can be simplified, and (17) becomes

$$-rac{1}{2}mnlpha_ au R\left(\epsilon_{kjl}\int_S n_i n_l \mathrm{d}S v_i \omega_j + \epsilon_{ijl}\int_S n_i n_l \mathrm{d}S v_k \omega_j
ight).$$

The second term within the bracket vanishes since the tensor $\int_S n_i n_l dS$ is symmetric. For the sphere the following identity holds:

$$\int_{S} n_i n_j \mathrm{d}S = \frac{4\pi}{3} R^2 \delta_{ij}.$$

This can be understood by forming the trace of the equality. Thus the force becomes

 $-\frac{2\pi}{3}R^3mn\alpha_{\tau}\epsilon_{klm}\omega_{l}v_{m},$ $-\alpha_{\tau}\frac{2}{3}\pi R^3mn\boldsymbol{\omega}\times\boldsymbol{v}.$ (18)

or

5. Effects of the nonuniform heating of the moving sphere

5.1. Heat conduction equation

To calculate (13) we need the surface temperature of the sphere. To that end, the heat equation is solved for the sphere.

We assume that the heat conduction is much faster than the rate of change of ω and v. An inertial coordinate frame moving with the sphere with its origin at the center of the sphere is introduced. In this frame we naturally choose \mathbf{e}_z parallel to ω . The stationary heat equation describing the heat flux within the rotating sphere then takes the form

$$\omega \frac{\partial \tau}{\partial \phi} = k \nabla^2 \tau, \tag{19}$$

where $\tau \equiv T_B/T - 1$. Here T_B is the temperature field within the sphere, $\dot{\phi} = \omega$ and $k = \kappa/\rho c_p$, where κ is the heat conductivity, ρ is the density of the body and c_p is the heat capacity of the body. The term on the left-hand side stems from the convective time derivative due to the rotation.

The angular part of the heat equation (19) is solved by spherical harmonics $Y_{lm}(\theta, \phi)$ with l = 0, 1, 2 (higher l-terms will not enter into the solution since the boundary condition (25) is truncated at \mathcal{U}^2). The integer m takes the values $-l \leq m \leq l$. The value of m characterises the spherical harmonic and should not be confused with the molecular mass, although we have used the same notation for both. The radial part of

the solution depends on the m-value. This is due to the fact that the heat equation distinguishes between rotation parallel and anti-parallel to ω through the term $\omega \partial \tau / \partial \phi$. The variables are separated according to

$$au = \sum_{l=0}^{2} \sum_{m=-l}^{l} R_{lm}(r) Y_{lm}(\theta, \phi),$$

and after substitution into (19), the equation for $R_{lm}(r)$ becomes

$$\frac{1}{r^2} \frac{\mathrm{d}}{\mathrm{d}r} \left[r^2 R_{lm}(r) \right] - \left[\frac{l(l+1)}{r^2} + im \frac{\omega R^2}{k} \right] R_{lm}(r) = 0.$$
 (20)

The solution to this equation is, for $l \neq 0$, given by

$$R_{lm}(r) = A_{lm} j_l \left(\frac{1 - \operatorname{sgn}(m)i}{\sqrt{2}} \sqrt{|m| \frac{\omega R^2}{k}} r \right), \tag{21}$$

where $j_l(x)$ is the spherical Bessel function of order l, and where $\operatorname{sgn}(m)$ is the sign of m. For the case of m = 0, we obtain

$$R_{l0}(r) = A_{l0}r^l. (22)$$

5.2. Boundary condition

The unknown amplitudes A_{lm} should be determined by the boundary condition that expresses the net energy flux through the surface of the sphere. First we denote the influx of kinetic energy from the gas to a resting surface element with outward normal \boldsymbol{n} by $E^{(i)}$. Due to Maxwell's boundary condition, we get $E^{(r)} = (1 - \alpha_{\tau})E^{(i)} + \alpha_{\tau}E^{(w)}_{M}$, where $E^{(w)}_{M} = 2k_{B}T^{(w)}N^{(i)}$ is the energy leaving the surface by the diffusely reflected stream. Here $N^{(i)}$ is given by (14). Thus the net influx of energy becomes

$$E = E^{(i)} - E^{(r)} = \alpha_{\tau} \left[E^{(i)} - 2k_B T^{(w)} N^{(i)} \right].$$
 (23)

The incident energy can be calculated for the moving gas[13, 14], and we get to second order

$$E^{(i)} = -\int_{c_j n_j < 0} \frac{m}{2} c^2 c_i n_i f d^3 c =$$

$$E_M \left[1 - \frac{5}{4} \sqrt{\pi} \mathcal{U}_j n_j + \frac{1}{2} \mathcal{U}^2 + \frac{3}{2} (\mathcal{U}_j n_j)^2 \right]. \tag{24}$$

The left side of (23) must equal $-\kappa \mathbf{n} \cdot \nabla T^{(\mathrm{w})}$. Ordinary spherical coordinates are now introduced, with $r \equiv \sqrt{x^2 + y^2 + z^2}/R$.

The boundary condition is now found to be (note that here, $\mathcal{U} = -\sqrt{m/2k_BT}(\boldsymbol{v} + R\boldsymbol{\omega} \times \boldsymbol{n})$)

$$\frac{\partial \tau}{\partial r} = \chi \left[1 - \frac{5}{4} \sqrt{\pi} \boldsymbol{\mathcal{U}} \cdot \boldsymbol{n} + \frac{1}{2} \boldsymbol{\mathcal{U}}^2 + \frac{3}{2} (\boldsymbol{\mathcal{U}} \cdot \boldsymbol{n})^2 - (1 + \tau) \left(1 - \sqrt{\pi} \boldsymbol{\mathcal{U}} \cdot \boldsymbol{n} + (\boldsymbol{\mathcal{U}} \cdot \boldsymbol{n})^2 \right) \right]. \tag{25}$$

Here

$$\chi = \alpha_{\tau} \frac{nk_B R}{\kappa} \sqrt{\frac{k_B T}{2\pi m}}.$$
 (26)

The order of magnitude of χ is $(c_s R/k) \cdot (mn/\rho)$, which according to our assumptions is $\ll 1$. In (25), terms independent of \boldsymbol{n} are proportional to Y_{00} , terms linear in \boldsymbol{n} corresponds to l=1, and those quadratic in \boldsymbol{n} corresponds to l=2. We have

$$Y_{00} = \frac{1}{\sqrt{4\pi}}$$

$$Y_{10} = \sqrt{\frac{3}{4\pi}} \sqrt{1 - n_x^2 - n_y^2}$$

$$Y_{1\pm 1} = \mp \sqrt{\frac{3}{8\pi}} (n_x \pm i n_y)$$

$$Y_{20} = \sqrt{\frac{5}{16\pi}} (2 - 3n_x^2 - 3n_y^2)$$

$$Y_{2\pm 1} = \mp \sqrt{\frac{15}{8\pi}} (n_x \pm i n_y) \sqrt{1 - n_x^2 - n_y^2}$$

$$Y_{2\pm 2} = \sqrt{\frac{15}{32\pi}} (n_x \pm i n_y)^2$$

As mentioned earlier, the heat equation (19) distinguishes between positive and negative values of m as the body rotates itself.

5.3. Temperature distribution on the surface of the body. On the body surface the temperature to first order in \mathcal{U} becomes

$$\tau_{[1]} = \frac{\sqrt{\pi}}{4} \chi \sqrt{\frac{m}{2k_B T}} \left[\operatorname{Re}(z) \boldsymbol{n} + \frac{\operatorname{Im}(z)}{\omega} \left(\boldsymbol{\omega} \times \boldsymbol{n} \right) \right] \cdot \boldsymbol{v}, \tag{27}$$

where the complex number z is given by

$$z = \frac{j_1(\frac{1-i}{\sqrt{2}}\sqrt{\frac{\omega R^2}{k}})}{\chi j_1(\frac{1-i}{\sqrt{2}}\sqrt{\frac{\omega R^2}{k}}) + \frac{1-i}{\sqrt{2}}\sqrt{\frac{\omega R^2}{k}}j_1'(\frac{1-i}{\sqrt{2}}\sqrt{\frac{\omega R^2}{k}})},$$
 (28)

where $j_1(x)$ is the spherical Bessel function corresponding to l = 1, and $j'_1(x)$ is its derivative. z is plotted in fig 1.

Note that to this order the solution has vector character corresponding to l=1.

To second order in \mathcal{U} , we get three different solutions corresponding to l=0,1,2. Here, we only seek the l=1 part of the distribution, as this is the only part that will contribute to the force (13). The remaining parts (l=0,2) of the temperature field will give a force that vanishes when integrated over the sphere.

The l=1 part becomes

$$\tau_{[2]} = -\chi R \frac{m}{2k_B T} \left[\text{Re}(z) \boldsymbol{n} + \frac{\text{Im}(z)}{\omega} (\boldsymbol{\omega} \times \boldsymbol{n}) \right] \cdot (\boldsymbol{\omega} \times \boldsymbol{v}). \tag{29}$$

The first of the terms will give another contribution to the transversal force. The second term will result in a force proportional to ω .

5.4. Forces from the temperature field

We can now from these expressions calculate the force (13). Three different terms are obtained:

$$-\alpha_{\tau} \frac{\pi}{12} pR^2 \sqrt{\frac{\pi m}{2k_B T}} \chi \operatorname{Re}(z) \boldsymbol{v}$$
 (30)

$$+\alpha_{\tau} \frac{1}{6} \pi R^{3} m n \chi \left[\operatorname{Re}(z) + \sqrt{\frac{2\pi k_{B}T}{m}} \frac{1}{4\omega R} \operatorname{Im}(z) \right] \boldsymbol{\omega} \times \boldsymbol{v}$$
 (31)

$$-\alpha_{\tau} \frac{1}{3} \pi R^{3} m n \chi \frac{\operatorname{Im}(z)}{\omega} \boldsymbol{\omega} \times (\boldsymbol{\omega} \times \boldsymbol{v}). \tag{32}$$

The complex number z is given by (28), and is plotted in fig 1. The first term (30) is a contribution to the damping force, that depends on ω through z. The second (31) is a transversal force. The third force is proportional to $\omega \times (\omega \times v) = (\omega \cdot v)\omega - \omega^2 v$, and has thus a contribution in both the direction of ω as well as in the direction of v.

6. Results for the force on the sphere

The total force becomes

$$egin{aligned} oldsymbol{F} &= -lpha_{ au}rac{\pi}{12}pR^2\sqrt{rac{\pi m}{2k_BT}}\chi\mathrm{Re}(z)oldsymbol{v} \ &-lpha_{ au}\xirac{2}{3}\pi R^3mn\,oldsymbol{\omega} imesoldsymbol{v} \end{aligned}$$

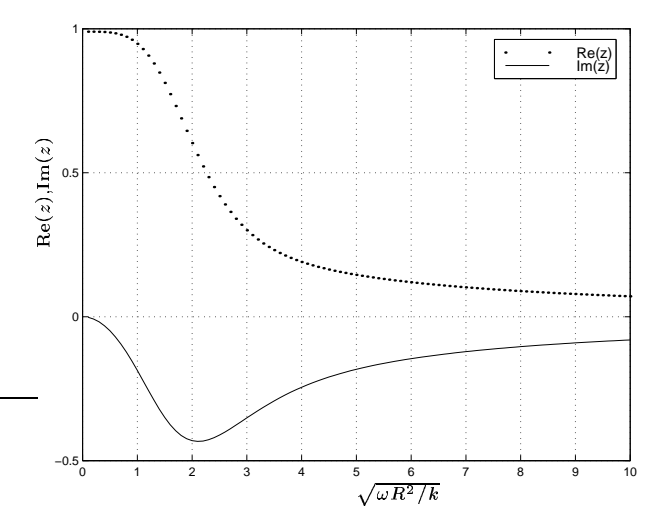


FIGURE 1. The real and imaginary part of z plotted against $\sqrt{\omega R^2/k}$, for $\chi=0.01$. As $\sqrt{\omega R^2/k}\to 0$, $\mathrm{Re}(z)\to (1+\chi)^{-1}$ and $\mathrm{Im}(z)\to 0$. As $\sqrt{\omega R^2/k}\to \infty$, both $\mathrm{Re}(z)$ and $\mathrm{Im}(z)$ tends to zero $\sim \sqrt{\omega R^2/k}^{-1}$.

$$-\alpha_{\tau} \frac{1}{3} \pi R^{3} mn \chi \frac{\operatorname{Im}(z)}{\omega} \boldsymbol{\omega} \times (\boldsymbol{\omega} \times \boldsymbol{v}). \tag{33}$$

Here the dimensionless number ξ is given by

$$\xi = 1 - \frac{1}{4}\chi \left[\operatorname{Re}(z) + \sqrt{\frac{2\pi k_B T}{m}} \frac{1}{4\omega R} \operatorname{Im}(z) \right], \tag{34}$$

where χ is given by (26), and where the complex number z is given by (28).

We have already seen that due to our assumption that the heat conduction of the sphere is much faster than the rate of change of the velocity and the angular velocity, $\chi \ll 1$. Thus the first and the third contribution to the force (33) will be small as they are proportional to χ . Further, ξ , given by (34), is for the same reason close to unity in (33).

In the limit of infinite thermal conductivity, χ tends zero. Thus the forces parallel to \boldsymbol{v} and $\boldsymbol{\omega}$ vanish. In the same limit, ξ tends to unity and the total force (33) is reduced to

$$\boldsymbol{F} = -\alpha_{\tau} \frac{2}{3} \pi R^3 m n \, \boldsymbol{\omega} \times \boldsymbol{v}, \tag{35}$$

which is the force (18) obtained in Section 4.

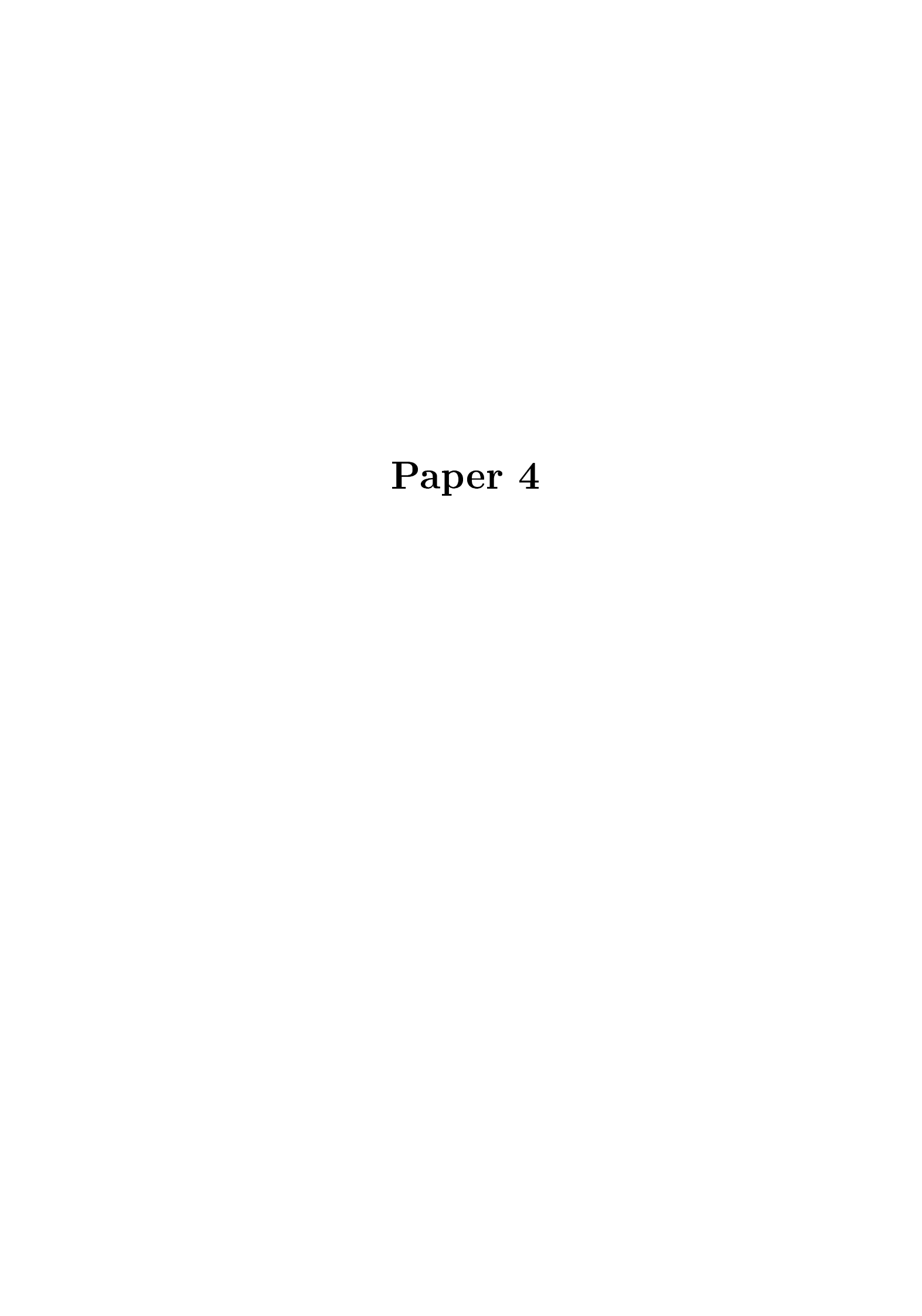
7. Conclusions

Apparently the transversal force derived here will have the opposite sign compared to the corresponding force in the hydrodynamical limit. It is interesting to note that the transversal force will vanish in some intermediate region of the density. Where this critical point is met requires however further investigation.

Just as there is a simple explanation of the ordinary Magnus effect in terms of Bernoulli's theorem there is a simple and natural explanation of the effect found here. The gas molecules will hit the sphere preferentially on that hemisphere which faces into the head wind, and these molecules are likely to be deflected in the spinward direction. Therefore the sphere will tend to be deflected in the opposite direction. This is an intuitive justification of the results of the present work.

References

- [1] G. A. Tokaty, A history and philosophy of fluid mechanics (Foulis, Henley on Thames, UK, 1971).
- [2] S. I. Rubinov and J. B. Keller, "The transverse force on a spinning sphere moving in a viscous fluid," J. Fluid Mech. 11, 447 (1961).
- [3] R. D. Mehta, "Aerodynamics of sports balls," Ann. Rev. Fluid Mech. 17, 151 (1985).
- [4] R. G. Watts and R. Ferrer, "The lateral force on a spinning sphere: Aerodynamics of curveball," Am. J. Phys. **55**, 40 (1987)
- [5] H. M. Barkla and L. J. and Auchterlonie, "The Magnus or Robins effect on a rotating sphere," J. Fluid Mech. 47, 437 (1971)
- [6] D. J. Tritton, *Physical Fluid Dynamics*, 2nd ed, (Clarendon Press, Oxford, UK, 1988).
- [7] T. E. Faber, Fluid Dynamics for Physicists (Cambridge University Press, Cambridge, UK, 1995).
- [8] J. M. Bowyer, Drag on a rotating cylinder apparatus near conditions of free molecule flow. PhD thesis, University of California, 1956.
- [9] N. M. Kogan, Rarefied Gas Dynamics (Plenum Press, New York, USA, 1969).
- [10] S. A. Schaaf, "Mechanics of Rarefied Gases," in *Handbuch der Physik* (Springer, Berlin, 1963), Vol. VIII/2, p. 591.
- [11] L. Waldmann, "Über die Kraft eines inhomogenen Gases auf kleine suspendierte Kugeln," Z. Naturforsch. **14a**, 589 (1959).
- [12] P. S. Epstein," On the resistance experienced by spheres in their motion through gases," Phys. Rev. Series 2, 23, 710 (1924)
- [13] S. Bell and S. A. Schaaf 1953, "Aerodynamic Forces on a Cylinder for the free molecule flow of a Nonuniform gas," Journal of the American Rocket Society, 23, 314 (1953).
- [14] L. H. Söderholm, "Equilibrium Temperature of a Convex Body in Free Molecular Shearing Flow," 031204, Phys. Rev. E 66, (2002)



Effects of the reversed Magnus force on a Kepler orbit in a rarefied gas

By Karl I. Borg and Lars H. Söderholm

Department of Mechanics Royal Institute of Technology SE-100 44 Stockholm, Sweden

The force and torque acting on a spinning sphere with homogeneous surface temperature moving with arbitrary speed in a rarefied gas are calculated. It is found that the transversal component of the force is the same as the corresponding force in the small speed limit. The torque is found to have two components: one perpendicular to the velocity and one parallel to the velocity. The effects of this force and torque acting on a spinning sphere in an initially circular orbit are investigated using perturbation theory. The result is that the orbital plane will rotate slowly.

1. Introduction

It is well-known that a sphere rotating in a fluid will experience a transverse force, that is, a force perpendicular to its velocity. This force is usually referred to as the Magnus force or the Robins effect [1]. Rubinov and Keller [2] calculated the effect in the fluid dynamical limit using the Navier-Stokes equations, assuming a small Reynolds number, Re, and

found that the force acting on a sphere of radius R, velocity v, and angular velocity ω , is given by

$$\mathbf{F} = [1 + \mathcal{O}(Re)]\pi R^3 mn\,\boldsymbol{\omega} \times \boldsymbol{v},\tag{1}$$

where m is the mass of a molecule and n is the number density of molecules.

In a recent paper by the present authors together with H. Essén [3], it was shown that for a body of moderately high thermal conductivity, the transverse force experienced by a rotating sphere moving through a rarefied gas with a speed small compared to the thermal speed, the Magnus force is reversed, and is given by

$$oldsymbol{F} = -lpha_{ au}\xi rac{2}{3}\pi R^3 mn\,oldsymbol{\omega} imesoldsymbol{v},$$

where α_{τ} is the accommodation coefficient of tangential momentum, and where the dimensionless factor ξ is close to unity, but depends on ω and on κ , the heat conductivity of the body. The Magnus force thus changes sign when the gas is rarefied.

In the present work, the transverse force acting on a spinning sphere moving in a rarefied gas is calculated for all speeds. Also, the total torque acting on the rotating sphere is calculated. In doing this, we shall assume that the temperature is homogeneous over the surface of the sphere. The gas is taken to be rarefied enough for the mean free path of the gas to be large compared to the radius of the sphere. Therefore we employ the method of free molecular flow [4]. The distribution function describing the stream of molecules incident on the body surface can then be approximated by the distribution function of the gas in the absence of the body. Maxwell's boundary condition will be used, for which a fraction $1 - \alpha_{\tau}$ of the stream of molecules incident on the body surface is reflected specularly, i.e. like a ball elastically hitting a solid wall, and a fraction α_{τ} of the stream reaches thermal equilibrium with the surface, and is reflected like a local Maxwellian. The parameter α_{τ} is the accommodation coefficient of tangential momentum. Further, we assume complete energy accommodation. For further results on this method, see Schaaf [5].

2. The distribution function

If we introduce a frame of reference with origin at the centre of the sphere, the velocity of a point x_i on the surface of the sphere is given by $v_i + \epsilon_{ijk}\omega_j x_k$. For a sphere, the vector from the centre of the sphere

to a point on the surface can be written as $x_i = Rn_i$, where n is the unit normal in the point, and R is the radius. It is convenient to make the calculations in a frame of reference in which the surface element is momentarily at rest. In this frame, the surrounding gas has the velocity $u_i = -(v_i + R\epsilon_{ijk}\omega_j n_k)$. The gas is described by the distribution function

$$f(\mathbf{c}) = n \left(\frac{2\pi k_B T}{m}\right)^{-3/2} \exp\left[-\frac{m(c_i - u_i)^2}{2k_B T}\right]. \tag{2}$$

Here, n is the number density of the gas, k_B is Boltzmann's constant, T is the temperature, m is the mass of a gas molecule and c_i is the velocity of a gas molecule. This is the Maxwell distribution function describing a gas in local equilibrium subjected to the homogeneous flow u_i . The number density is given by

$$n = \int f(\boldsymbol{c}) \mathrm{d}^3 c,$$

where d^3c is the element of volume in velocity space. We introduce the non-dimensional velocities $C_i \equiv c_i/\sqrt{\frac{2k_BT}{m}}$ and $U_i \equiv u_i/\sqrt{\frac{2k_BT}{m}}$. For a mono atomic gas, $\mathcal{V} = v/\sqrt{\frac{2k_BT}{m}} = \sqrt{\frac{6}{5}}M$, where M is the Machnumber, here based upon the translation of the body. We also define a corresponding dimensionless variable based on the angular velocity according to $W_i \equiv \omega_i R/\sqrt{\frac{2k_BT}{m}}$.

3. The force on a body surface element

We shall now calculate a general expression for the net force exerted by the surrounding gas on a resting surface element $dS_i = n_i dS$. Here n_i is the unit outward normal of the surface element. This force is given by the difference of the momentum brought to the surface element by the incident stream of gas molecules and the momentum carried out by the reflected stream, and can be written

$$dF_k = \left[P_k^{(i)} - P_k^{(r)} \right] dS, \tag{3}$$

where the momentum flux incident on the surface element $P_k^{(\mathrm{i})}$ is given by

$$P_k^{(i)} = -\int_{c_j n_j < 0} m c_k c_j n_j f^{(i)} d^3 c.$$
 (4)

If the surrounding gas is described by a resting Maxwellian distribution, $P_k^{(i)}$ takes the value $-P_M n_i$, where

$$P_M = \frac{1}{2}nk_BT. (5)$$

The momentum flux carried out by reflected molecules $P_k^{(r)}$ is given by

$$P_k^{(r)} = \int_{c_j n_j > 0} m c_k c_j n_j f^{(r)} d^3 c.$$
 (6)

Here, $f^{(i)}$ and $f^{(r)}$ are the distribution functions of the stream of molecules incident and reflected on the surface element. Since the body is small compared to the mean free path of the gas, and as the body is convex, the incident stream of molecules can be approximated by the distribution function describing the gas in the absence of the body, that is, $f^{(i)} = f$. The reflected stream of gas molecules is given by Maxwell's boundary condition, cf Kogan [4]. One part is specularly reflected. The remaining part has reached thermal equilibrium with the surface, and is reflected as a Maxwellian. Thus we have

$$f^{(r)}(\boldsymbol{c}) = (1 - \alpha_{\tau}) f^{(i)}(\boldsymbol{c} - 2(\boldsymbol{c} \cdot \boldsymbol{n}) \boldsymbol{n})$$
$$+ \alpha_{\tau} n^{(w)} \left(\frac{2\pi k_B T^{(w)}}{m} \right)^{-3/2} \exp\left(-\frac{mc^2}{2k_B T^{(w)}} \right), \tag{7}$$

where α_{τ} is the accommodation coefficient of tangential momentum. $T^{(\mathrm{w})}$ is the temperature of the surface of the body. The unknown number density $n^{(\mathrm{w})}$ is determined from the condition that the net particle flux through the surface vanishes, that is, $0 = N^{(\mathrm{i})} - N^{(\mathrm{r})}$, where the incident particle flux $N^{(\mathrm{i})}$ is given by

$$N^{(i)} = -\int_{c_i n_i < 0} c_j n_j f^{(i)} d^3 c.$$
 (8)

For a Maxwellian distribution at rest $N^{(i)}$ takes the value

$$N_M = n\sqrt{\frac{k_B T}{2\pi m}}. (9)$$

The reflected particle flux $N^{(\mathrm{r})}$ is found from (7) to be

$$N^{(r)} = (1 - \alpha_{\tau}) N^{(i)} + \alpha_{\tau} N_{M}^{(w)}, \tag{10}$$

where $N_M^{(w)}$ is given by (9) but with wall-values of T and n. Therefore, due to conservation of gas molecules at the surface, $n^{(w)}$ fulfils

$$N^{(i)} = n^{(w)} \sqrt{\frac{k_B T^{(w)}}{2\pi m}}.$$
 (11)

We are now in a position to calculate the net momentum flux transferred to the surface element according to (3). In the case of pure specular reflection, it is given by $2n_k n_j P_j^{(i)}$. In case of purely diffuse reflection, the corresponding momentum can be written $P_M^{(w)} n_i$, where $P_M^{(w)}$ is (5) with wall-values of T and n. $P_M^{(w)}$ can be written

$$P_M^{(\mathrm{w})} = \sqrt{rac{T^{(\mathrm{w})}}{T}} rac{N^{(\mathrm{i})}}{N_M} P_M.$$

Here, (11) has been used. The force on the surface element (3) is thus

$$dF_k = \left[(1 - \alpha_\tau) 2n_k n_j P_j^{(i)} + \alpha_\tau \left(P_k^{(i)} - \sqrt{\frac{T^{(w)}}{T}} \frac{N^{(i)}}{N_M} P_M n_k \right) \right] dS.$$

$$(12)$$

The first term is the momentum transferred to the body from the specularly reflected stream. The second term, $\alpha_{\tau}P_k^{(\mathrm{i})}$, is the part of the incident momentum to be reflected diffusely. The last term is the momentum carried out from the surface by the diffusely reflected stream. Note that N_M and P_M depend on the gas parameters only. The influence of the wall is collected in $T^{(\mathrm{w})}$. We shall assume that the temperature is constant over the surface of the sphere. The case of a perfect conductor is treated in Section 5.

4. Calculation of the force from a moving Maxwellian

For a moving Maxwellian, the influxes of particles $N^{(i)}$ and momentum $P_i^{(i)}$ can be calculated [4, 6] and are given by

$$N^{(i)} = N_M \left[e^{-\mathcal{U}_n^2} - \sqrt{\pi} \mathcal{U}_n \left(1 + \operatorname{erf}(-\mathcal{U}_n) \right) \right],$$

$$P_i^{(i)} = \frac{2}{\sqrt{\pi}} P_M \left\{ \left(\mathcal{U}_i - \mathcal{U}_n n_i \right) \left[e^{-\mathcal{U}_n^2} - \sqrt{\pi} \mathcal{U}_n \left(1 + \operatorname{erf}(-\mathcal{U}_n) \right) \right] - \left[\mathcal{U}_n e^{-\mathcal{U}_n^2} - \sqrt{\pi} \left(\frac{1}{2} + \mathcal{U}_n^2 \right) \left(1 + \operatorname{erf}(-\mathcal{U}_n) \right) \right] n_i \right\}.$$

$$(13)$$

110

Here.

$$\operatorname{erf}(x) = \frac{2}{\sqrt{\pi}} \int_0^x e^{-t^2} dt,$$

and the shorthand $U_n \equiv U_l n_l$ is the normal component of the velocity. Substituting these expressions into (12) yields

$$dF_{i} = P_{M} \left\{ (2 - \alpha_{\tau}) \left[\frac{2}{\sqrt{\pi}} \mathcal{U}_{n} \chi(-\mathcal{U}_{n}) - (1 + \operatorname{erf}(-\mathcal{U}_{n})) \right] n_{i} \right.$$

$$\left. + \alpha_{\tau} \frac{2}{\sqrt{\pi}} \mathcal{U}_{i} \chi(-\mathcal{U}_{n}) - \alpha_{\tau} \sqrt{\frac{T^{(w)}}{T}} \chi(-\mathcal{U}_{n}) n_{i} \right\} dS, \tag{15}$$

where the function $\chi(x)$ has been introduced for convenience, and is given by

$$\chi(x) = \exp(-x^2) + \sqrt{\pi}x \left[1 + \text{erf}(x)\right]. \tag{16}$$

This expression will now be integrated over the surface of the sphere to give the total force acting on the body. In doing this, we make use of the assumption that the temperature of the sphere is constant. This is the case if the body is a perfect heat conductor. We first recall that

$$\mathcal{U}_i = -\left(\mathcal{V}_i + \epsilon_{ijk} \mathcal{W}_j n_k\right),\,$$

where $W_i = \sqrt{m/2k_BT}R\omega_i$. Consequently, $U_n = -V_n \equiv -V_l n_l$. From this substitution, the force is seen to contain one term linear in W_i and one independent of W_i . The first term is given by

$$-\alpha_{\tau} P_{M} \frac{2}{\sqrt{\pi}} \epsilon_{ijk} \mathcal{W}_{j} \int_{S} \left[e^{-\mathcal{V}_{n}^{2}} + \sqrt{\pi} \mathcal{V}_{l} n_{l} \left(1 + \operatorname{erf}(\mathcal{V}_{l} n_{l}) \right) \right] n_{k} dS.$$

Here, S denotes the surface of the sphere. From symmetry it follows that integrands odd in n cancel when integrated over the sphere surface. For this reason, only the first part of the second term within the square brackets will contribute to the force. Further, for a sphere, the following identity holds:

$$\int_{S} n_l n_k dS = \frac{4\pi R^2}{3} \delta_{lk},$$

and thus this part of the force becomes

$$-lpha_{ au}P_{M}rac{8\pi R^{2}}{3}\epsilon_{ijk}\mathcal{W}_{j}\mathcal{V}_{k},$$

or, expressed in dimensional variables,

$$-\alpha_{\tau} \frac{2\pi R^3}{3} mn\boldsymbol{\omega} \times \boldsymbol{v}. \tag{17}$$

Here we have used $P_M = nk_BT/2$. This is a transverse force of opposite direction compared to the so-called Magnus force acting on a spinning ball in the continuum limit. This result coincides with the force obtained in [3] for a perfect conductor under the assumption that v and ωR are much smaller than the thermal speed $\sqrt{2k_BT/m}$.

Using polar coordinates with $V_n = V \cos \theta$ the remaining part of the force can be integrated. This gives the well-known result [4] for the drag force

$$-\frac{\pi R^2}{6} \sqrt{\frac{2k_B T}{\pi m}} (8 + \pi) mn \, a(\mathcal{V}) \, \boldsymbol{v}, \tag{18}$$

where the coefficient $a(\mathcal{V})$ is given by

$$a(\mathcal{V}) = \frac{3}{32 + 4\pi} \left\{ \frac{1 + \alpha_{\tau}}{2} \left[\sqrt{\pi} \operatorname{erf}(\mathcal{V}) \left(-\frac{1}{\mathcal{V}^3} + \frac{4}{\mathcal{V}} + 4\mathcal{V} \right) + 2e^{-\mathcal{V}^2} \left(\frac{1}{\mathcal{V}^2} + 2 \right) \right] + \frac{4\pi}{3} \sqrt{\frac{T^{(w)}}{T}} \right\}$$
(19)

The last term within the curly brackets depends on $T^{(w)}$, the temperature of the surface of the body. It is calculated in Section 5 for the case of a perfect conductor. The qualitative behaviour of $a(\mathcal{V})$ is however rather insensitive to the choice of model for $T^{(w)}$: using the speed dependent perfect conductor model yields the same friction force as using a constant value of $T^{(w)}$. The choice of model only affects the numerical coefficient of $a(\mathcal{V})$.

The torque $dM_i = R\epsilon_{ijk}n_jdF_k$ acting on a surface element dS can be calculated in much the same way. From symmetry the torque acting on a sphere vanishes if $\omega = \mathbf{0}$, and thus only the part of the force depending on ω will contribute. Integrating dM_i over the surface of the sphere gives the torque:

$$M_i =$$

$$-\alpha_{\tau} \frac{4\pi R^4}{3} nm \sqrt{\frac{2k_B T}{\pi m}} \left[b_{\perp}(\mathcal{V}) \left(\delta_{ij} - \frac{1}{\boldsymbol{v}^2} v_i v_j \right) + b_{\parallel}(\mathcal{V}) \frac{1}{\boldsymbol{v}^2} v_i v_j \right] \omega_j. \quad (20)$$

Here

$$b_{\perp}(\mathcal{V}) = \frac{3}{64} \left[\sqrt{\pi} \operatorname{erf}(\mathcal{V}) \left(\frac{1}{\mathcal{V}^3} + \frac{4}{\mathcal{V}} + 12\mathcal{V} \right) - 2e^{-\mathcal{V}^2} \left(\frac{1}{\mathcal{V}^2} - 6 \right) \right]$$
(21)

and

$$b_{\parallel}(\mathcal{V}) = rac{3}{32} \left[\sqrt{\pi} \mathrm{erf}(\mathcal{V}) \left(rac{-1}{\mathcal{V}^3} + rac{4}{\mathcal{V}} + 4\mathcal{V}
ight) + 2e^{-\mathcal{V}^2} \left(rac{1}{\mathcal{V}^2} + 2
ight) \right]. \quad (22)$$

The first contribution to the torque damps the component of ω perpendicular to the velocity, and the second term damps the component of ω parallel to the velocity. Note that the torque does not depend on the temperature of the sphere's surface.

5. Equilibrium temperature of a perfect conductor

The purpose of this section is to calculate the temperature of the sphere under the assumption that the body is a perfect conductor, or put in other words, has infinite thermal conductivity. First we denote the influx of kinetic energy from the gas to a resting surface element with outward normal \boldsymbol{n} by $E^{(i)}$. Due to Maxwell's boundary condition, we get $E^{(r)} = (1 - \alpha_{\tau})E^{(i)} + \alpha_{\tau}E^{(w)}_{M}$, where $E^{(w)}_{M} = 2k_{B}T^{(w)}N^{(i)}$ is the energy leaving the surface by the diffusely reflected stream. Here $N^{(i)}$ is given by (4). Thus the net influx of energy becomes

$$E = E^{(i)} - E^{(r)} = \alpha_{\tau} \left[E^{(i)} - 2k_B T^{(w)} N^{(i)} \right].$$
 (23)

The incident energy can be calculated for the moving gas, and we get [4, 7]

$$E^{(i)} = -\int_{c_j n_j < 0} \frac{m}{2} c^2 c_i n_i f d^3 c =$$

$$E_M \left[\left(1 + \frac{1}{2} \mathcal{U}^2 \right) e^{-\mathcal{U}_n^2} - \sqrt{\pi} \mathcal{U}_n \left(\frac{5}{4} + \frac{1}{2} \mathcal{U}_n^2 \right) \operatorname{erf}(-\mathcal{U}_n) \right]. \tag{24}$$

For a perfect conductor, the temperature of the body adjusts itself so that the total influx of energy equals the total outflux. Thus, (23) is integrated over the sphere and equated to zero [7], and one obtains

$$2k_B T^{(\mathrm{w})} \int_S N^{(\mathrm{i})} \mathrm{d}S = \int_S E^{(\mathrm{i})} \mathrm{d}S.$$

Performing the integrals yields

$$\frac{T^{(\mathrm{w})}}{T} = \frac{1}{8} \frac{\sqrt{\pi} \mathrm{erf}(\mathcal{V}) \left(3 + 28\mathcal{V}^2 + 4\mathcal{V}^4\right) + 2\mathcal{V}e^{-\mathcal{V}^2} \left(13 + 2\mathcal{V}^2\right)}{\sqrt{\pi} \mathrm{erf}(\mathcal{V}) \left(1 + 2\mathcal{V}^2\right) + 2\mathcal{V}e^{-\mathcal{V}^2}}$$

$$\mathcal{V}^2 \sqrt{\pi} \mathrm{erf}(\mathcal{V}) \left(1 - 3\cos^2\psi + (1 + \cos^2\psi)\mathcal{V}^2\right) + 6\mathcal{V}e^{-\mathcal{V}^2}\cos^2\psi$$

$$+\frac{W^{2}}{2V^{2}}\frac{\sqrt{\pi}\mathrm{erf}(\mathcal{V})\left(1-3\cos^{2}\psi+(1+\cos^{2}\psi)\mathcal{V}^{2}\right)+6\mathcal{V}e^{-\mathcal{V}^{2}}\cos^{2}\psi}{\sqrt{\pi}\mathrm{erf}(\mathcal{V})\left(1+2\mathcal{V}^{2}\right)+2\mathcal{V}e^{-\mathcal{V}^{2}}}.$$
 (25)

Here ψ is the angle between \mathcal{W} and \mathcal{V} . The dependence on \mathcal{W} has been collected in the second term.

To use (25) is a rough model, but it is apparent from (18) that the model for the homogeneous temperature of the surface of the sphere only affects the friction force in terms of a numerical coefficient. Neither the the transverse force nor the torque depends on the value of $T^{(w)}$.

Substituting the expression for the temperature into $a(\mathcal{V})$, the coefficient in the damping force (18), completes the expressions for the forces and torques acting on a rotating sphere moving in a rarefied gas. The coefficients a, b_{\perp} and b_{\parallel} are plotted in figure 1 for the case where $|\omega R| \ll |v|$: It is then legitimate to regard the second term in (25) as a negligible correction to the first term. We end this section by calculating the coefficients a, b_{\perp} and b_{\parallel} in the supersonic limit $(M \to \infty)$, and we get

$$a(\mathcal{V}) \approx \frac{\pi + 3\sqrt{\pi}(1 + \alpha_{\tau})}{16 + 2\pi} \mathcal{V}, \quad b_{\perp}(\mathcal{V}) \approx \frac{9\sqrt{\pi}}{16} \mathcal{V}, \quad b_{\parallel}(\mathcal{V}) \approx \frac{5\sqrt{\pi}}{16} \mathcal{V}. \quad (26)$$

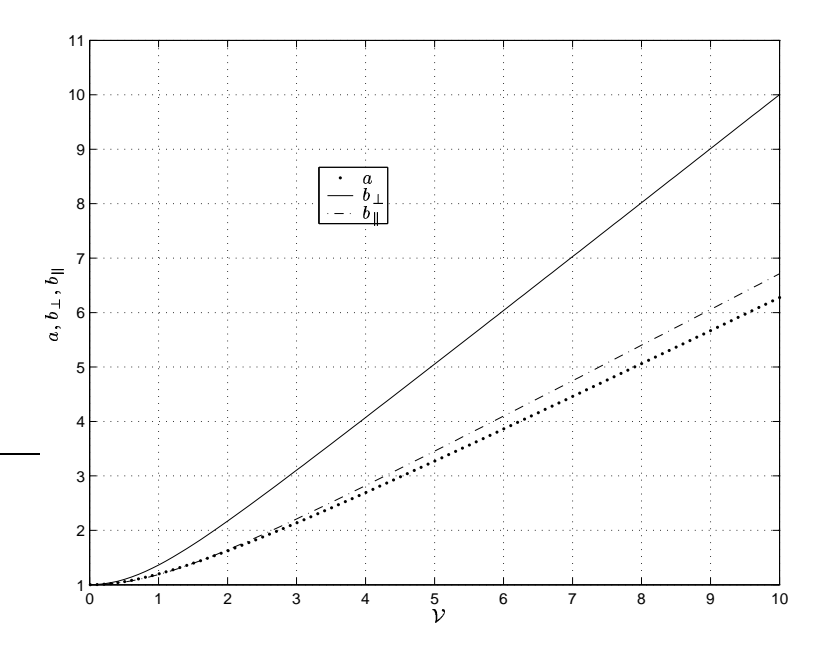


FIGURE 1. The coefficients a, b_{\perp} and b_{\parallel} are plotted as functions of \mathcal{V} for a perfect conductor in the limit $|\boldsymbol{\omega}R| \ll |\boldsymbol{v}|$. In this figure, $\alpha_{\tau} = 1$. In the supersonic limit, the functions a, b_{\perp} and b_{\parallel} grow linearly with the speed.

It is interesting to compare the transverse force (17) and the friction force (18) to the corresponding forces in the fluid-dynamic limit. The transverse force is in this limit given by (1). It has been shown experimentally [8, 9, 10] that (1) is reasonable also for high Reynolds numbers.

The drag force in the continuum limit is given by [10]

$$oldsymbol{F}_D = -
horac{\pi R^2}{2}\,C_D |oldsymbol{v}|oldsymbol{v},$$

$$C_D \sim \frac{6\pi}{Re}, Re < 1 \text{ and } C_D \sim 1, Re > 1.$$
 (27)

It is apparent that for small velocities, both the friction force (18) and the corresponding fluid dynamic drag force (27) are linear in the velocity, but the coefficients are different: the transverse force is for small speeds larger compared to the drag force in the fluid-dynamic limit than in the rarefied gas.

As the speed increases, both the fluid-dynamic drag forces and the friction force (18) become quadratic in the speed. The speed at which the transitions take place differs however between the two. In the fluid-dynamic limit, the transition occurs when $Re \sim 1$, but in the rarefied gas when the Mach number $M \sim 1$. Thus, for large but sub sonic speeds, the transverse force is larger compared to the drag force in the rarefied gas than in the fluid-dynamic limit.

6. Perturbation of Kepler orbit

In this section a spinning body moving in a circular orbit in the gravitation field of the Earth, under the influence of the thermosphere [11] is considered. As a starting point we review the Kepler problem (here G is the gravitational constant, M is the mass of the Earth, and r is the position vector of the satellite with respect to an inertial system with its origin at the centre of gravity)

$$\frac{\mathrm{d}^2 \mathbf{r}}{\mathrm{d}t^2} = -GM|\mathbf{r}|^{-3}\mathbf{r}.$$
 (28)

For a body in a circular orbit, the orbit radius r_0 and the period time of the orbit τ_0 are related by Kepler's third law:

$$r_0 = \left(\frac{GM\tau_0^2}{4\pi^2}\right)^{1/3}. (29)$$

Now the influence of the thin thermosphere on the orbit of the body is considered. For simplicity the body is chosen to be a spinning sphere and thus we add to the Kepler problem (28) the damping force (18) as well as the transverse force (17) calculated in a previous section. Further, the torque (20) damping the angular velocity of the spinning sphere is also taken into account. We assume that the sphere is homogeneous and has the radius R, the density ρ and the homogeneous surface temperature $T^{(w)}$. The temperature and number density of the thermosphere are denoted T and n. These vary over a 24-hour period, and we shall here use time averages for the values of T and n. The number density will decrease rapidly with height, and also the temperature T will vary with height. We also allow $T^{(w)}$ to vary with height. Now we define the non-dimensional variables n^* and T^* according to

$$n = n_0 n^*(r)$$
 and $T = T_0 T^*(r)$, (30)

where n_0 and T_0 are the initial values of the number density and the temperature. Here we also define the non-dimensional temperature of the sphere surface $T^{(w)*}$ according to $T^{(w)} = T_0 T^{(w)*}(r)$.

From the friction force (18) we get a damping time given by

$$\frac{8}{8+\pi} \frac{\rho}{mn_0} R \sqrt{\frac{\pi m}{2k_B T_0}} \frac{1}{n^*(r) \sqrt{T^*(r)}},\tag{31}$$

where m is the mass of a gas molecule. We now assume that this damping time is much larger than the period time of the unperturbed orbit τ_0 . This is the case for example for a satellite of a reasonable density with the radius 1 m at the height of 130 km above the surface of the Earth. Here we define the damping time τ_1 according to (31):

$$\tau_1 = \frac{8}{8 + \pi} \frac{\rho}{m n_0} R \sqrt{\frac{\pi m}{2k_B T_0}}.$$
 (32)

It is now convenient to define the initial non-dimensional speeds according to $V_0 = v_0 \sqrt{m/2k_B T_0}$ and $W_0 = R\omega_0 \sqrt{m/2k_B T_0}$, where v_0 is the initial speed and where $\omega_0 = |\omega_0|$.

The non-dimensional variables

$$t^* = 2\pi t/\tau_0$$
, $\boldsymbol{r}^* = \boldsymbol{r}/r_0$ and $\boldsymbol{\omega}^* = \boldsymbol{\omega}/\omega_0$

are now introduced. Here we define the small parameter ε as the quotient between the period time τ_0 and the damping time τ_1 according to

$$\varepsilon = \frac{\tau_0}{\tau_1} = \left(1 + \frac{\pi}{8}\right) \frac{mn_0}{\rho} \sqrt{\frac{2k_B T_0}{\pi m}} \frac{\tau_0}{R}.$$
 (33)

The corresponding non-dimensional equation of motion is then given by (the *-superscript will be dropped in what follows):

$$\frac{\mathrm{d}^2 \mathbf{r}}{\mathrm{d}t^2} = -|\mathbf{r}|^{-3} \mathbf{r} - \varepsilon \, n(r) k_1 \mathcal{V}_0 | \frac{\mathrm{d}\mathbf{r}}{\mathrm{d}t} | \frac{\mathrm{d}\mathbf{r}}{\mathrm{d}t} - \varepsilon \, n(r) k_2 \mathcal{W}_0 \boldsymbol{\omega} \times \frac{\mathrm{d}\mathbf{r}}{\mathrm{d}t}. \tag{34}$$

For convenience, the coefficients k_1, k_2 , given by

$$k_1 = rac{3}{32 + 4\pi} \left[2\sqrt{\pi}(1 + \alpha_{\tau}) + rac{4\pi}{3\mathcal{V}} \sqrt{rac{T^{(\mathrm{w})}(r)}{T(r)}}
ight], \quad k_2 = rac{4\sqrt{\pi}\alpha_{\tau}}{8 + \pi}$$

have been introduced. We note that according to (25), for a perfect conductor the square bracket has the constant value $2\sqrt{\pi}(1+\alpha_{\tau})+2\pi/3$ in the supersonic limit.

The initial conditions are chosen to be

$$r = e_x$$
 and $\frac{\mathrm{d}r}{\mathrm{d}t} = e_y$. (35)

In the absence of the forces (17), (18) these initial conditions defines a circular Kepler orbit. The time derivative of the angular momentum of the sphere equals the torque. Therefore, imposing the same scaling on this equation gives

$$\frac{\mathrm{d}\omega_i}{\mathrm{d}t} = -\varepsilon \, n(r) \mathcal{V}_0 \left| \frac{\mathrm{d}\boldsymbol{r}}{\mathrm{d}t} \right| \left[k_3 \left(\delta_{ij} - \frac{1}{\boldsymbol{v}^2} v_i v_j \right) + k_4 \frac{1}{\boldsymbol{v}^2} v_i v_j \right] \omega_j \tag{36}$$

where the coefficients k_3 and k_4 are given by

$$k_3 = \frac{9\sqrt{\pi}}{16} \frac{20\alpha_{\tau}}{8+\pi}, \quad k_4 = \frac{5\sqrt{\pi}}{16} \frac{20\alpha_{\tau}}{8+\pi}.$$

Here we have used that the moment of inertia of a sphere is $8\rho\pi R^5/15$. At t=0, ω is the unity vector parallel to the initial angular velocity.

The character of the equation (34) suggests a multiple-scale solution, cf. Kevorkian and Cole [12]. Accordingly, in addition to the non-dimensional time t we introduce a 'slow' time $\tilde{t} = \varepsilon t$, which corresponds to the typical time on which the damping from the thermosphere acts.

We now set $\mathbf{r} = \mathbf{r}^{(0)}(t, \tilde{t}) + \varepsilon \mathbf{r}^{(1)}(t, \tilde{t}) + ...$ and $\boldsymbol{\omega} = \boldsymbol{\omega}^{(0)}(t, \tilde{t}) + \varepsilon \boldsymbol{\omega}^{(1)}(t, \tilde{t}) + ...$ and seek a solution that to lowest order of approximation $(\varepsilon = 0)$ is a circle with slowly varying parameters, according to

$$\mathbf{r}^{(0)}(t,\tilde{t}) = r(\tilde{t}) \left[\cos \Phi(t,\tilde{t}) \mathbf{e}_1(\tilde{t}) + \sin \Phi(t,\tilde{t}) \mathbf{e}_2(\tilde{t}) \right]. \tag{37}$$

Substitution of this ansatz into the equation of motion (34) imposes two conditions:

$$1 - r^3(\tilde{t}) \left(\frac{\partial \Phi(t, \tilde{t})}{\partial t} \right)^2 = 0 \text{ and } r(\tilde{t}) \frac{\partial^2 \Phi(t, \tilde{t})}{\partial t^2} = 0.$$

The second equation can be integrated twice with respect to t, and yields

$$\Phi(t, \tilde{t}) = \Omega(\tilde{t})t + \phi(\tilde{t}),$$

where the angular frequency $\Omega(\tilde{t})$ and the phase $\phi(\tilde{t})$ are constants of integration with respect to t. Then, from the first equation, we get

$$r(\tilde{t}) = \Omega(\tilde{t})^{-2/3}. (38)$$

This is Kepler's third law. The boundary conditions (35) are now imposed on this solution (as the solution is already a circle, it is sufficient to apply only one of the two in (35)) and one obtains $\Omega(0) = 1$ and $\phi(0) = 0$. Thus we get

$$\mathbf{r}^{(0)} = \Omega(\tilde{t})^{-2/3} \left\{ \cos \left[\Omega(\tilde{t})t + \phi(\tilde{t}) \right] \mathbf{e}_1(\tilde{t}) + \sin \left[\Omega(\tilde{t})t + \phi(\tilde{t}) \right] \mathbf{e}_2(\tilde{t}) \right\}.$$
(39)

The equation (36) becomes to lowest order

$$\frac{\partial \boldsymbol{\omega}^{(0)}}{\partial t} = \mathbf{0}.\tag{40}$$

Thus the leading order term of the angular velocity only varies on the slow time scale, that is $\boldsymbol{\omega}^{(0)} = \boldsymbol{\omega}^{(0)}(\tilde{t})$.

To first order in ε we get the following equation for $r^{(1)}$:

$$\frac{\partial^{2} \boldsymbol{r}^{(1)}}{\partial t^{2}} + \Omega^{2} \boldsymbol{r}^{(1)}$$

$$-3\Omega^{2} \left[\sin \left(\Omega t + \phi \right) \left(\boldsymbol{r}^{(1)} \cdot \boldsymbol{e}_{1} \right) + \cos \left(\Omega t + \phi \right) \left(\boldsymbol{r}^{(1)} \cdot \boldsymbol{e}_{2} \right) \right] \left\{ \sin \left(\Omega t + \phi \right) \boldsymbol{e}_{1} + \cos \left(\Omega t + \phi \right) \boldsymbol{e}_{2} \right\}$$

$$= n(r) k_{1} \mathcal{V}_{0} \Omega^{2/3} \left[\cos \left(\Omega t + \phi \right) \boldsymbol{e}_{1} - \sin \left(\Omega t + \phi \right) \boldsymbol{e}_{2} \right]$$

$$-n(r) k_{2} \mathcal{W}_{0} \Omega^{1/3} \left[\cos \left(\Omega t + \phi \right) \left(\boldsymbol{\omega}^{(0)} \times \boldsymbol{e}_{1} \right) - \sin \left(\Omega t + \phi \right) \left(\boldsymbol{\omega}^{(0)} \times \boldsymbol{e}_{2} \right) \right]$$

$$-\frac{2}{3} \Omega^{-2/3} \frac{d\Omega}{d\tilde{t}} \left\{ \left[3\Omega t \sin \left(\Omega t + \phi \right) - \cos \left(\Omega t + \phi \right) \right] \boldsymbol{e}_{1} + \left[3\Omega t \cos \left(\Omega t + \phi \right) + \sin \left(\Omega t + \phi \right) \right] \boldsymbol{e}_{2} \right\}$$

$$+2\Omega^{1/3} \left[\cos \left(\Omega t + \phi \right) \frac{d\boldsymbol{e}_{1}}{d\tilde{t}} - \sin \left(\Omega t + \phi \right) \frac{d\boldsymbol{e}_{1}}{d\tilde{t}} \right]$$

$$-2\Omega^{1/3} \frac{d\phi}{d\tilde{t}} \left[\sin \left(\Omega t + \phi \right) \boldsymbol{e}_{1} + \cos \left(\Omega t + \phi \right) \boldsymbol{e}_{2} \right]$$

The right-hand side of this equation contains the leading order solution $\mathbf{r}^{(0)}(t,\tilde{t})$ given by the ansatz (39) containing the unknown slowly varying parameters $\Omega(\tilde{t})$, $\Phi(\tilde{t})$, and $\mathbf{e}_i(\tilde{t})$, i=1,2.

The character of the left-hand side predicts an oscillatory solution for $\mathbf{r}^{(1)}$. Accordingly, the amplitude of this solution will grow without bound with time if the right-hand side of the same equation contains 'driving' terms oscillating with the same frequency. From demanding that such terms in the right-hand side (r.h.s) vanish, one obtains equations for the slowly varying parameters $\Omega(\tilde{t})$, $\phi(\tilde{t})$, and $\mathbf{e}_i(\tilde{t})$ in the leading order solution $\mathbf{r}^{(0)}$, cf [12]. This is done by solving the equations

$$\frac{1}{\pi} \int_0^{2\pi} (\mathbf{r.h.s}) \cos \left(\Omega t + \phi\right) dt = \frac{1}{\pi} \int_0^{2\pi} (\mathbf{r.h.s}) \sin \left(\Omega t + \phi\right) dt = 0.$$

The equations we get are too few to completely determine all the unknowns. This is because a phase changing with time describes the same thing as the basis vectors rotating about the axis normal to the orbital plane. Therefore we further impose the restriction that the angular velocity of the basis vectors lies in the orbital plane spanned by e_1 and e_2 . Introducing for convenience the angular velocity γ of the basis vectors spanning the orbital plane according to

$$rac{\mathrm{d}oldsymbol{e}_i}{\mathrm{d} ilde{t}} = oldsymbol{\gamma} imes oldsymbol{e}_i, \quad (i=1,2)$$

we get

$$\left(\boldsymbol{\gamma} - \frac{1}{2}k_2n(r)\mathcal{W}_0\boldsymbol{\omega}^{(0)}\right) \cdot \boldsymbol{e}_i = 0, \quad (i = 1, 2), \tag{41}$$

$$\frac{\mathrm{d}\phi(\tilde{t})}{\mathrm{d}\tilde{t}} = \frac{3\pi}{5}n(r)k_1\mathcal{V}_0\Omega(\tilde{t})^{1/3} + k_2n(r)\mathcal{W}_0\boldsymbol{\omega}^{(0)} \cdot (\boldsymbol{e}_1 \times \boldsymbol{e}_2),\tag{42}$$

and

$$\frac{\mathrm{d}\Omega(\tilde{t})}{\mathrm{d}\tilde{t}} = \frac{3}{5}k_1 n(r) \mathcal{V}_0 \Omega(\tilde{t})^{4/3}.$$
 (43)

Equation (43) predicts that $\Omega(\tilde{t})$ increases slowly with time. This equation can be written in terms of the radius r by using (38) according to

$$\frac{\mathrm{d}r(\tilde{t})}{\mathrm{d}\tilde{t}} = -\frac{3}{2}k_1 n(r) \mathcal{V}_0 r(\tilde{t})^{1/2}.$$
(44)

Thus the orbit radius will decrease with time. The phase $\phi(\tilde{t})$ will, according to (42), change with time. Further, the phase will depend on the component of ω perpendicular to the orbital plane. The equation

(41) predicts that the orbital plane will rotate slowly with the angular velocity

$$\gamma = \frac{1}{2} k_2 n(r) \mathcal{W}_0 \, \boldsymbol{\omega}_{\text{orbital plane}}^{(0)}, \tag{45}$$

where $\boldsymbol{\omega}_{\text{orbital plane}}^{(0)}$ is the component of the initial angular velocity parallel to the orbital plane. There will thus be no rotation if the angular velocity is normal to the orbital plane. Returning to dimensional units, we get

$$\gamma = \alpha_{\tau} \frac{1}{4} \frac{mn}{\rho} \, \omega_{\text{orbital plane}}^{(0)}. \tag{46}$$

Note that γ does not depend on the value of the temperature on the sphere's surface.

Let us estimate the rotation of the orbital plane when the radius of the orbit contracts by Δr according to (the last expression is in dimensional units)

$$|\gamma \Delta \tilde{t}| = \frac{|\gamma|\Delta r}{|\frac{\mathrm{d}r}{\mathrm{d}\tilde{t}}|} \sim \frac{|\boldsymbol{\omega}_0|R}{|\boldsymbol{v}_0|} \frac{\Delta r}{r},$$
 (47)

where r is the initial orbit radius, which is essentially the radius of the Earth. Here we have used (45) and (44). In this expression, the variation in the number density n(r) drops out. As an example, consider a satellite in an orbit at the initial height ~ 300 km above the Earth, rotating with 1 revolution per second (with ω_0 parallel to the orbital plane). If the satellite has the radius 1 m this means that the forces and torques calculated in the previous section are valid down to the height ~ 130 km, where the mean free path of the gas is ~ 10 m. For this case the orbit of the satellite, when contracting from 300 km to 130 km, will rotate an angle $\sim 3 \cdot 10^{-6}$ radians. This corresponds to the orbit turning ~ 20 m, which in this context is a small effect.



FIGURE 2. The orbit in the figure above shows the evolution of an initially circular Kepler orbit of a sphere due to the damping and the action of the transverse force. The simulation exposes a slowly contracting orbit radius in a slowly rotating orbital plane. For this orbit, the angular velocity of the sphere has been exaggerated in order to produce a clearly visual effect on the orbit.

A simulation of the equations of motion, (34) and (36), yields the orbit shown in figure 2.

7. Conclusion

The force and torque acting on a rotating sphere of high conductivity are calculated. The force gets two contributions: one damping force parallel to the negative of the velocity, another is a transverse force. The torque damps the rotation and is found to have two contributions: one in the direction perpendicular and one parallel to the velocity.

It is shown that these forces and torques, when applied to a spinning sphere in a circular orbit, apart from slowly contracting the orbit radius also make the orbital plane of the sphere to slowly rotate with an angular velocity parallel to the projection of the angular velocity of the sphere on the orbital plane. A rough estimate of the rotation angle of the orbital plane when the orbit radius has contracted by Δr is given by

$$rac{|oldsymbol{\omega}_0|R}{|oldsymbol{v}_0|}rac{\Delta r}{r},$$

where ω_0 and v_0 are the initial rotation and velocity of the sphere, R its radius, and where r is the radius of the Earth.

Acknowledgement

We wish to thank Dr. Hanno Essén for valuable discussions.

References

- [1] Tokaty, G. A. 1971 A history and philosophy of fluid mechanics, Henley on Thames: Foulis.
- [2] Rubinov, S. I. and Keller, J. B. 1961 The transverse force on a spinning sphere moving in a viscous fluid J. Fluid Mech. 11: 447-459.
- [3] Borg, K. I., Söderholm, L. H. and Essén, H. 2003 Force on a spinning sphere moving in a rarefied gas Phys. Fluids, 15: 736-741.
- [4] Kogan, N. M. 1969 Rarefied Gas Dynamics New York: Plenum.
- [5] Schaaf, S. A. "Mechanics of Rarefied Gases," in *Handbuch der Physik* (Springer, Berlin, 1963), Vol. VIII/2, p. 591.
- [6] Waldmann, L. 1959 Über die Kraft eines inhomogenen Gases auf kleine suspendierte Kugeln. Z. Naturforsch. 14a: 589-99.
- [7] Söderholm, L. H. 2002 Equilibrium Temperature of a Convex Body in Free Molecular Shearing Flow, Phys. Rev. E, **66**: 031204.
- [8] Watts, R. G. and Ferrer, R. 1987 The lateral force on a spinning sphere: Aerodynamics of curveball Am. J. Phys. 55: 40-44.
- [9] Barkla, H. M. and Auchterlonie, L. J. 1971 The Magnus or Robins effect on a rotating sphere J. Fluid Mech. 47: 437-447.
- [10] Tritton, D. J. 1988 Physical Fluid Dynamics, 2nd ed. Oxford: Clarendon Press.
- [11] Tascione, T. F. 1994 Introduction to the space environment, 2nd ed., Krieger Publishing Company, Malabar, Florida, USA.
- [12] Kevorkian, J., and Cole, J. D. 1981 Perturbation Methods in Applied Mathematics, Springer-Verlag New York Inc.